LA-13288-MS

UC-000
Issued: May 1997

Design Summary of the Magnet Support Structures for the Proton Storage Ring Injection Line Upgrade

J. D. Bernardin
J. E. Ledford
B. G. Smith

HH

Los Alamos
NATIONAL LABORATORY
Los Alamos, New Mexico 87545

TABLE OF CONTENTS

Design Summary of the Magnet Support Structures for the Proton Storage Ring Injection Line Upgrade

by

J. D. Bernardin, J. E. Ledford, and B. G. Smith

Abstract

This report summarizes the technical engineering and design issues associated with the Proton Storage Ring (PSR) Injection Line upgrade of the Los Alamos Neutron Science Center (LANSCE). The main focus is on the engineering design calculations of several magnet support structures. The general procedure based upon a set number of design criteria is outlined, followed by a case-by-case summary of the engineering design analyses, reutilization or fabrication callouts, and design safety factors.

1. Facility Overview and Project Introduction

This report presents a summary of technical engineering and design issues associated with the Proton Storage Ring (PSR) Injection Line upgrade of the Los Alamos Neutron Science Center (LANSCE). This upgrade, the details of which can be found elsewhere [1], was initiated to reduce the beam losses of a direct injection H^- beam. The upgrade consists of adding several additional magnets and monitoring instruments to effectively reduce the beam lossses and hence increase the output current. Figure 1 displays the proposed PSR Injection Line upgrade with the magnets and instrumentation noted at the top of the figure. The legend at the lower corner of the figure is provided to describe the short-hand notation.

This report focuses on the engineering design calculations of several magnet support structures. The general procedure based upon a set number of design criteria is outlined in the next section, followed by a case-by-case summary of the engineering

design analyses, reutilization or fabrication callouts, and design safety factors. For the latter three structures (RI-BM-01, RI-BM-02, and RI-QF-02), significant utilization of COSMOS was made. Consequently, the Von Mises stress plots generated for the various subcomponents of these structures are also included in this document. The actual design drawings, rigorous engineering calculations, and general information are provided in an additional document.

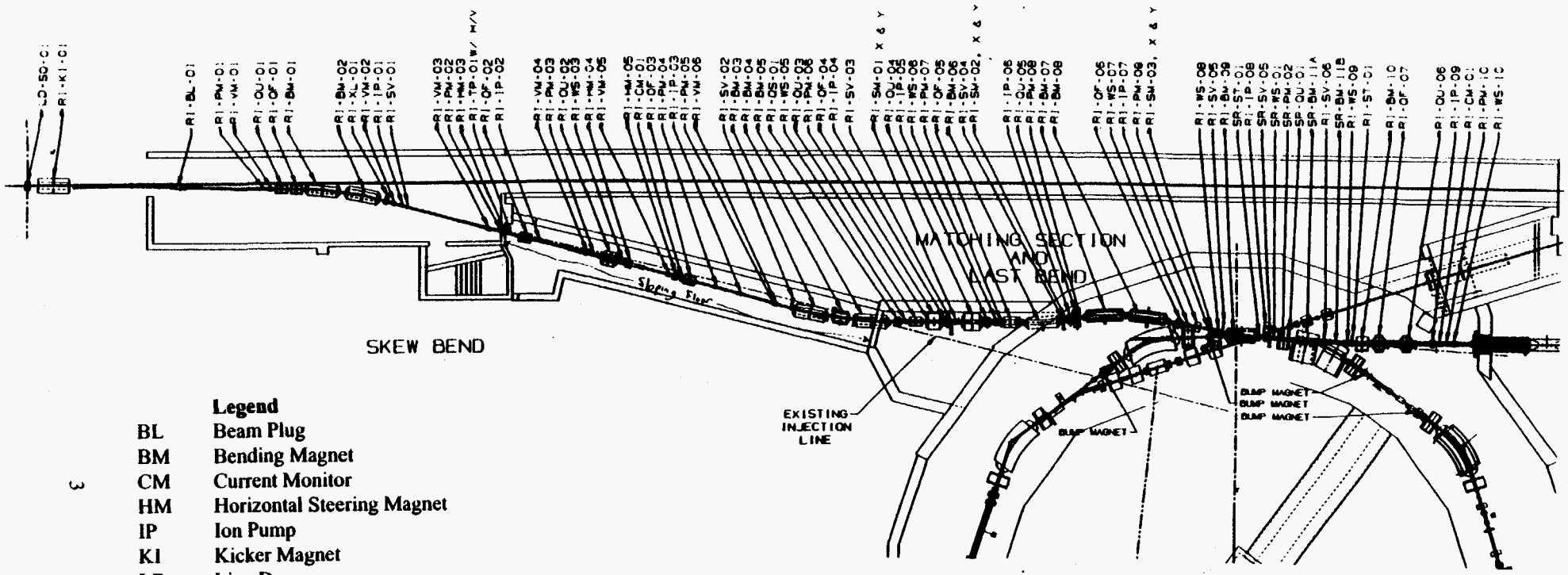

Legend

BL	Beam Plug
BM	Bending Magnet
CM	Current Monitor
HM	Horizontal Steering Magnet
IP	Ion Pump
KI	Kicker Magnet
LD	Line D
PM	Position Monitor
QF	Focusing Quadrupole Magnet
QU	Defocusing Quadrupole Magnet
RI	Injection Line
SM	Steering Magnet
SQ	Sqew Magnet
ST	Stripper Foil or Magnet
SV	Solenoid Valve
SR	Storage Ring
VM	Vertical Steering Magnet
WS	Wire Scanner

Figure 1. Schematic diagram of the Proton Storage Ring Injection Line Upgrade.

2. Engineering Design Procedure

The engineering design procedure for the magnet support structures was comprised of the following three steps:

(1) Preliminary engineering design drawings for a particular magnet support stand were completed which satisfied mounting and alignment requirements.

(2) Strength calculations for various structural components on a stand were performed both with the commercial finite element code COSMOS/M and by hand.

(3) Where required, design changes were made to satisfy strength safety factor requirements and finalized engineering design drawings were produced.

The strength calculations consisted of a static stress analysis of all major subcomponents of the magnet support structures. The two loading conditions considered consisted of the magnet and support structure weight as well as a seismic load. The seismic issue considered was in accordance with DOE STD 1020-94 [2] which was applied to the design of both new structures as well as modification of existing structures. The PSR facility at LAMPF was classified as a performace category PC 2, which was determined from safety and mission importance perspectives [3]. As stated in DOE STD 1020-94 [2], the seismic condition for a PC 2 can be evaluated using the methodology given in the Uniform Building Code (UBC) in which seismic activity is accounted for through the use of a static horizontal seismic loading condition. In particular, Section 1630 of the 1994 UBC provides the following equation for the static lateral seismic force of equipment mounted on structures:

$$F_p = Z\, I_p\, C_p\, W_p$$

where

F_p = Total design lateral seismic force
Z = Seismic zone factor: For PC 2, $Z = 0.20$
I_p = Importance factor: For PC 2, $I_p = 1.5$
C_p = Horizontal force factor: For equipment, $C_p = 1.50$
(accounts for non-rigid or flexible mounted equipment)
W_p = Operating weight of equipment

So, for the PC 2 design, the lateral seismic load, which can act in any horizontal direction, is given as:

$$F_p = 0.45\, W_p$$

The lateral seismic force was considered to act in two perpendicular directions, but not concurrently. Also note that vertical seismic forces were not considered for PC 2.

In addition, the following design criteria were utilized in the engineering analyses:

i) A minimum safety factor of 2 was utilized for existing hardware while a safety factor of 3 was used for all new hardware. As outlined in [4], the selection of the safety factor in this range was based on the following: S.F. = 1.5 to 2.0 for well known materials, under reasonably constant environmental conditions, subjected to loads and stresses that can be determined readily. S.F. = 2.0 to 2.5 for average materials operated in ordinary environments and subjected to loads and stresses that can be determined. S.F. = 2.5 -3.0 for less tried or for brittle materials under average conditions of environment, load, and stress.

ii) Standard Mohr Theory was used for static failure analysis [4].

iii) Common, low grade steel (A-36, yield strength = 35 ksi) was used in components and grade 2 fasteners were used for joining. Threaded rod (B-7 steel, yield strength = 105 ksi) was used for most vertical adjusters.

iv) Design must allow for easy installation and alignment.

v) Wherever possible, reutilization of existing hardware should be made to reduce costs and wastes. (existing structural components have a certain degree of low radioactivity).

As a final design consideration, the natural frequency and harmonics of the RI-KI-01 support structure were determined experimentally with a Bruel & Kjaer Type 2034 dual channel signal analyzer, a type 2813 line drive power supply, and two type 8318 accelerometers (sensitivity of 3070 μA/g, frequency band from 0.1 to 1600 Hz). The RI-KI-01 kicker magnet extracts the beam off of a main line (D) and delivers it to the proton storage ring. A primary concern was that vibrations in this magnet could lead to considerable beam losses in the storage ring. To investigate this potential problem, the natural frequencies and corresponding mode shapes of the RI-KI-01 structure were determined. Next, the natural frequencies were compared to the impulse frequencies (10, 20 and 30 Hz) of the dipole magnet to determine if potential resonating problems existed. In cases where resonance was a concern, the magnet displacements incurred from the pulsing magnet were measured and evaluated with magnet operating criteria.

3. Magnet Support Structures

The next four subsections summarize the engineering design analyses for four different magnet support structures found in the injection and skew lines of the PSR. Each subsection is composed of the following:

1. A descriptive summary of the engineering analyses performed on various structural components of the support structure is provided. These components are indicated on an accompanying engineering drawing of the support structure.

2. Where appropriate, meshed component drawings, produced in COSMOS, showing loading and fixturing conditions are provided in an associated appendix. In addition, Von Mises stress plots are included along with calculated safety factors for worst-case conditions.

3. An engineering design summary, containing designed safety factors and recommended design modifications for each of the various structural components completes each subsection. In addition, the final engineering drawing numbers are provided.

While only a summary of the engineering analyses is provided in this document, a complete set of engineering drawings, hand calculations, COSMOS data, and design modifications can be found in the engineering design file for the PSR upgrade (three ring binder).

3.1 LD-SQ-01

Engineering Analyses of LD-SQ-01

1. Hex Head Cap Screws - Shear and tensile stresses for all screws on Angle Block #1 were determined along with the bearing stresses in the screw threads. COSMOS was employed to solve for reaction forces and all stresses were determined by hand [5, 6].
2. Angle Block #1 - Tensile stress in vertical members and shear stresses in welds were determined by hand and a COSMOS analysis was performed on the worst loaded horizontal plate member.
3. Threaded Rod - Shear and tensile (loading and bending) stresses were determined for the worst loaded threaded rod. In addition, the bearing stresses in the screw threads were determined. COSMOS was employed to solve for reaction forces and all stresses were determined by hand.
4. Ceiling Plate - COSMOS was used to determine the loading on the ceiling plate. From this, the shear force on the ceiling weld was determined. Based on the maximum allowable stresses for fillet welds, as specified by the AISC for E-70 electrodes used to weld A-36 steel, the required weld length was determined.
5. Adjustment Plate - COSMOS was used to determine the loading on the adjustment plate. For the worst-loaded region of the plate (at 4 in. from end, hole with a stress concentration factor of 2), the shear and maximum tensile (loading and bending) stresses were calculated.
6. Angle Block #2 - COSMOS was used to determine the loading on angle block #2. From this, the maximum tensile stress (loading and bending) was determined in the vertical members. Next, maximum tensile stresses in the fasteners were determined. Finally, the maximum tensile stress in the block's base plate was determined at a worst-loaded region (with a stress concentration factor of 3 due to bolt holes).

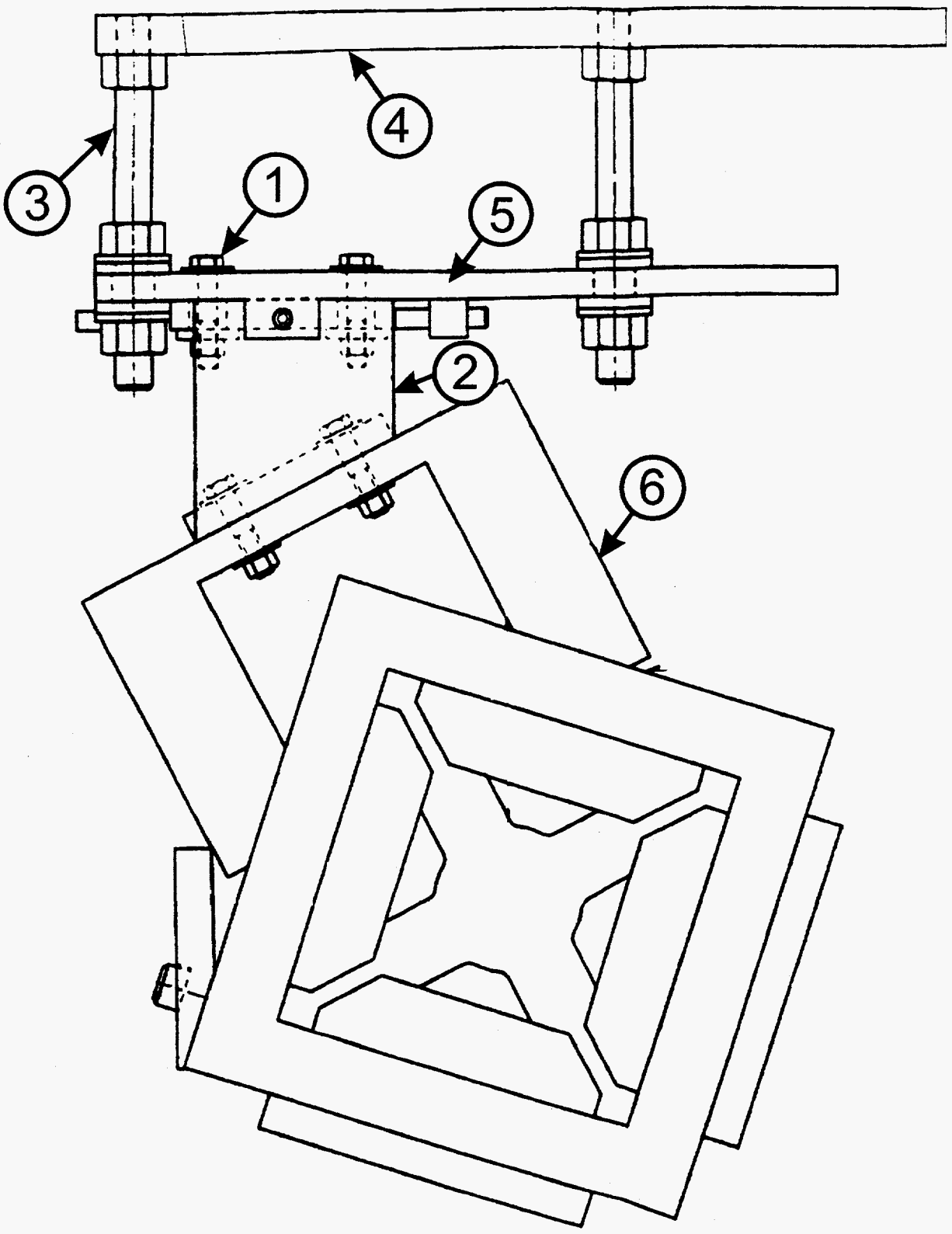

Figure 2. LD-SQ-01 magnet and support structure.

Design Summary of LD-SQ-01

1. Hex Head Cap Screws - COSMOS reaction forces and hand calculations showed that a safety factor of 2.6 exists for the worst loaded screw (1" diam.) on the top of angle block #1. Calculations indicated that 4 screws were insufficient on the bottom or sloping part of the angle block and that **design modification** was necessary. Using 6, 1" grade 2 fasteners gave a safety factor of 4.0 for the worst loaded screw. Nut bearing stresses were found to be sufficiently low (S.F.>3.0).
2. Angle Block #1 - Tensile and shear stresses in the angle block components and welds were found to be sufficiently low (S.F. >3.0). The angle block had to be redesigned to accept 6 rather than four fasteners on the lower side.
3. Threaded Rod - A safety factor of 15.4 was determined for the worst loaded threaded rod. If the loaded ends were modeled as pinned rather than fixed (assuming the spherical washers slipped), then the maximum stress would double and the safety factor would be reduced to 7.7.
4. Ceiling Plate - The weld lengths (for a 3/8" weld) called out in the design drawing will provide a safety factor >> 3.0. The strengths of the ceiling plates were deemed more than adequate from the RI-KI-01 analysis which was for a much heavier magnet but same size plates.
5. Adjustment Plate - A safety factor of 2.4 was determined for the worst loaded portion of the plate.
6. Angle Block #2 - The fasteners have a designed safety factor of 4.4 and the block's base plate has a safety factor of 6.3. The top plate of the angle block required **design modification**. The plate must be redrilled to accept 6 1" fasteners, rather than 4 which was originally called for.

Final Design Drawing Number: 95Y225663

3.2 RI-KI-01

Engineering Strength Analyses of RI-KI-01:

1. Ceiling Plate and Welds - The loads and moments created by the seismic force and magnet weight on the ceiling plate were determined using COSMOS. Von Mises stress plots were generated to determine the stress distribution and magnitude within the plate. The resultant forces on the welds holding the plate in place were also determined with COSMOS. Next, the reaction forces at the fixed nodes (representing the welds) were computed and compared with the maximum allowable stresses for fillet welds (as specified by the AISC for E-70 electrodes used to weld A-36 steel) to determine the required weld length.
2. Threaded Rod - The threaded rods (1" diameter, 6.5" exposed length includes the 1" adjustment and 1" support block added to mount tower) were modeled on COSMOS. The two rods (half of magnet and stand - symmetry) were fixed w.r.t. all six degrees of freedom on their top-most end, and attached to a large and very stiff beam (representing the magnet and lower supports). The seismic load and the magnet weight were applied to the center of the stiff beam. Two separate analyses were performed with the seismic load acting in opposite directions nonconcurrently. Von Mises stress plots were generated and reaction forces at the fixed ends of the rods were calculated. An extended analysis was performed to check out the possible consequences of the lower end of the rods being allowed to rotate (pin connection to represent spherical washer). This had a net effect of doubling the stress within the worst-loaded section of the threaded rods. A final refined model which was felt to be most realistic, incorporated a corrected length rod of 6.5", use of the minor thread diameter of 0.87" (rather than the 1" O.D.), and allowed rotation of the loaded threaded rod ends.
3. Midway Plate - The reaction forces at the threaded rod ends (determined above) were applied to the midway plate and a moment diagram of the resultant loading was generated. From the moment diagram, the stresses in the worst loaded region of the plate were determined through hand calculations. A stress concentration factor of 3 was applied to the hole where the threaded rod passed through. This procedure was done for each of the seismic loading directions investigated.
4. Threaded Rod Mount Tower - The reaction forces at the threaded rod ends (determined above) were used to determine the maximum shear, tension, and bending stresses in the threaded rod mount towers for seismic loads acting in opposite directions nonconcurrently. The regions of highest concern were around the threaded rod hole in the cross support member (stress concentration factor of 1.5) and at the welds at the base of the mount tower. All stress calculations were performed by hand and Mohr's theory was used to determine the maximum principle stresses. The minor thread diameter was used for the stress computations.
5. Ceiling Mounts and Fasteners - The reaction forces at the ceiling mounts were determined with COSMOS. These loads were then transferred to the mounting bolts to determine the maximum tensile stresses in the fasteners.

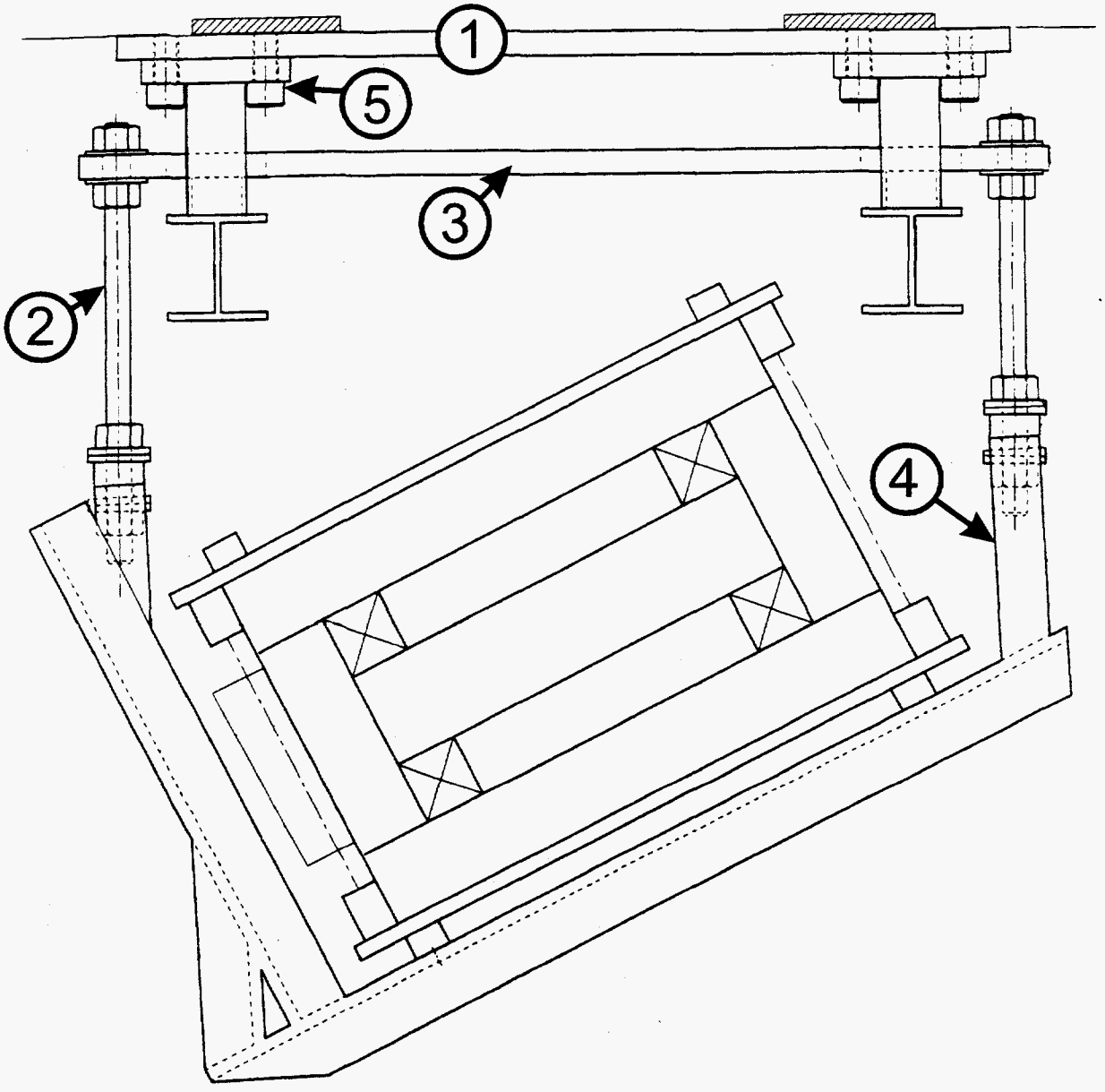

Figure 3. RI-KI-01 magnet and support structure.

Frequency Analyses of RI-KI-01:

As mentioned previously, the natural frequency and harmonics of the RI-KI-01 support structure were determined experimentally with a Bruel & Kjaer Type 2034 dual channel signal analyzer and two type 8318 accelerometers (sensitivity of 3070 μA/g, frequency band from 0.1 to 1600 Hz). The experimental procedure for these measurements was as follows:

1) The accelerometers were placed on the magnet along one of the three major axes orientations and the vibration response of the structure to background noise was measured. The coordinate system used in reference to the magnet is shown in Figure 2. Note that the magnet horizontal is tilted 23° from true horizontal. A single frequency response was averaged from 20 measurements. This was repeated for the other two orientations.
2) The procedure in step #1 was repeated except that the structure was excited prior to each measurement with a single pulse from a rubber mallet. In each orientation, a single frequency response was averaged from 10 measurements.
3) The procedure in step #1 was again repeated except that the magnet was pulsed at 10 Hz (202 Amps). In each orientation, a single frequency response was averaged from 20 measurements. This entire procedure was repeated for magnet excitation frequencies of 20 and 30 Hz.

The output from each measurement consisted of the power spectral density PSD function of the response signal. The PSD identifies which frequencies and their corresponding relative strengths that are present in the apparent noisy accelerometer

response signal. To determine the mode shapes of the support structure, the phase difference between the two accelerometers was measured. For example, where no phase difference was present, the support structure was found to be resonating in a purely translational state along one of the major axes. For a 180° phase difference, the support structure was resonating in a purely torsional state about one of the major axes. In addition to the frequency analyses, the magnet displacements were estimated by integrating the RMS function twice with respect to time. This function was performed within the spectrum analyzer.

Strength Design Summary of RI-KI-01

1. Ceiling Plate and Welds - COSMOS Von Mises stess results indicated that the ceiling plates have a designed safety factor of 6.4. Hand calculations indicated that a total weld length of 6 inches on each end of the ceiling plate (to the ceiling I-beams) would provide a safety factor of 10.5.
2. Threaded Rod - For the worst-case loading condition in which the loaded end (closest to magnet) of the threaded rod is allowed to rotate (assuming the spherical washers slipped completely) and hence has a pinned boundary condition on the loaded end, an exposed rod length of approximately 6.5 inches (including the 1" max. adjustment) between the mounting nuts (note: this length was computed after the support block for the threaded rod mount tower was added) and the rod minimum thread diameter, a worst-case safety factor of 2.1 was obtained.
3. Midway Plate - COSMOS results and hand calculations indicate that the threaded rod hole in the midway plate is the region of highest stress for the worst-case loading condition. The current design provides a safety factor of 3.1.
4. Threaded Rod Mount Tower - For worst-case loading conditions, the current threaded rod mount towers are insufficient and possess bending stresses approaching the yield strength. A design modification was proposed which included attaching a reinforcement block on top of the horizontal structural piece of each mount tower (the part through which the lower end of the threaded rod passes through). All welds were checked and found to provide a safety factor of 2.8.
5. Ceiling Mounts and Fasteners - COSMOS results and hand calculations indicate that the current fasteners are inadequate and redesign must occur. For the top four fasteners on the upper flange of the ceiling mount, using 1" grade 2 bolts will give a safety factor greater than 3 for the worst loaded bolt. It was recommended that the bottom four fasteners be replaced by a continuous weld due to clearance and safety factor limitations. In meeting clearance criteria for the upper 1" fasteners, the entire ceiling mount had to be redesigned and the old mounts had to be scrapped.

Frequency Design Summary of RI-KI-01:

Table 1 summarizes the natural frequencies of the RI-KI-01 structure within the band of 4 to 400 Hz, as measured along the three major axes (defined in Figure 4) by exciting the magnet with a mallet. The phase angle between the two accelerometers indicates whether the mode of vibration for each frequency is purely translational (θ =

Table 1. Natural frequencies and harmonics of RI-KI-01 structure for various accelerometer orientations (measured with hammer excitation).

Accelerometer Displacement Direction	Frequency (Hz)	Phase Angle Between Accelerometer Signals
Z (beam direction)	8.5	0
	16	-180
	41	-90
	62	-45
	125	0
	160	160
	250	160
	290	-90
	350	-160
	375	0
Y (perpendicular to beam)	11	0
	27.5	0
	40	0
	53	-180
	65	180
	125	45
	170	90
	200	-180
	250	-180
	290	0
	350	0
	390	30
X (perpendicular to beam)	11	0
	16	-180
	27.5	0
	45	-180
	68	-180
	120	-90
	140	160
	165	-180
	175	90
	210	0
	280	0
	300	-90
	350	160
	390	180

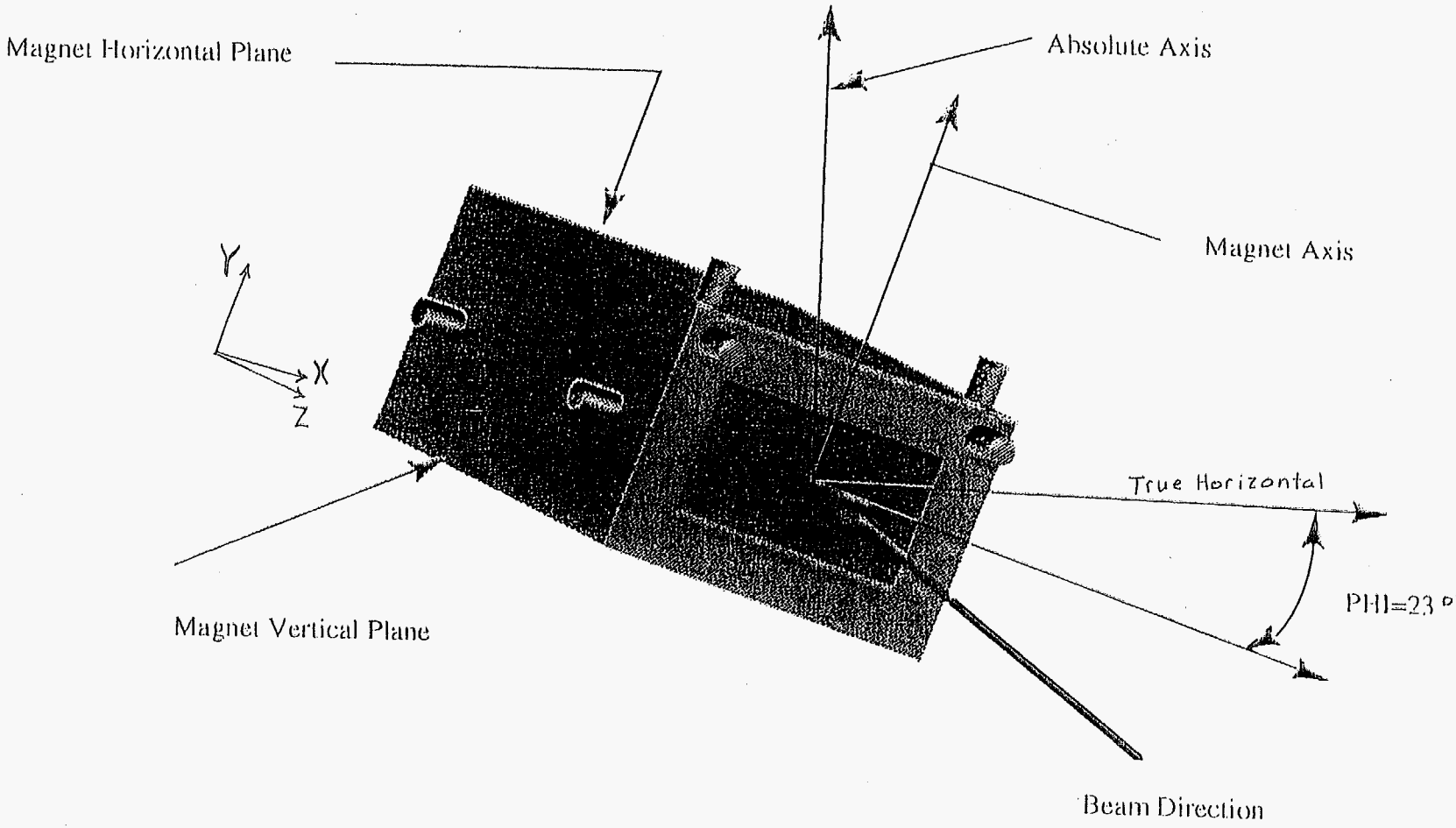

Figure 4. Schematic diagram of the accelerometer placement on the RI-KI-01 magnet.

0°), purely torsional ($\theta = 180°$), or a combination of both ($0° < \theta < 180°$). For example, in the beam direction, there is a purely translational vibration mode at 8.5 Hz and a purely torsional vibration mode at 16 Hz. The data for the background noise in which the magnet was not excited with the mallet, was nearly identical to the data in Table 1 and thus will not be presented. This similarity was expected since the effect of the mallet was to enhance the response signal of the natural frequencies. The PSD data output for all experimental measurements is contained in Appendix D.

Upon observation of the data in Table 1, it is apparent that the RI-KI-01 structure possesses natural frequencies which correspond closely with the magnet excitation frequencies and harmonics, i.e. 11 and 27.5 Hz. Consequently, the structure will resonate when the magnet is pulsed. The magnitude of the displacements, as determined in part by the amount of internal damping, was measured in the three major axis directions while operating the magnet at 10, 20 and 30 Hz. Table 2 lists the total RMS displacements (the sum of the displacements from all frequencies between 4 and 400 Hz) for the three axis directions and three magnet pulsing frequencies. In each case, the magnitude of the displacements is on the order of 1 μm, well below the magnitude sufficient to disrupt the beam. Consequently, while the RI-KI-01 structure has natural frequencies which correspond to the excitation frequencies of the magnet, internal damping is sufficient and no additional stiffening of the structure is required.

Final Design Drawing Number: 95Y225665

Table 2. Summary of the RMS displacements of the RI-KI-01 structure at various magnet excitation frequencies.

	Magnet Excitation Frequency (Hz)					
	10		20		30	
Displacement Direction	Channel A (μm)	Channel B (μm)	Channel A (μm)	Channel B (μm)	Channel A (μm)	Channel B (μm)
Z	0.94	0.99	0.76	1.06	0.81	0.85
Y	1.11	1.22	1.17	1.53	0.83	1.04
X	1.27	1.49	1.24	0.79	1.04	0.91

3.3 RI-BM-01 and RI-BM-02

Engineering Analyses of RI-BM-01 and RI-BM-02

The stands and magnets for RI-BM-01 and RI-BM-02 are identical, except that the pedestals for RI-BM-01 are slightly taller. Consequently, the analyses were performed for the worst-case loadings for RI-BM-01 and all designs for this stand will be more than satisfactory for RI-BM-02.

1. Mounting Jacks -
   Shaft, Main Body and Welds - Hand calculations were used to determine the reaction forces at each jack. For the worst-loaded conditions (jack stand B), bending and axial stresses were determined in the shaft and main body, and shear forces on the main body welds were calculated. As a secondary check, a COSMOS analysis was also used to determine the stress in the main jack body and the shear loading on its base weld.
   Collar Plate and Mounting Screws - A COSMOS stress analysis was performed on the collar plate. The loading on the collar plate from the seismic and magnet loads was distributed uniformly around a circular contour representing the contact line between the collar plate and base of the main jack body. The direction of the seismic load was chosen so as to provide the worst-case loading on the mounting bolts. The collar plate was fixed with respect to all translations and the mounting bolt holes and reaction forces at these holes (the effective loading on the bolts) were determined. Hand calculations were then used to determine the stresses within the worst loaded bolt.
   Pusher Bolts - A worst case loading condition in which a single pusher bolt resisted the seismic loading through the jack body was analyzed to determine the maximum compression force. This compression force was then compared to that required to buckle the bolt.
2. Jack Stand Pedestals -
   Base Plate and Floor Mounting Bolts - Using jack stand B as a worst case loading condition, a COSMOS analysis was performed to determine the maximum bending stress in the base plate. The bolt holes were assumed to be fixed with respect to all three translations and the load was evenly distributed around a contour representing the weld connecting the main body riser tube. Two different loading orientations were considered. For the worst of these two, the reactions forces at the bolt holes were determined. These forces were used in a hand calculation to determine the maximum tensile stresses in the mounting bolts.
3. *Main Riser Tube and Welds* - Using jack stand B as a worst case loading condition, a COSMOS analysis was performed to determine the maximum bending stress in the main riser tube. One end of the tube was assumed to be fixed with respect to all six degrees of freedom (weld to base plate) and the load was evenly distributed around

the outer contour on the other end of the tube. Next, since the weld area (for a 3/16" weld) is greater than the cross-sectional area of the riser tube, it was assumed that the stresses in the base of the riser tube, as determined by the COSMOS analysis, would be representative of those found in the fillet welds (for A-36 steel).

4. Jack Stand Pads - Bearing stresses in the pads were determined from hand calculations. Hand calculations were also used to determine the designed safety factor of the welds used to fasten the pads to the magnet body.

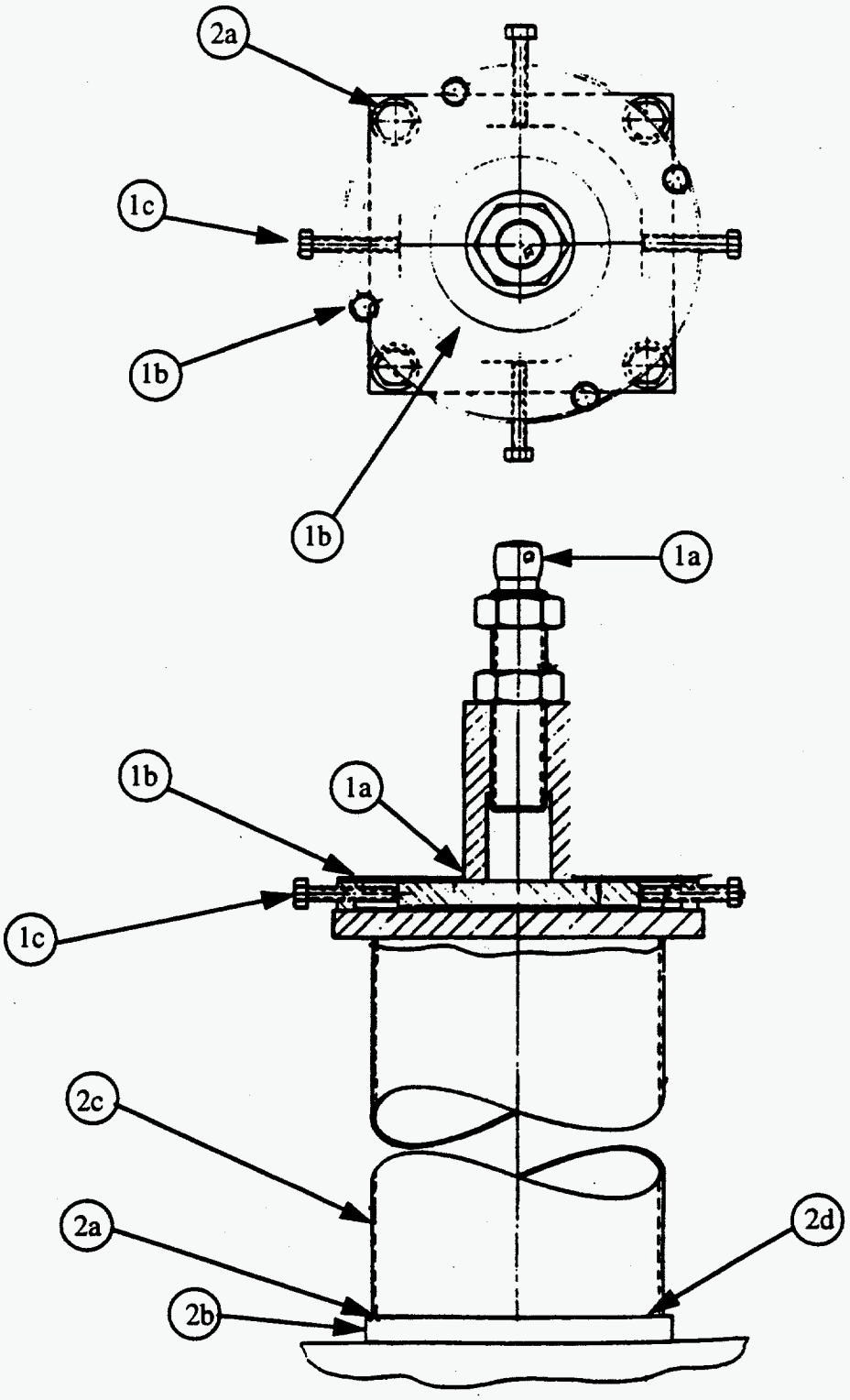

Figure 5. RI-BM-01 adjustment jack and support pedestal.

Design Summary of RI-BM-01 and RI-BM-02

1. Mounting Jacks -
   Shaft, Main Body and Welds - COSMOS results (in agreement with hand calculations) indicated that the stress in the main body and weld are acceptable and gave a safety factor greater than 3. Hand calculations showed, however, that the bending stresses in the jack shaft were too high and redesign of this component was necessary. Several options exist for this redesign and are presented below under *Required Design Modifications for RI-BM-01 stands.*
   Collar Plate and Mounting Screws - COSMOS results indicated that the current collar plate thickness was unsatisfactory and redesign must occur. A plate thickness of 0.75" (versus 0.25" in current design) gave a safety factor of 4.1. Hand calculations using the COSMOS determined resultant forces on the mounting screws resulted in a safety factor of 2.0 for grade 2 fasteners.
   Pusher Bolts - For the worst-case loading conditions, hand calculations gave a safety factor of 35 for the pusher bolts.
2. Jack Stand Pedestals -
   Base Plate and Floor Mounting Bolts - COSMOS results indicated that stresses in the 0.75" thick base plate were too high and that redesign was necessary. Increasing the plate thickness to 1.00" reduced the stresses and provided a safety factor greater than 3.0. Hand calculations gave a safety factor of 3.4 for the worst loaded floor mounting bolt.
   Main Riser Tube and Welds - COSMOS results indicated that stresses in the riser tube and welds were low and that a designed safety factor of 3.2 existed. It was recommended that a continuous rather than an intermittent weld be used between the riser tube and the two end plates.
3. Jack Stand Pads - Hand calculations gave safety factors greater than 10 for the bearing stresses in the pad bodies and shear stresses in the welds.

A design review for the RI -BM stands was convened on January 28, 1997 to determine whether or not the old stand design or a completely new design would be used. The following outline was provided at the design review:

Required Design Modifications for RI-BM-01 stands:

1) A tie-down is recommended to keep magnet from lifting off of jacks.
2) A new collar plate is required for all jack stands. The thickness must be increased from 0.25" to 0.75".
3) The base plate thickness must be changed from 0.75" to 1.00".
4) The weld joining the riser to the base plate should be made continuous with a thickness of 3/16".
5) A containment ring should be welded on to the underside of the jack stand A pad to keep the magnet from sliding off of the jack.

6) The current threaded shaft on the jack stand is insufficient for supporting against a seismic load (S.F. = 1.5). The following 3 options are proposed to rectify this situation:
    (i) Build a new shaft (diameter > 2.25") and corresponding jack body out of mild steel.
    (i) Build a new shaft (diameter = 1.5") from a high grade steel and retain the old jack body for continued use.
    (ii) Use a set of spacers to limit the spacing between the two lock nuts on the threaded shaft to a quarter inch. Use a go-nogo gauge to inspect clearance.

Advantages of using old system:

1) Kinematic system has been used successfully in the past. No complicated cradle structure is required for the magnet underside, thus making the system universal.
2) Design and layout drawings as well as a thorough engineering analysis have been completed.
3) Machining of new components can be initiated now while shop load for PSR upgrade is low.
4) Pedestals can be reused with suitable spacers welded to base plate.
5) Pads on bottom of magnets do not have to be removed or replaced.
6) Less machining and fabrication time required compared to a new stand.

Disadvantages of using old system:

1) Current stand is not universal in its operating, as may be the case if a new universal stand design is selected for majority of the magnet support structures.
2) Machining must be done on possibly 'hot' materials.
3) A significant amount of machining and refabrication must take place.

At the time of printing this document, a decision had not been reached as whether or not the old design discussed here would be used.

Final Design Drawing Number: (Not yet available)

3.4 RI-QF-02

Engineering Analyses of RI-QF-02

1. Ceiling Plate and Welds - COSMOS was used exclusively to determine the stresses within the ceiling plate. Seismic and magnet loads were distributed across the center nodes of the COSMOS model and welds were approximated by fixing the outer edges of the plate with respect to all six degrees of freedom. Von Mises stress plots were generated to determine the stress distribution and magnitude within the plate and welds. As a secondary check on the welds, the reaction forces at the fixed nodes (representing the welds) were computed and compared with the maximum allowable stresses for fillet welds (as specified by the AISC for E-70 electrodes used to weld A-36 steel) to determine the required weld length.
2. Upper Plate and Fasteners - COSMOS was used exclusively to determine the stresses within the upper plate. Seismic and magnet loads were distributed across a circular contour on the plate, which represented the weld which attached the riser tube to the upper plate. Von Mises stress plots were generated to determine the stress distribution and magnitude within the plate and reaction forces at each of the four bolt holes were determined. These reaction forces were then used to determine the maximum tensile stress in the worst-loaded fastener.
3. Riser Tube and Weld - The riser tube and weld were modeled on COSMOS as a thin-walled cylinder and fixed edge, respectively. Seismic and magnet loads were distributed across the inner contour of the non-fixed end of the cylinder. Von Mises stress plots were generated to determine the stress distribution and magnitude within the riser tube and reaction forces at the fixed end were determined. These reaction forces at the fixed nodes (representing the welds) were compared with the maximum allowable stresses for fillet welds (as specified by the AISC for E-70 electrodes used to weld A-36 steel) to determine the required weld length. Finally, the maximum stresses in the riser tube were performed by hand to verify the COSMOS results.
4. Upper Adjuster Plate - The upper adjuster plate was modeled on COSMOS. Seismic and magnet loads were distributed evenly across the contours of the three holes where the threaded rods passed through the plate. A second analysis was performed in which non-uniformly distributed loads were applied to the three holes. These forces were determined from the COSMOS analysis on the threaded rods (reaction forces at the location of contact between the rods and adjuster plate). An inner contour on the top face of the plate was fixed with respect to all six degrees of freedom to represent the welded attachment of the riser tube. Two different loading orientations (90 degrees rotation in the horizontal plane of the plate) were considered to determine a worst-case scenario. Von Mises stress plots were generated to determine the stress distribution and magnitude within the adjuster plate for both loading orientations.
5. Threaded Rod - The threaded rods (1" diameter, 5" length) were modeled on COSMOS. The three rods were fixed w.r.t. all six degrees of freedom on their top-most end, and attached to a large and very stiff beam (representing the magnet and lower supports). The seismic load and moment, as well as the magnet weight, were applied to the center of the stiff beam. Von Mises stress plots were generated and

reaction forces at the fixed ends of the rods were calculated. An extended analysis was performed to check out the possible consequences of the lower end of the rods being allowed to rotate (pin connection to represent spherical washer). This had a net effect of doubling the stress within the worst-loaded section of the threaded rods.

6. Lower Adjuster Plate - The lower adjuster plate was modeled on COSMOS. Seismic and magnet loads were distributed evenly across the contours of the four holes used to attach the lower magnet assembly. The contours of the three holes for the threaded rods were fixed w.r.t. all six degrees of freedom. Only a single orientation was considered as the results for the upper adjuster plate noted similar stresses for two different loading orientations. Von Mises stress plots were generated to determine the stress distribution and magnitude within the adjuster plate.
7. Lower Magnet Attachment Blocks and Fasteners - These features are currently under redesign. All strength calculations will be obtained during the analysis of structure RI-QU-01 which employs identical components.

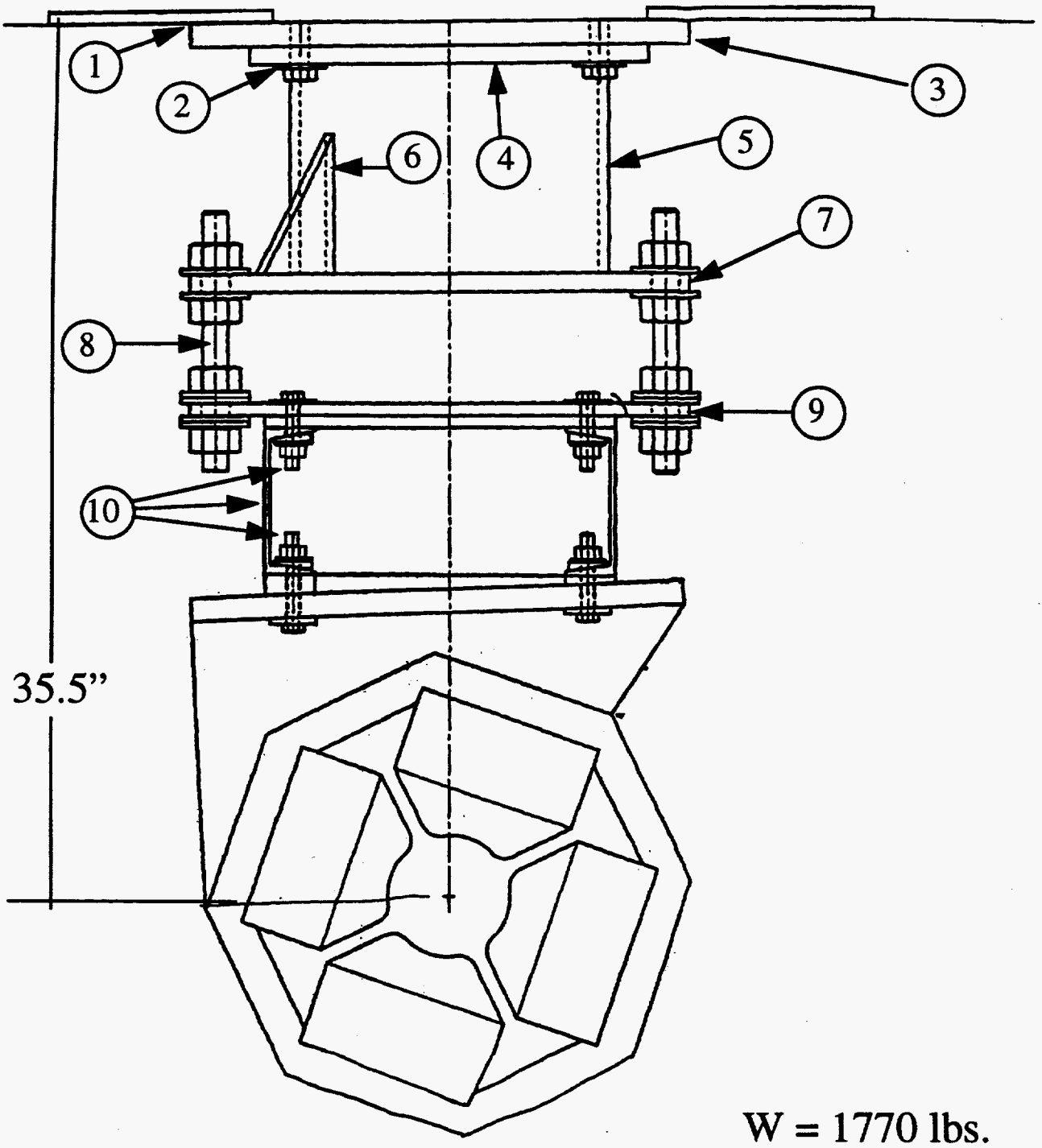

Figure 6. RI-QF-02 magnet and support structure.

Design Summary of RI-QF-02

1. Ceiling Plate and Welds - A COSMOS analysis of the ceiling plate and associated welds gave a designed safety factor greater than 18 for these components under worst-case loading conditions.
2. Upper Plate and Fasteners - A COSMOS analysis of the upper plate indicated that the worst loaded region on the plate had a safety factor of 3.2 and that the high stresses in the region near the bolt holes would be further reduced by washers which were not provided in the model. Using reaction force data provided by COSMOS, the fasteners were found to have a safety factor of 8.0.
3. Riser Tube and Weld - COSMOS results gave a safety factor of 31.8 for the riser tube and reaction force data from COSMOS indicated that the welds connecting the riser tube to the upper plate and adjuster plates provided a safety factor of 20.3.
4. Upper Adjuster Plate - A worst-case loading condition modeled with COSMOS gave a maximum stress region (less than 5% of the plate) that had a corresponding safety factor of 2.8. The majority of the plate possessed considerably lower stresses.
5. Threaded Rod - A COSMOS model indicated that the proposed design using grade B-7 steel had a safety factor of 9.1 assuming both ends of the threaded rod were fixed relative to any rotation. A worst-case condition was modeled in which the loaded end (closest to magnet) of the threaded rod was allowed to rotate (assuming the spherical washers slipped completely) and hence had a pinned boundary condition on the loaded end, giving a maximum stress that was twice as high and thus a designed safety factor of 4.55.
6. Lower Adjuster Plate - A COSMOS analysis indicated that the lower adjuster plate required thickening to reduce stress levels. Increasing the plate thickness to 1" gives a safety factor of 4.4.
7. Lower Magnet Attachment Blocks and Fasteners - The strength analysis for these components can be found in the results for magnet RI-QU-01. This magnet has the same stand design and at the time of the analysis for RI-QF-02, these components were under redesign.

Following the completion of this strength analysis for RI-QF-02, a few design changes were made in the threaded rod and adjuster plates (increasing their diameter and thicknesses, respectively). While these design enhancements were not necessary for RI-QF-02, they were deemed necessary in the engineering analyses for RI-QU-01. Since stand consistency was desired, these changes were incorporated in RI-QF-02 and can be noted in the latest design drawings.

Final Design Drawing Number: 95Y225671

Appendix A - Magnet Specifications Required for Stand Designs

Magnet Specifications Required for Stand Design

Magnet Name	Old(in line) /SemiNew (new to line) /New (Brand new) - Type	Weight (lbs)	Max. Overal Dimensions H/W/L(cm) (no mounting hardware)	Mount (Ceiling, floor, pipe)
LD-QS-01	Old-4Q11	600	50/50/43	Ceiling
RI-KI-01	Old-Kicker	2,130 (3,500)	39/60/126	Ceiling
LD-QS-02	SemiNew-4Q16	1,250	43/43/61	
LD-QS-03	SemiNew-4Q16	1,250	43/43/61	
LD-QS-04	SemiNew-4Q11	600	50/50/43	
RI-VM-01	Old-Steerer	120	36/20/25	Pipe
RI-QU-01	Old-4Q20	1,764	53/53/67	Floor
RI-QF-01	Old-4Q20	1,764	53/53/67	Floor
RI-BM-01	Old-H10-IV-62	5,100	35/63/177	Floor
RI-BM-02	Old-H10-IV-62	5,100	35/63/177	Floor
RI-VM-02	Old-Steerer	120	36/20/25	Pipe
RI-VM-03	Old-Steerer	120	36/20/25	Pipe
RI-HM-03	Old-Steerer	120	36/20/25	Pipe
RI-QF-02	Old-4Q20	1,764	53/53/67	Ceiling
RI-VM-04	Old-Steerer	200	42/25/28	Pipe
RI-QU-02	Old-6Q24	3150	84/84/86	Ceiling
RI-HM-04	Old-Steerer	200	42/25/28	Pipe
RI-VM-05	Old-Steerer	120	36/20/25	Pipe
RI-HM-05	Old-Steerer	120	36/20/25	Pipe
RI-QF-03	Old-4Q20	1,764	53/53/67	Floor
RI-VM-06	Old-Steerer	120	36/20/25	Pipe
RI-BM-03	Old-H10-IV-62	5,100	35/63/177	Floor
RI-BM-04	SemiNew-H10-IV-27	2,000	35/63/59	Floor
RI-BM-05	Old-H10-IV-62	5,100	35/63/177	Floor
RI-QS-01	SemiNew-4Q8	570	46/46/36	Floor
RI-QU-03	Old-4Q20	1,764	53/53/67	Floor
RI-QF-04	New-6Q24	3150	84/84/86	Floor

RI-SM-01	New-Steerer	340	33/33/23	(pipe)
RI-QU-04	SemiNew-8Q32	6,200	89/89/99	Floor
RI-QF-05	SemiNew-10Q27	6,700	100/56/100	Floor
RI-BM-06	Old-H10-IV-62	5,100	35/63/177	Floor
RI-SM-02	New-Steerer	340	33/33/23	(pipe)
RI-QU-05	SemiNew-5Q8	3,200	100/100/30	Floor
RI-BM-07	New-H10-VI-75	6,100	35/63/211	Floor
RI-BM-08	New-H10-VI-75	6,100	35/63/211	Floor
RI-QF-06	SemiNew-4Q8	570	46/46/36	Floor
RI-SM-03	New-Steerer	340	33/33/23	(pipe)
RI-BM-09	New-P16-VI-56	5,500	35/63/176	Floor
SR-QU-01	Old-PSR Quad	3,500		Floor
SR-BM-11A	SemiNew-C16-VI-36	40,000	163/147/114	Floor
SR-BM-11B	SemiNew-C16-VI-36	40,000	163/147/114	Floor
RI-BM-10-H-V	New-P10-VI-16	1,500	45/59/64	Floor
RI-QF-07	SemiNew-12Q16	5,000	90/90/82	Floor
RI-QU-06	SemiNew-12Q16	5,000	90/90/82	Floor

Appendix B - COSMOS model and Von Mises Stress Plots for LD-SQ-01

Top plate of angle block #1

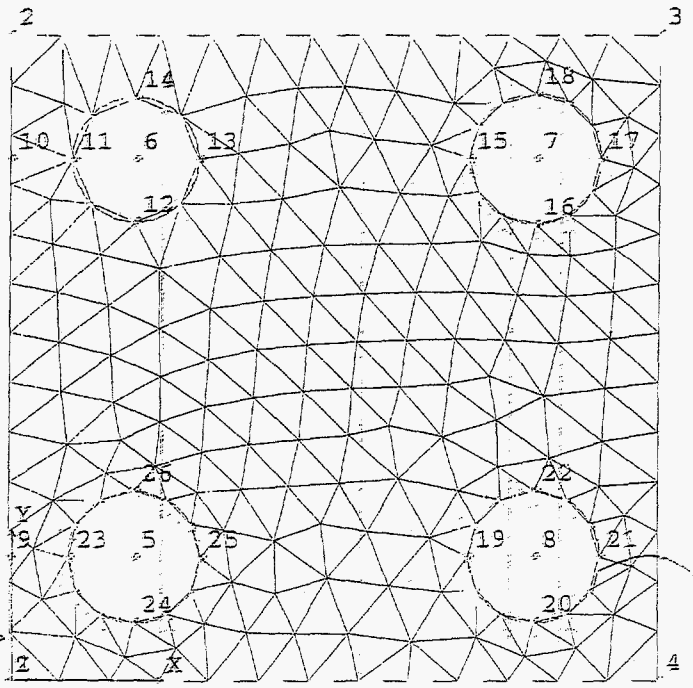

0.75 thick → 3D - Thin Shell elements

Bolt holes fixed w.r.t. all 3 translations

Seismic load, magnet weight load, & moment created by seismic load are evenly distributed along top & bottom edges.

GeoStar 1.75: SQ011

Stress plot of top plate

Lin STRESS Load

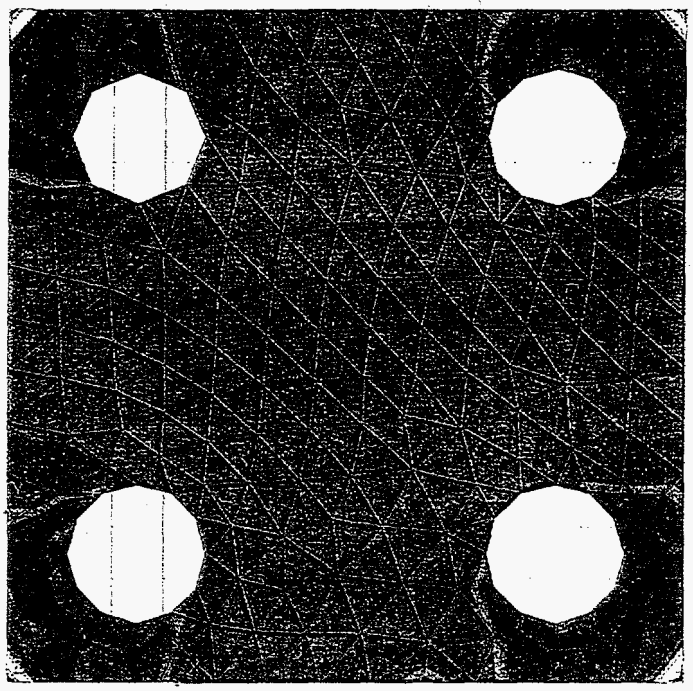

$$S.F. = \frac{35\ KSI}{10.2\ KSI} = 3.43$$

Appendix C - COSMOS model and Von Mises Stress Plots for RI-KI-01

Ceiling Plate

Fixed w.r.t. all 6 DOF

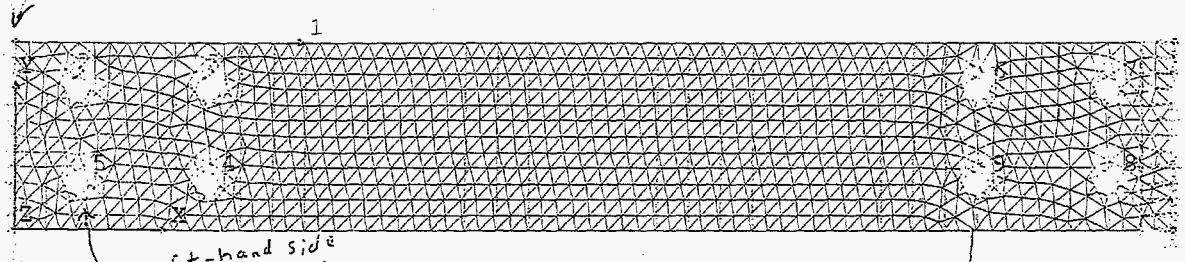

left-hand side loads distributed uniformly across 4 hole contours

right-hand loads (dif. from left) applied uniformly across 4 hole contours

GeoStar 1.75: KI011

Ceiling Plate
Stress Plot

Lin STRESS Load

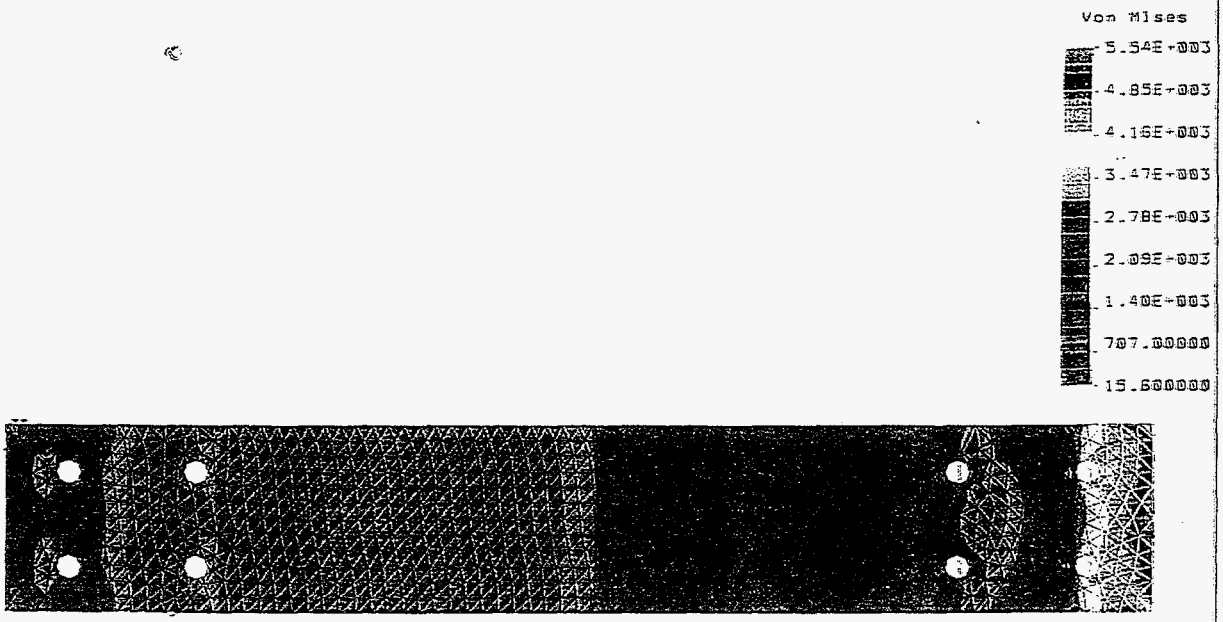

$$S.F. = \frac{\sigma_y}{\sigma_{max}} = \frac{35}{5.5} = 6.4$$

GeoStar 1.75: KI011

Stress plot with exaggerated deformations

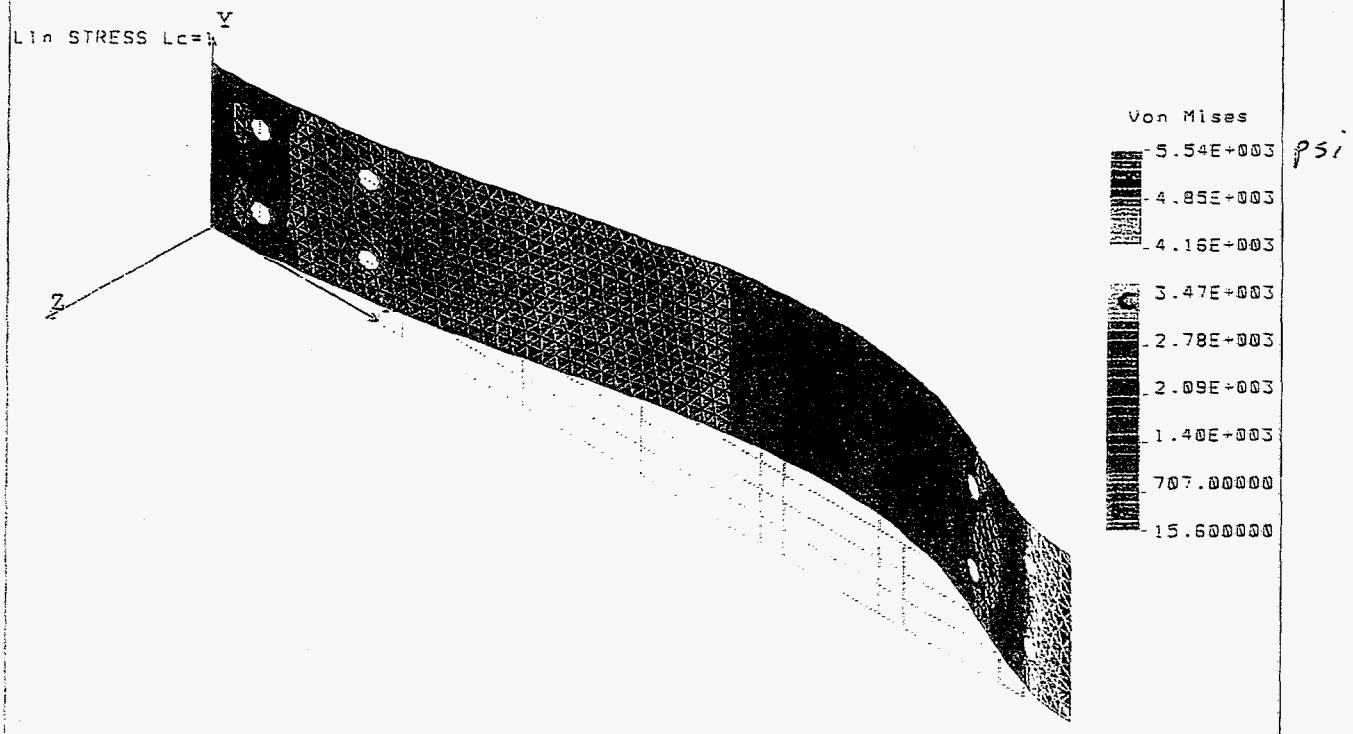

$$S.F = \frac{\sigma_y}{\sigma_{max}} = \frac{35\,ksi}{5.5\,ksi} = 6.4$$

Threaded Rods
Seismic load to the left

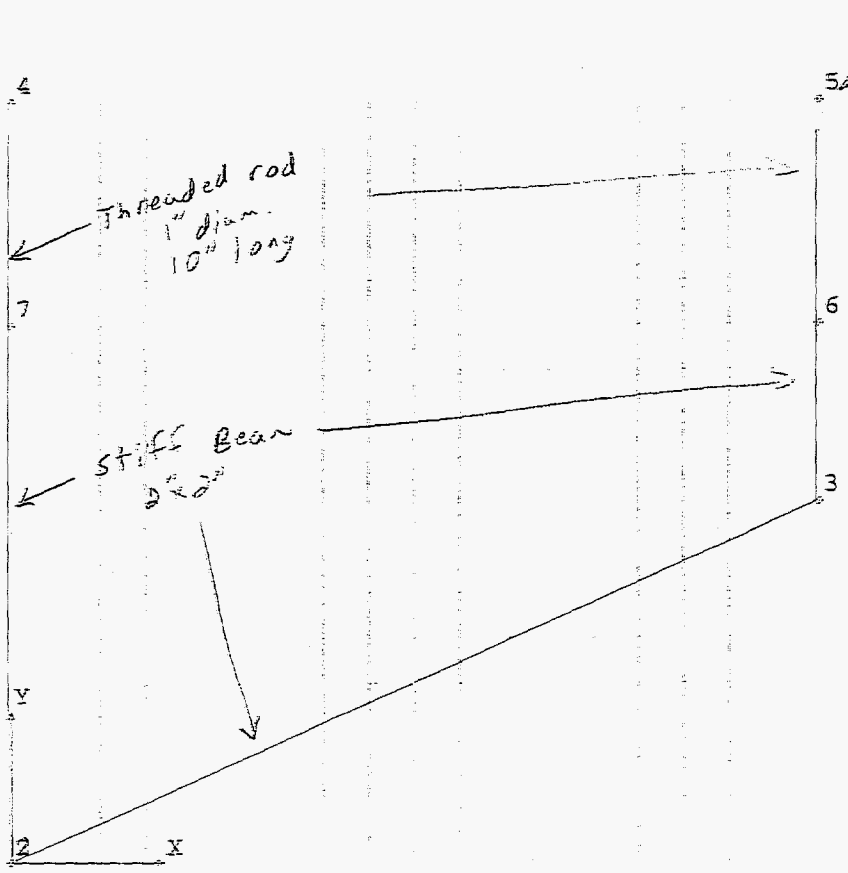

GeoStar 1.75: KI012

Stress Plot

Seismic load to the left

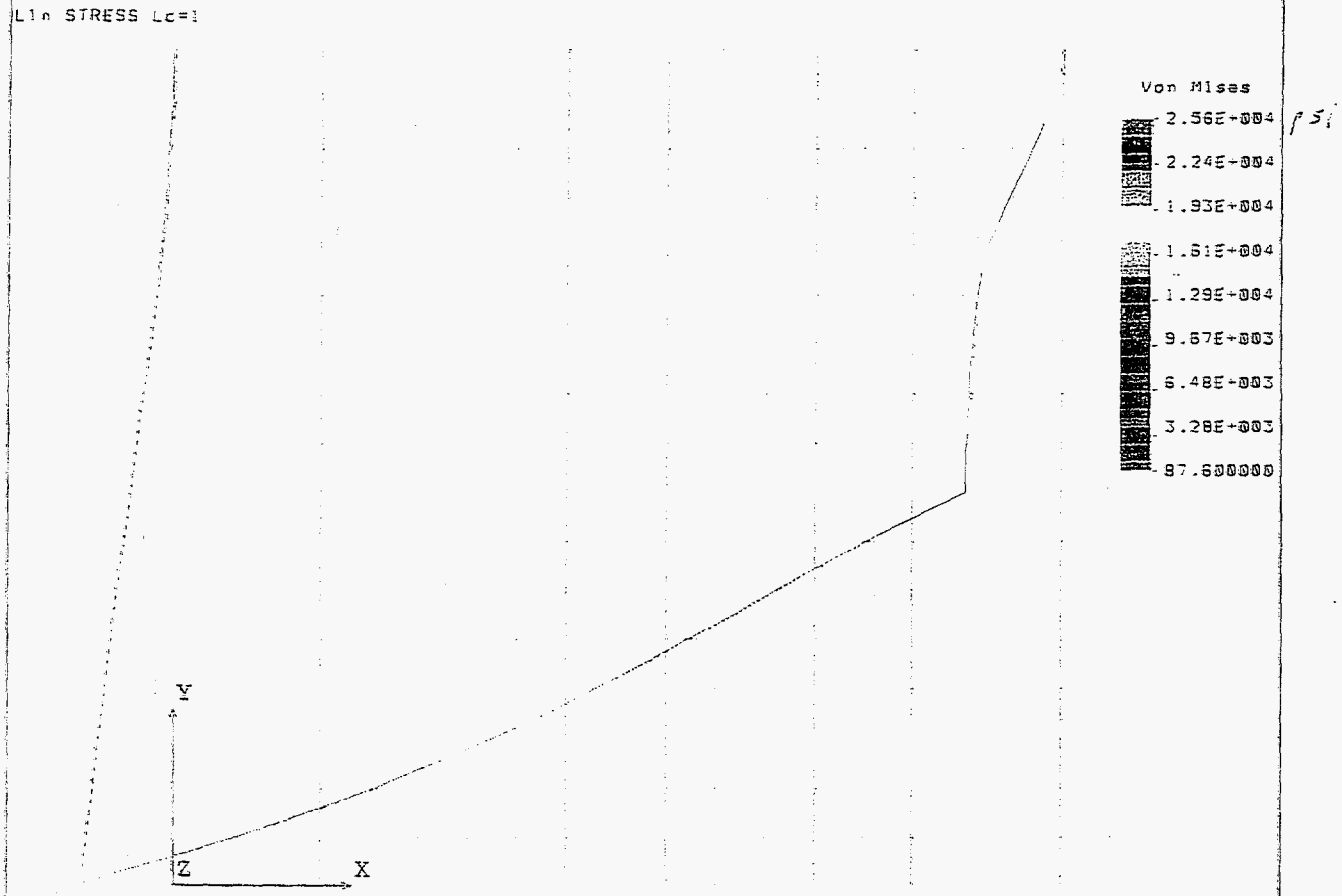

$$S.F. = \frac{\sigma_Y}{\sigma_{max}} = \frac{105\ ksi}{25.6\ ksi} = 4.1$$

GeoStar 1.75: KI012

Stress Plot

Seismic load to the right

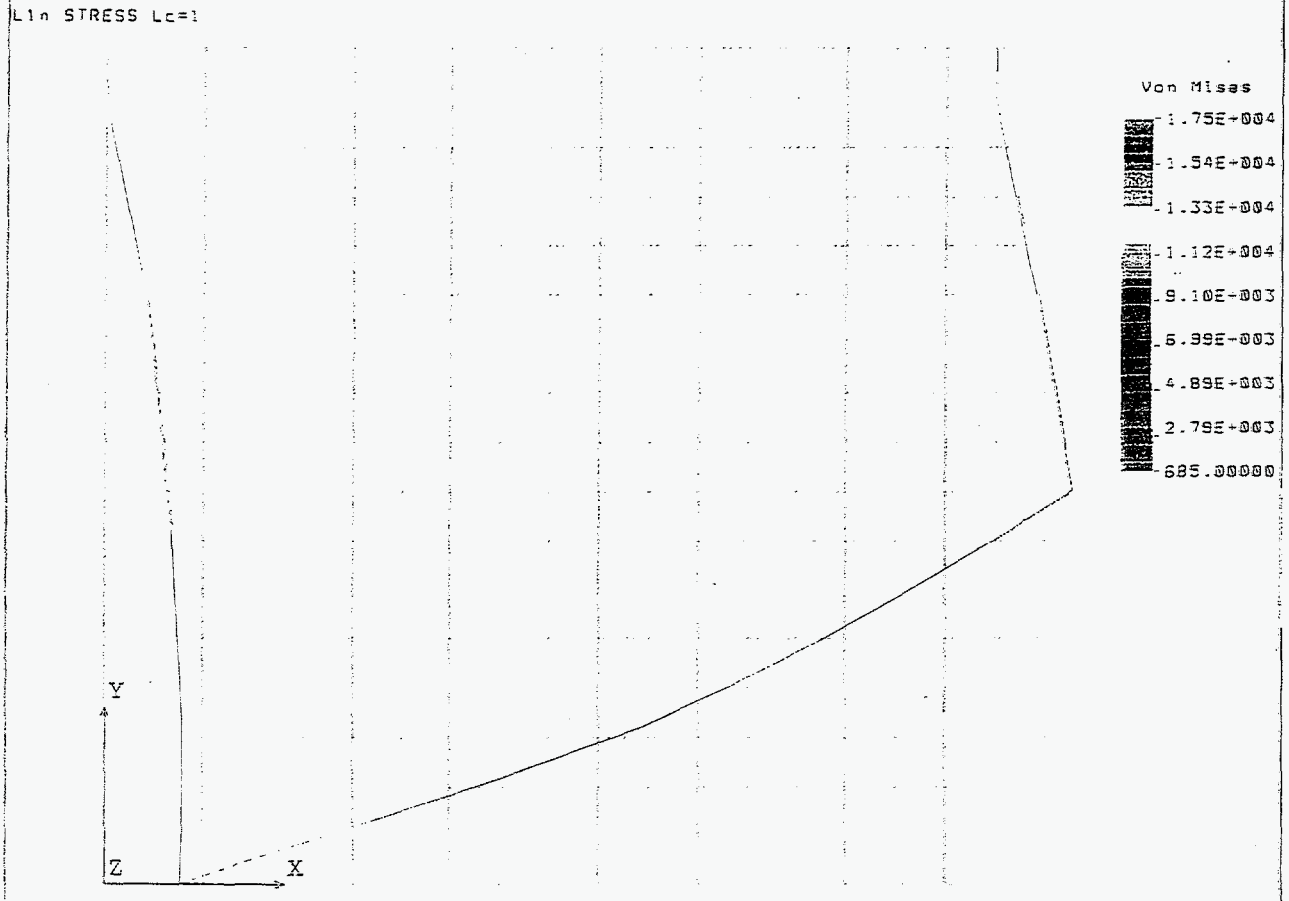

Appendix D - Vibration Frequency Data for RI-KI-01

Test Number	Description	Accelerometer Placement
0	Pretest with magnet pulsed	Top and side of magnet
1	Background noise	Top and side
2	Impulsed with mallet	Top and side
3	Impulsed with mallet	Top and side
4	Background noise	Side (measure disp. in x dir)
5	Impulsed with mallet	Side of magnet
6	Background noise	Top (measure disp. in y dir)
7	Impulsed with mallet	Top of magnet
8	Background noise	End (measure disp. in z dir)
9	Impulsed with mallet	Ends of magnet
10	Magnet pulsed @ 30Hz	Ends
11	Magnet pulsed @ 30Hz	Top
12	Magnet pulsed @ 30Hz	Side
13	Magnet pulsed @ 30Hz	I-beam and magnet side
14	Magnet pulsed @ 30Hz	I-beam and magnet top
15	Magnet pulsed @ 20Hz	Ends
16	Magnet pulsed @ 20Hz	Top
17	Magnet pulsed @ 20Hz	Side
18	Magnet pulsed @ 10Hz	Side
19	Magnet pulsed @ 10Hz	Top
20	Magnet pulsed @ 10Hz	End
21	Impulsed with mallet	End (same end meas. Phase)
22	Impulsed with mallet	Top (same end meas. Phase)
23	Impulsed with mallet	Side (meas. Phase diff.)
24	Magnet pulsed @ 20Hz	Side

Note: Test # written in bottom left-hand corner of each data sheet.

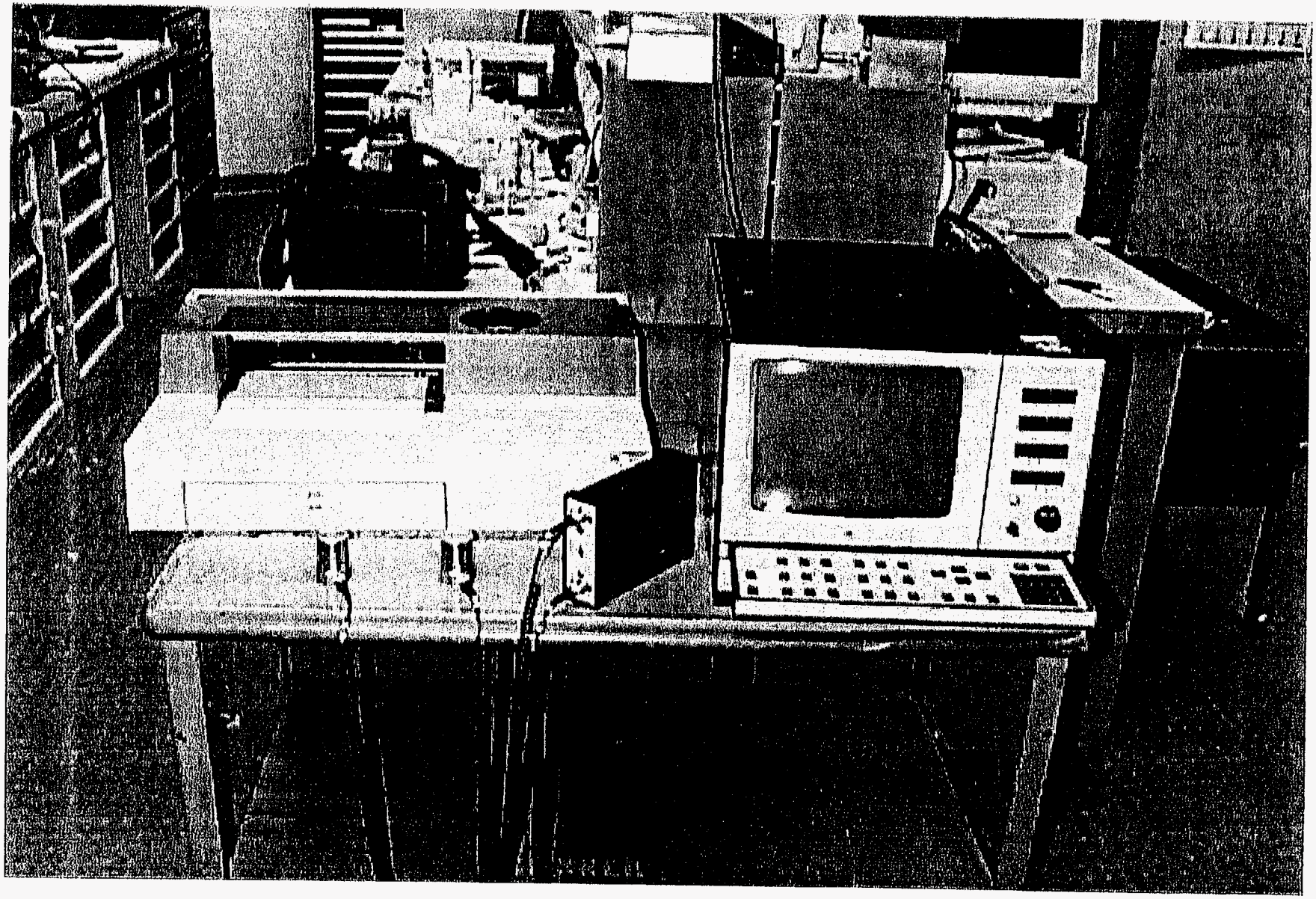

Bruel Kjær

Type 2034

Page No.
57

Sign.:

Meas.
Object:

Comments:

Test:a
magnet pulsed
@ 24 Hz

W2 AUTO SPEC CH.A
Y: 28.4mU /Hz PSD 80dB
X: 4Hz TO 400Hz LOG
SETUP W12 #A: 20

MAIN Y: 41.5E-9U /Hz
X: 201.5Hz

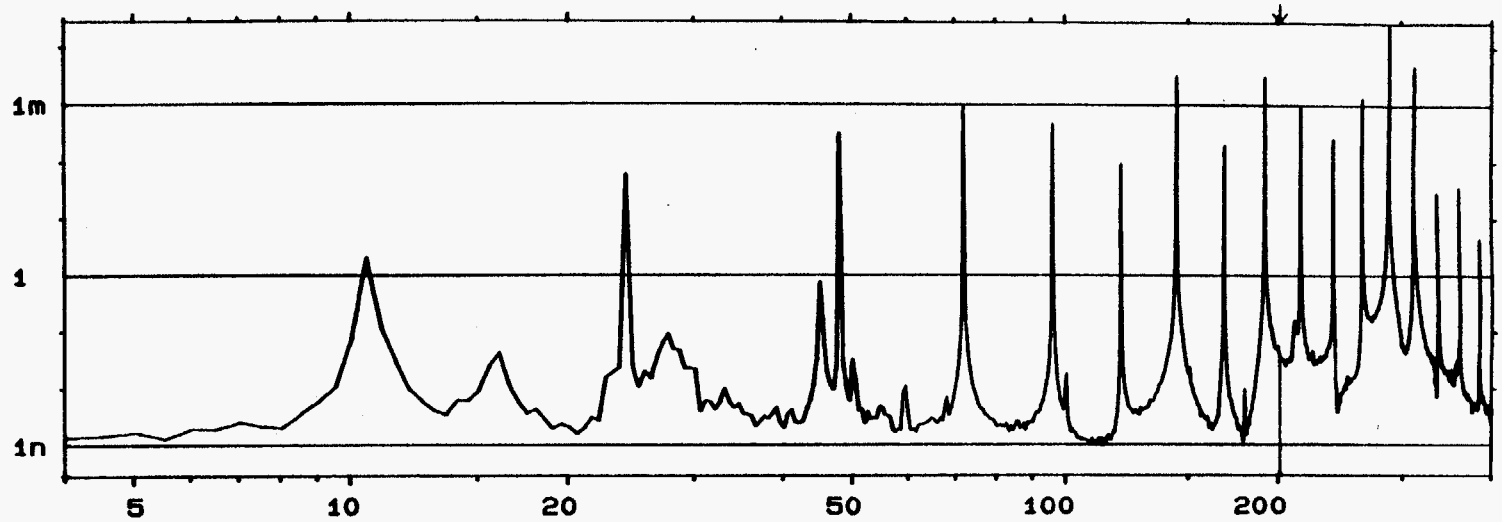

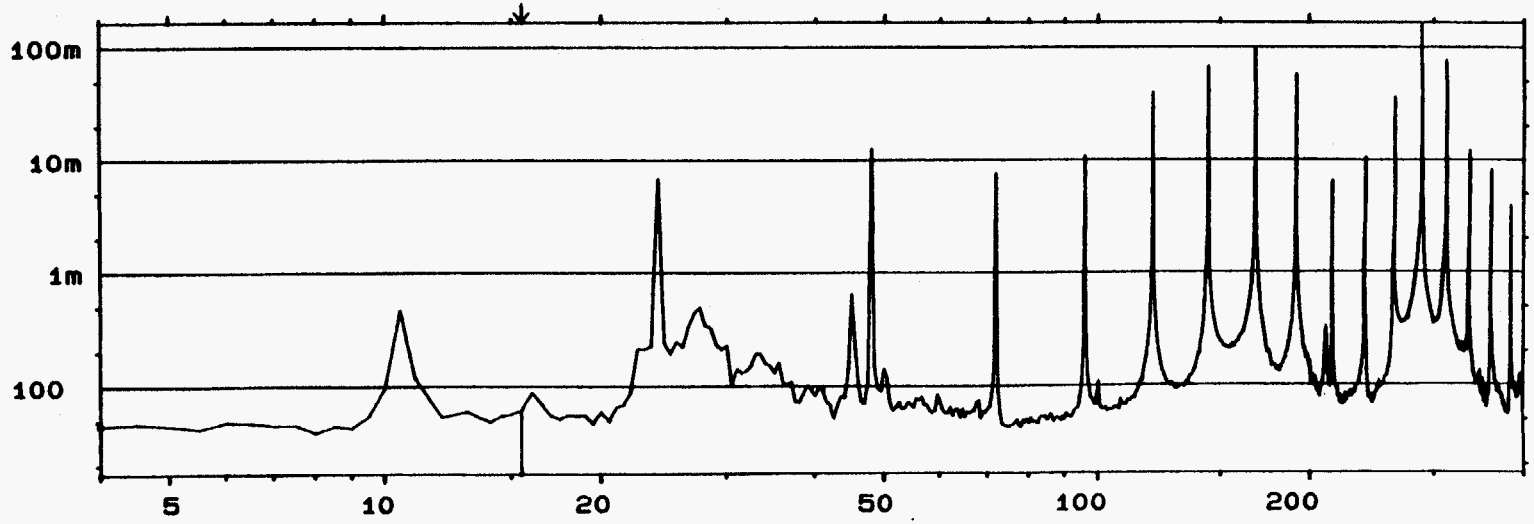

W2 AUTO SPEC CH.B
Y: 166mU RMS 80dB
X: 4Hz TO 400Hz LOG
SETUP W12 #A: 20

MAIN Y: 61.4 U
X: 15.5Hz

Brüel Kjær

Type 2034

Page No.
58

Sign.:

Meas.
Object:

Comments:

Test 1

W2 AUTO SPEC CH.B
Y: 10.3E-9U²/Hz PSD 40dB
X: 4Hz TO 400Hz LOG
#A: 20

MAIN Y: 59.7E-12U²/Hz
X: 15.5Hz

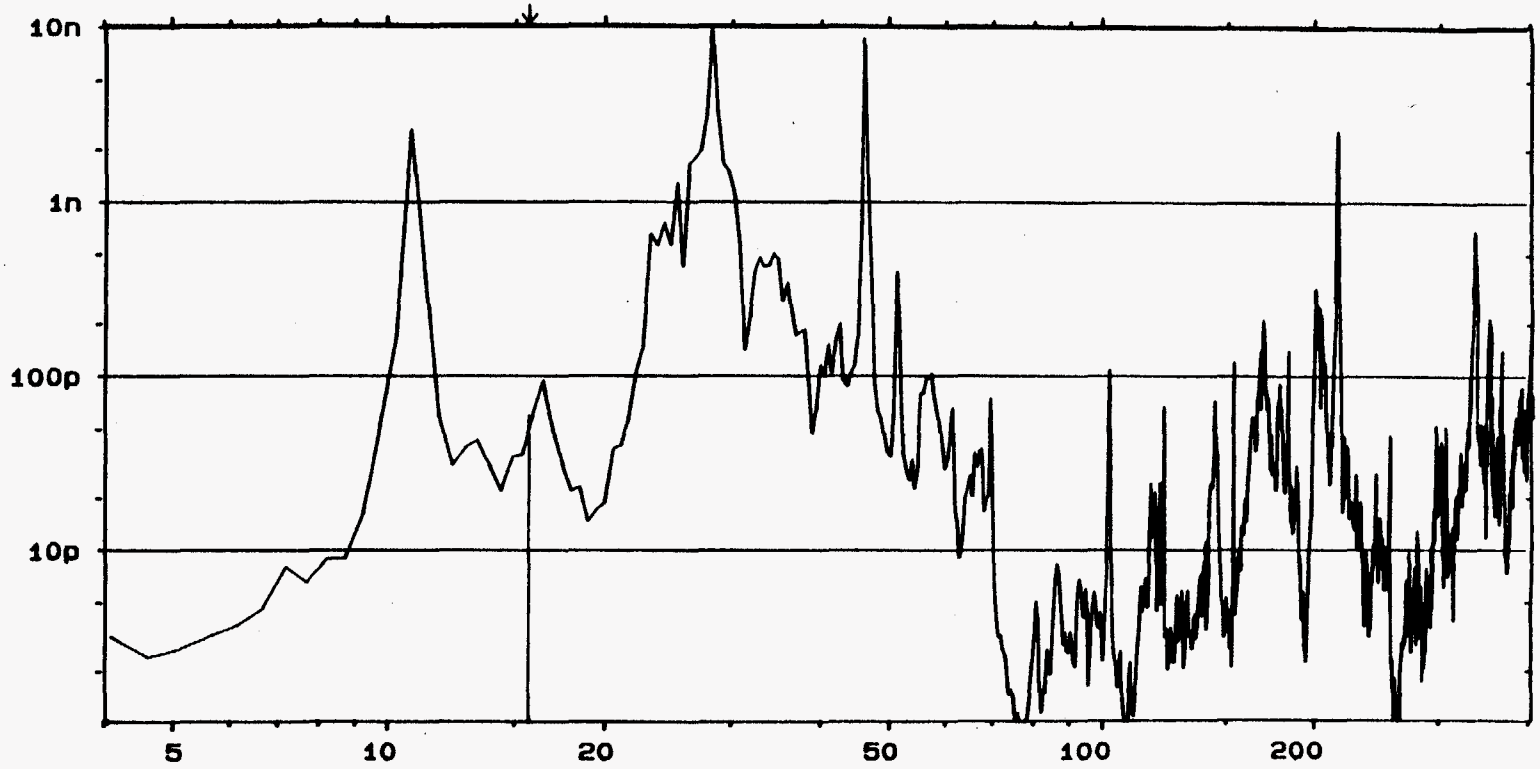

SETUP W12

MEASUREMENT:	DUAL SPECTRUM AVERAGING			
TRIGGER:	FREE RUN			
DELAY:	CH.A B: 0.00ms			
AVERAGING:	LIN 20	OVERLAP: 0%		
FREQ SPAN:	400Hz	F: 0.5Hz	T: 2s	T: 977 s
CENTER FREQ:	BASEBAND			
WEIGHTING:	RECTANGULAR			
CH.A:	300mV +	3Hz DIR	FILT: 25.6kHz	3.15V/G
CH.B:	400mV +	3Hz DIR	FILT: 25.6kHz	3.13V/G
GENERATOR:	VARIABLE SINE	OFF		

Bruel Kjær

Type 2034

Page No.
59

Sign.:

Meas.
Object:

Comments:

Test

W2 AUTO SPEC CH.A [ ] INPUT MAIN Y: 14.8E-12U²/Hz
Y: 12.3E-9U²/Hz PSD 40dB X: 201.5Hz
X: 4Hz TO 400Hz LOG
SETUP W12 #A: 20

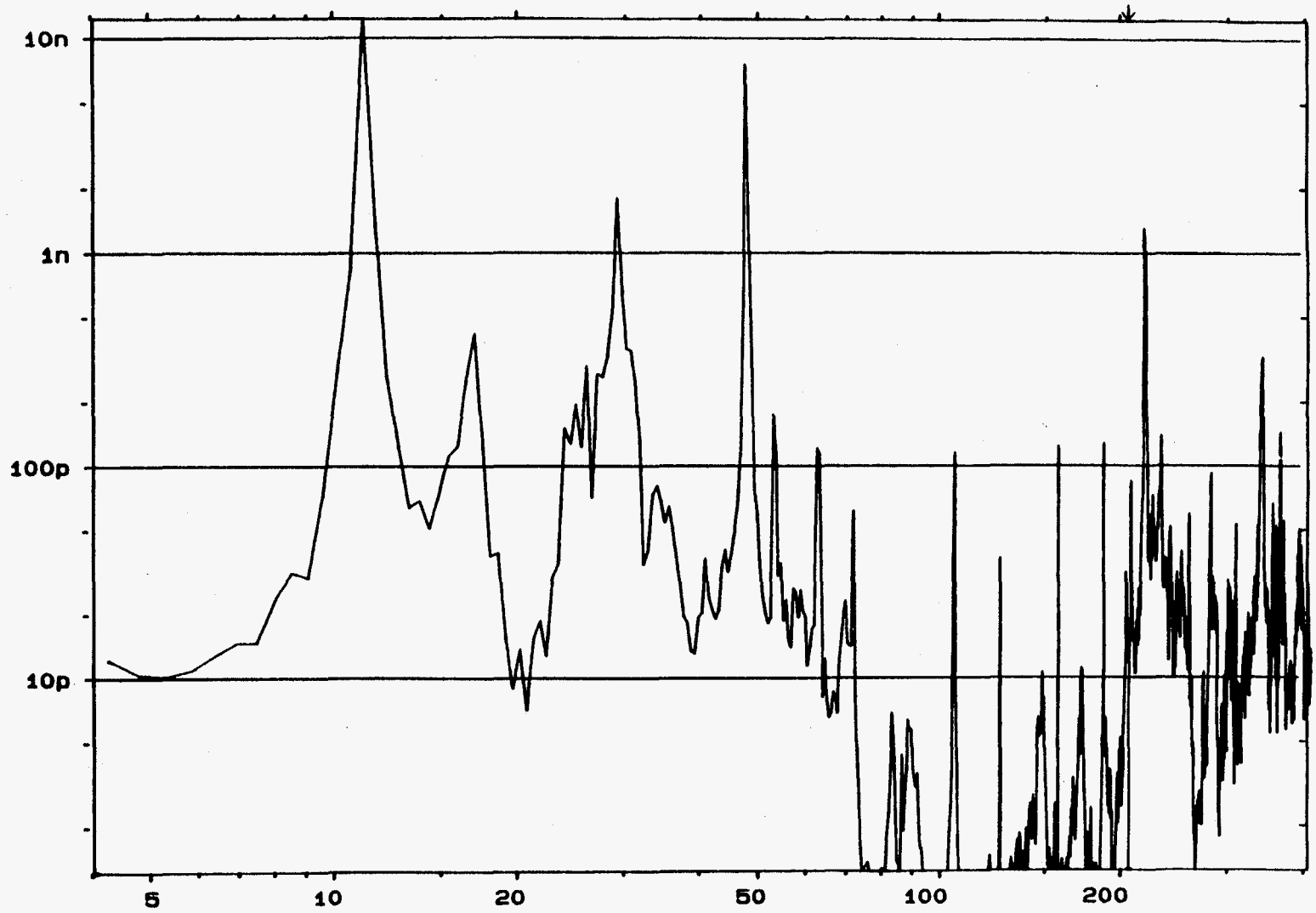

Bruel Kjær

Type 2034

Page No.
60

Sign.:

Meas.
Object:

Comments:

Test 1

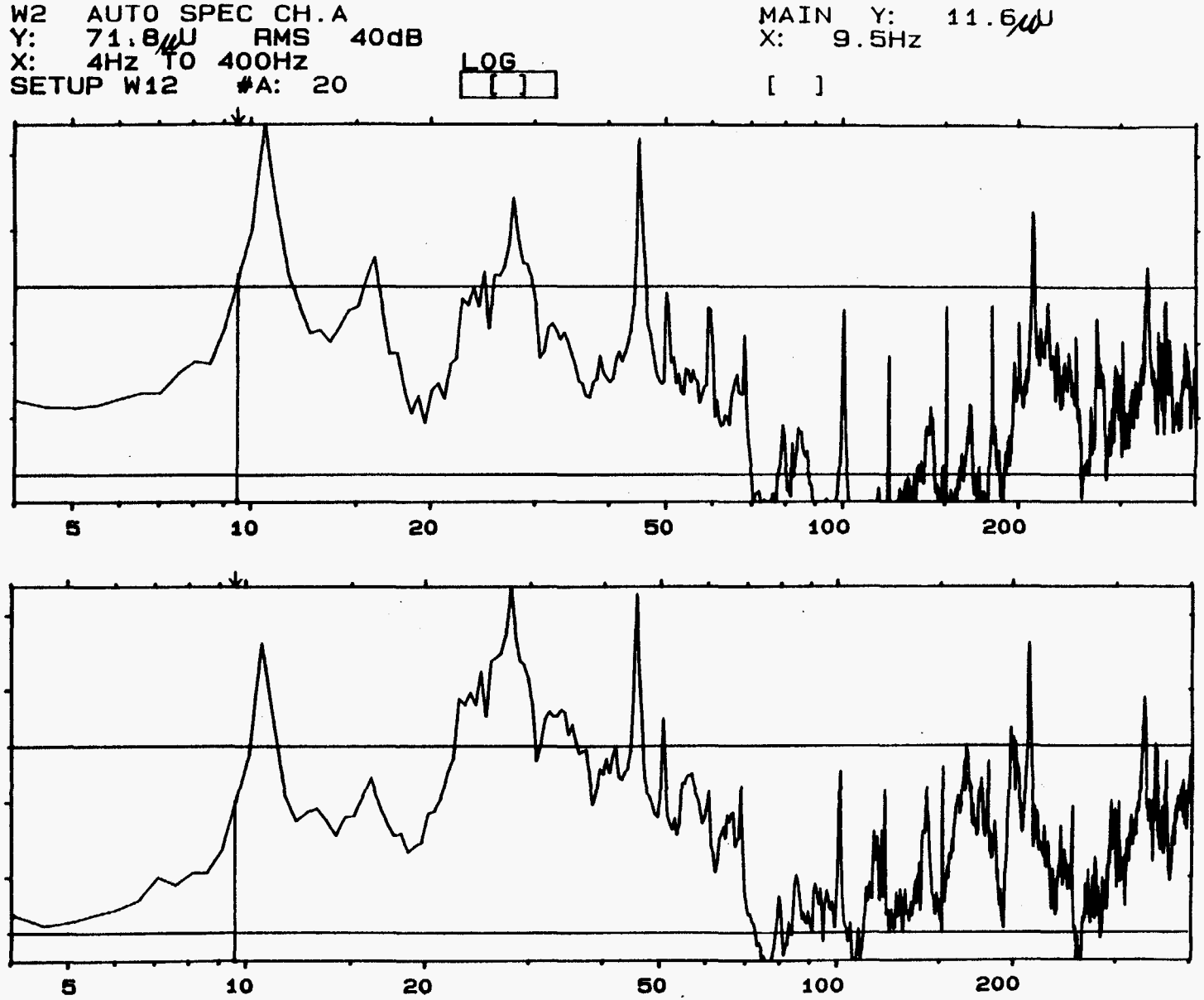

Bruel Kjær

Type 2034

Page No.
61

Sign.:

Meas.
Object:

Comments:

Test #1

W2 AUTO SPEC CH.A
Y: 5.15E-9U²/Hz PSD 40dB
X: 4Hz TO 400Hz LOG
SETUP W12 #A: 20

MAIN Y: 252E-12U²/Hz
X: 15.5Hz

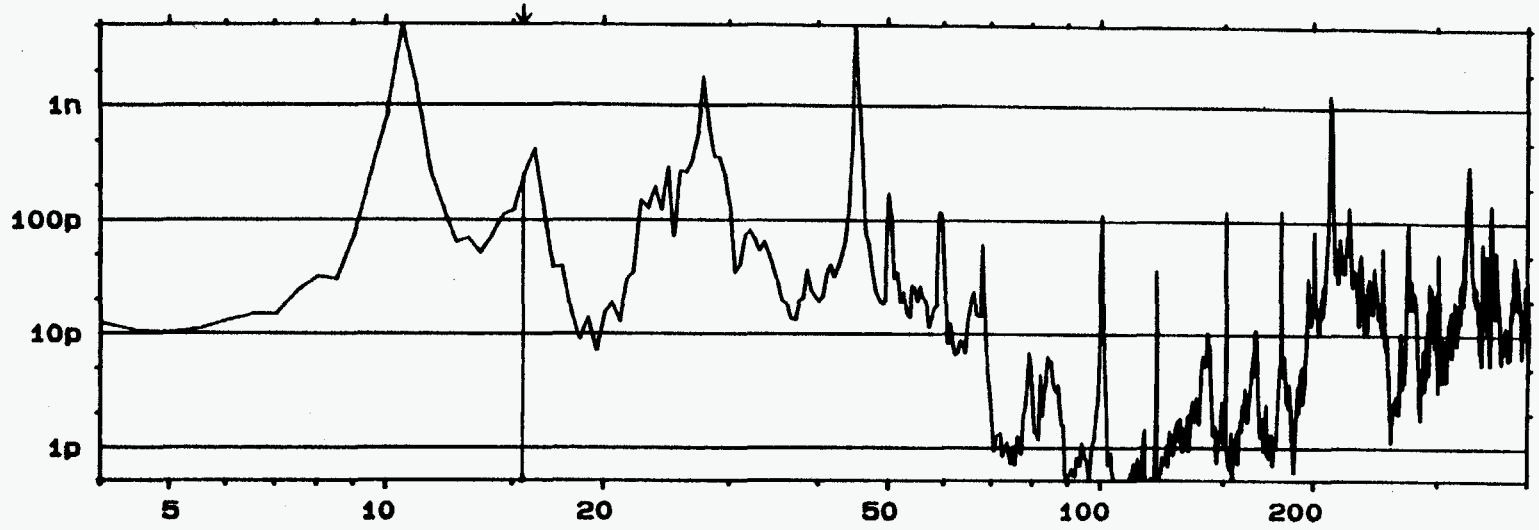

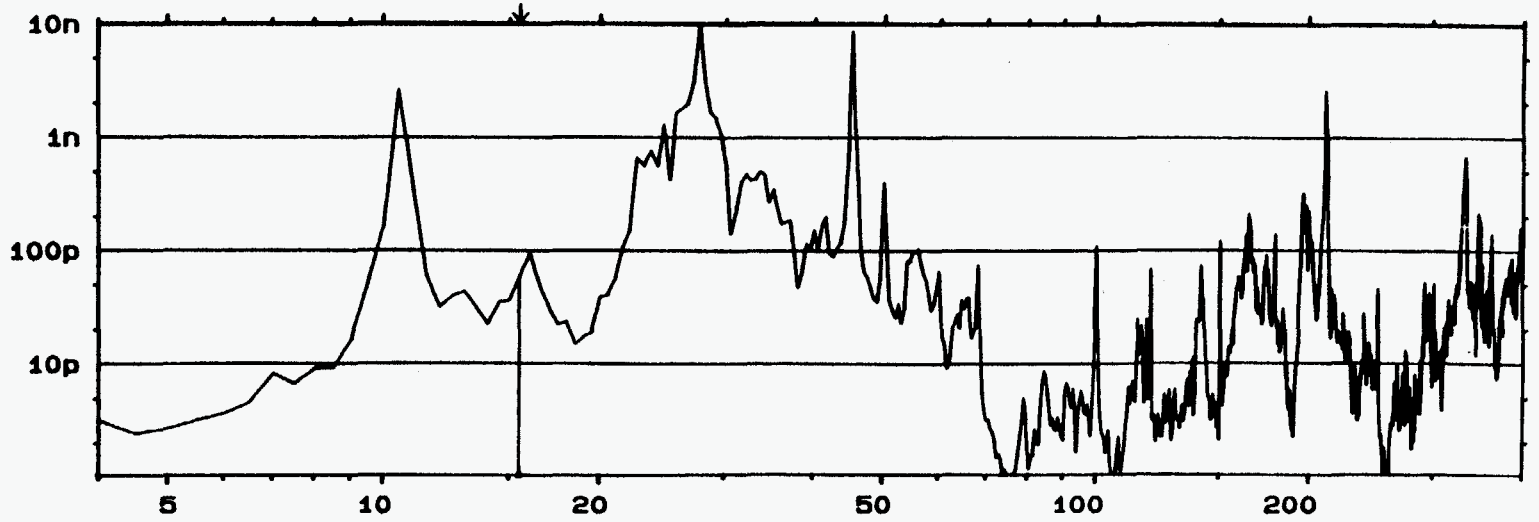

W2 AUTO SPEC CH.B
Y: 10.3E-9U²/Hz PSD 40dB
X: 4Hz TO 400Hz LOG
SETUP W12 #A: 20

MAIN Y: 59.7E-12U²/Hz
X: 15.5Hz

Bruel Kjær

Type 2034

Page No.
62

Sign.:

Meas.
Object:

Comments:

Test 2

W2 AUTO SPEC CH.A
Y: 6.04 U /Hz PSD 40dB
X: 4Hz TO 400Hz LOG
SETUP W12 #A: 10

MAIN Y: 5.18 U /Hz
X: 15.5Hz

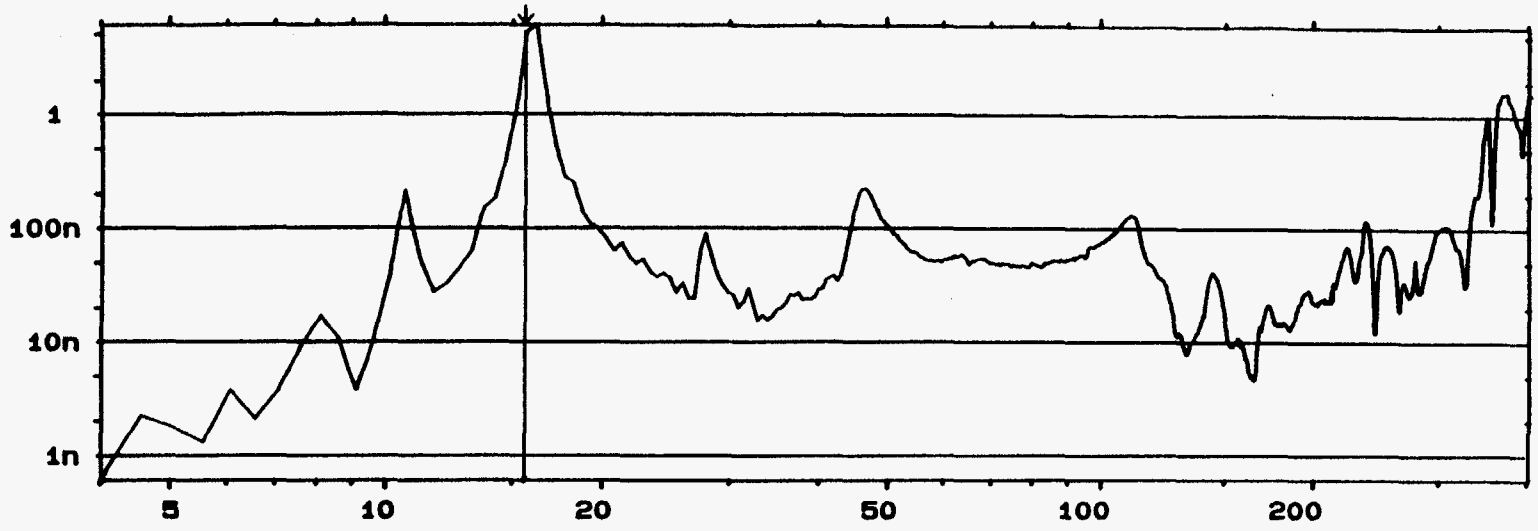

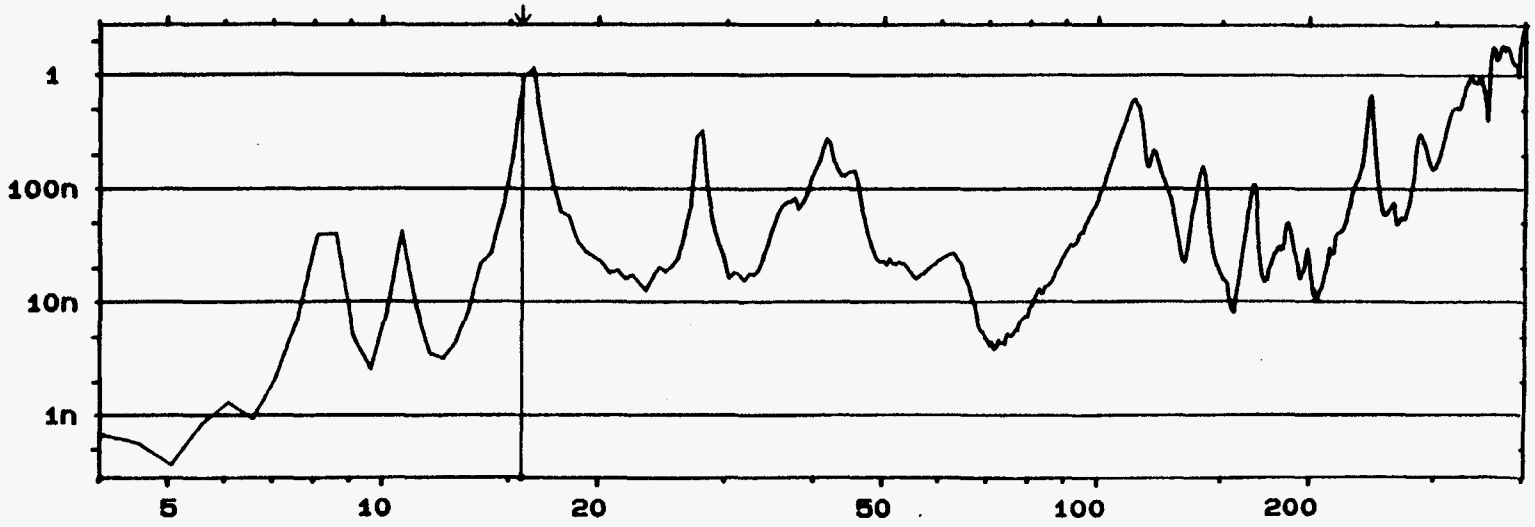

W2 AUTO SPEC CH.B
Y: 2.81 U /Hz PSD 40dB
X: 4Hz TO 400Hz LOG
SETUP W12 #A: 10

MAIN Y: 957E-9U /Hz
X: 15.5Hz

Bruel Kjær

Type 2034

Page No.
63

Sign.:

Meas.
Object:

Comments:

Test #3

W2 AUTO SPEC CH.A [ ] INPUT MAIN Y: 852E-9U /Hz
Y: 30.2 U /Hz PSD 40dB X: 15.5Hz
X: 4Hz TO 400Hz LOG
SETUP W12 #A: 10

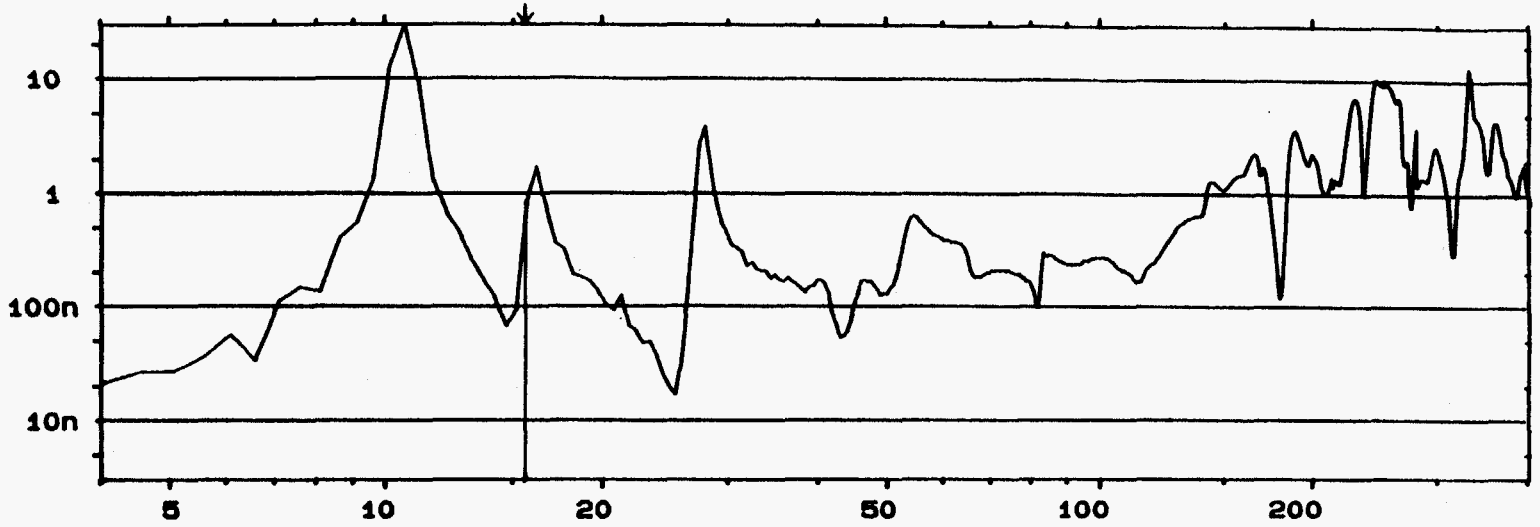

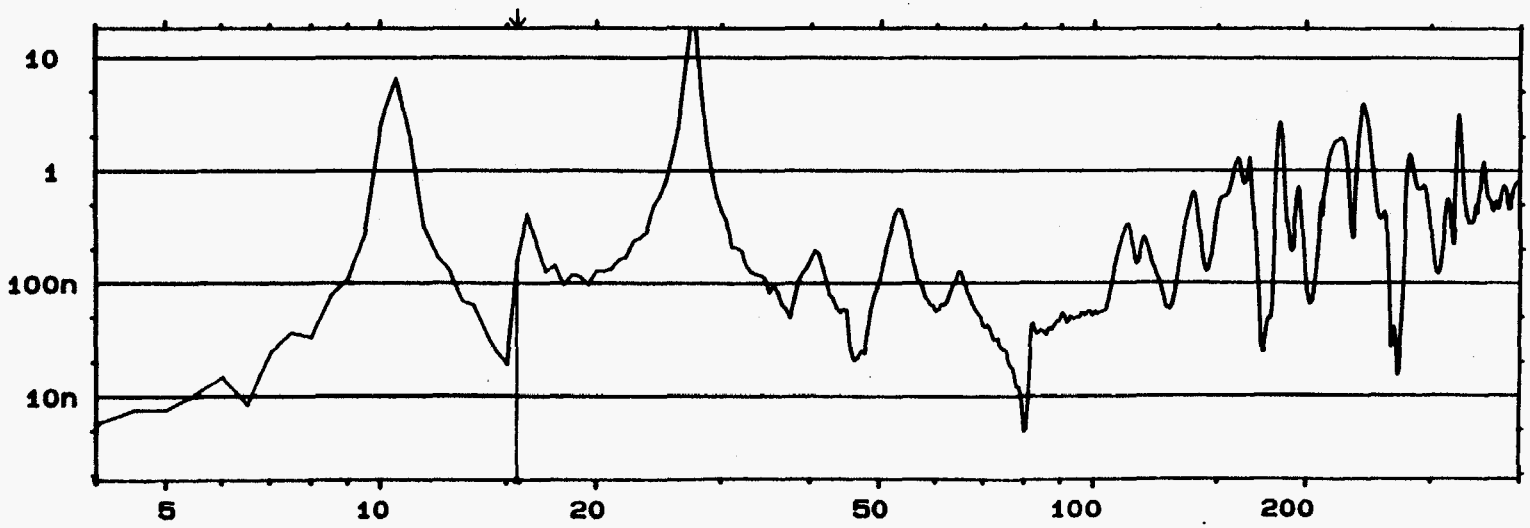

W2 AUTO SPEC CH.B MAIN Y: 158E-9U /Hz
Y: 18.1 U /Hz PSD 40dB X: 15.5Hz
X: 4Hz TO 400Hz LOG
SETUP W12 #A: 10

Bruel Kjær

Type 2034

Page No.
64

Sign.:

Meas.
Object:

Comments:

Test 4

W2 AUTO SPEC CH.A
Y: 21.4E-9U /Hz PSD 40dB
X: 4Hz TO 400Hz LOG
SETUP W12 #A: 20

MAIN Y: 300E-12U /Hz
X: 15.5Hz

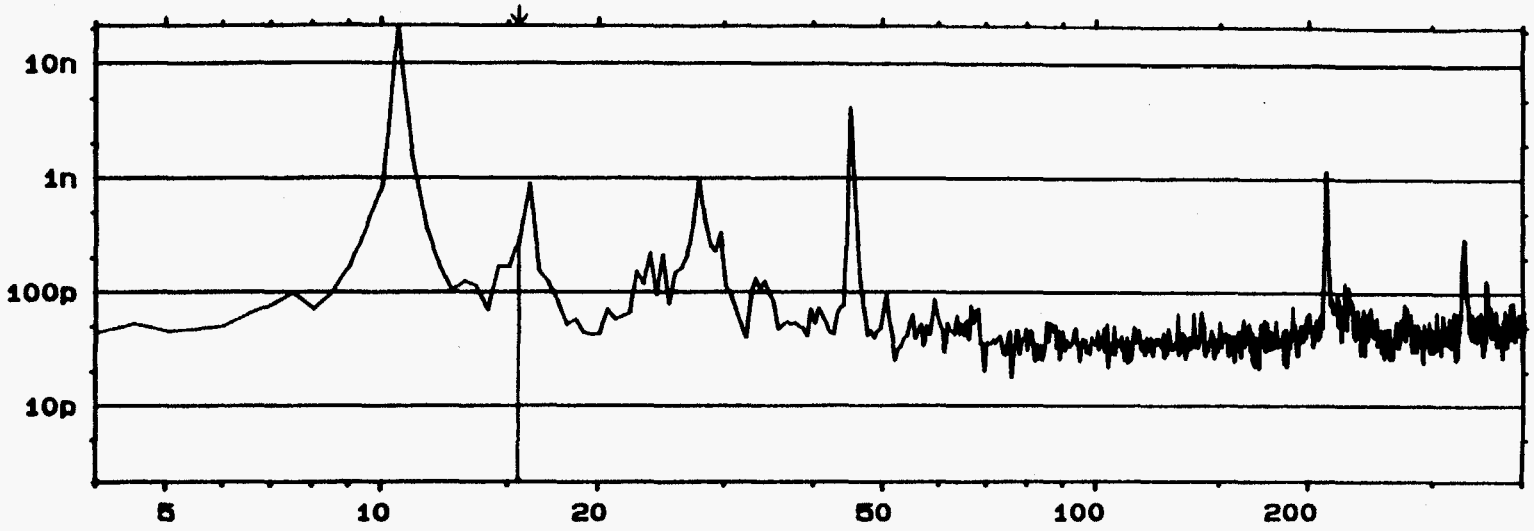

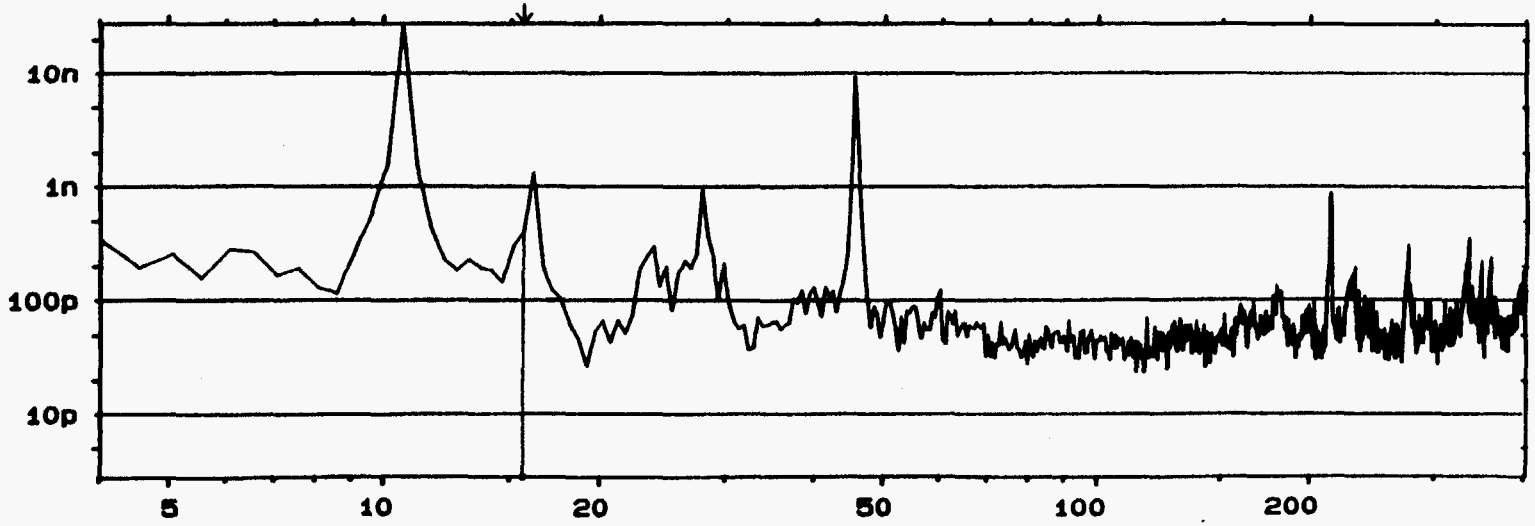

W2 AUTO SPEC CH.B
Y: 27.6E-9U /Hz PSD 40dB
X: 4Hz TO 400Hz LOG
SETUP W12 #A: 20

MAIN Y: 403E-12U /Hz
X: 15.5Hz

Bruel Kjær

Type 2034

Page No.
65

Sign.:

Meas.
Object:

Comments:

Test 6

W2 AUTO SPEC CH.A
Y: 33.8 U /Hz PSD 40dB
X: 4Hz TO 400Hz LOG
SETUP W12 #A: 10

MAIN Y: 380E-9U /Hz
X: 15.5Hz

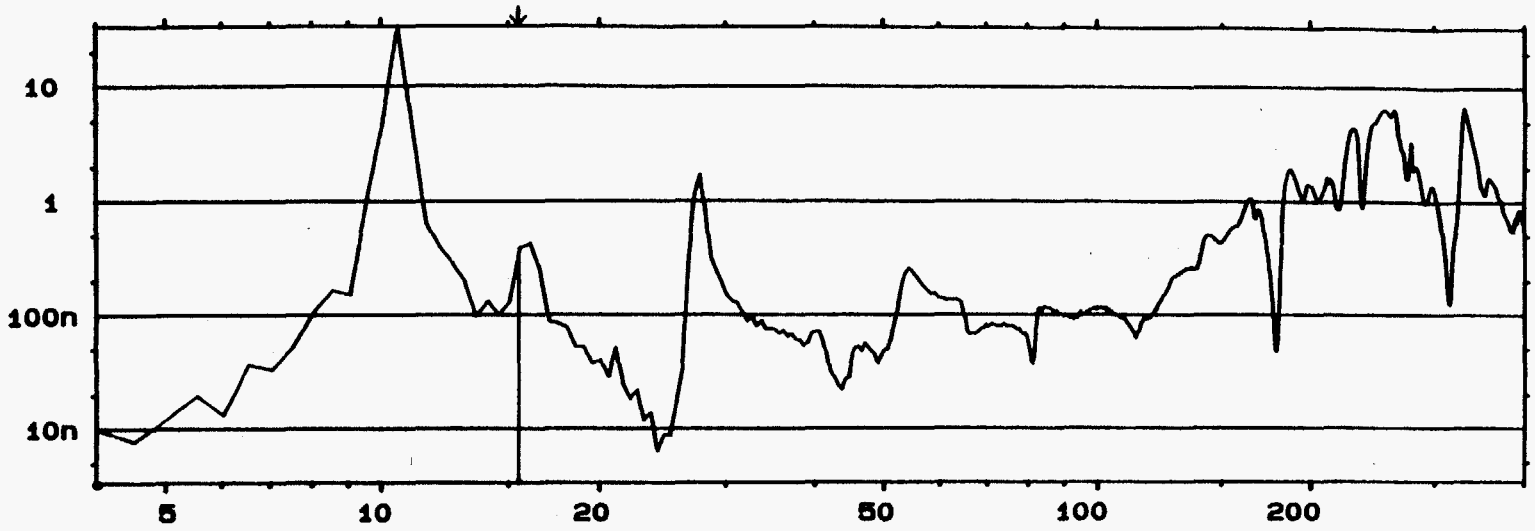

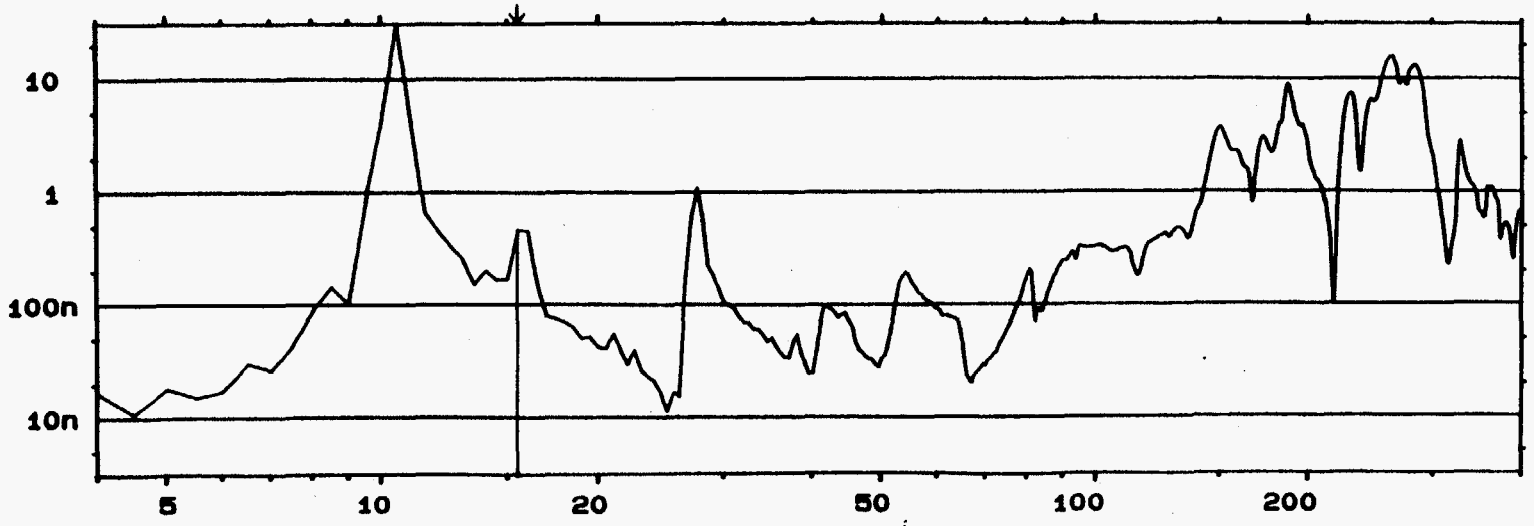

W2 AUTO SPEC CH.B
Y: 31.2 U /Hz PSD 40dB
X: 4Hz TO 400Hz LOG
SETUP W12 #A: 10

MAIN Y: 462E-9U /Hz
X: 15.5Hz

Bruel Kjær

Type 2034

Page No.
66

Sign.:

Meas.
Object:

Comments:
Test 6

W2 AUTO SPEC CH.A
Y: 14.4E-9U /Hz PSD 40dB
X: 4Hz TO 400Hz LOG
SETUP W12 #A: 20

MAIN Y: 93.9E-12U /Hz
X: 15.5Hz

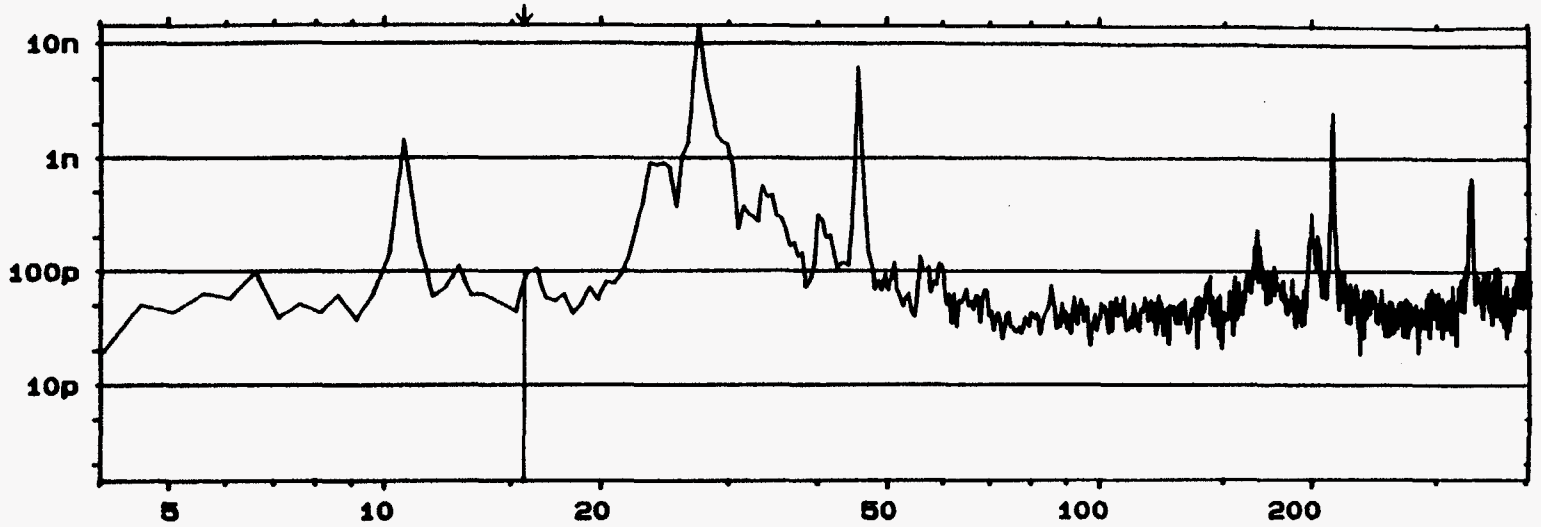

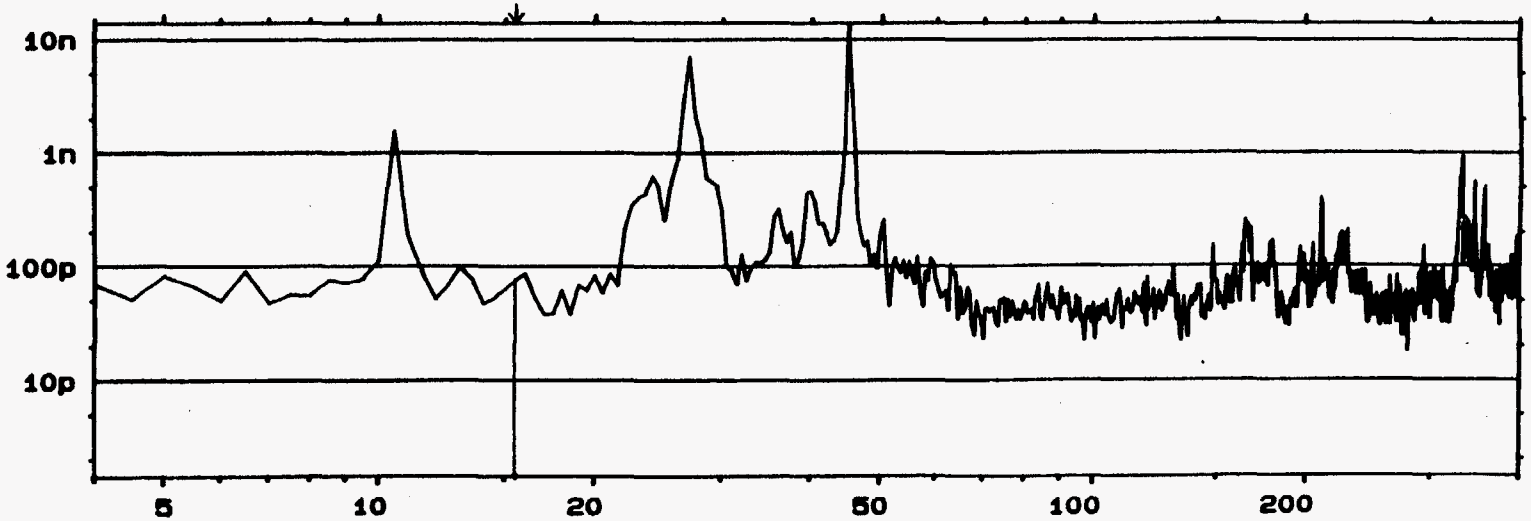

W2 AUTO SPEC CH.B
Y: 14.0E-9U /Hz PSD 40dB
X: 4Hz TO 400Hz LOG
SETUP W12 #A: 20

MAIN Y: 75.6E-12U /Hz
X: 15.5Hz

Bruel Kjaer

Type 2034

Page No.
67

Sign.:

Meas.
Object:

Comments:

KS2#7

W2 AUTO SPEC CH.A
Y: 17.0 U /Hz PSD 40dB
X: 4Hz TO 400Hz LOG
SETUP W12 #A: 10

MAIN Y: 54.1E-9U /Hz
X: 23.0Hz

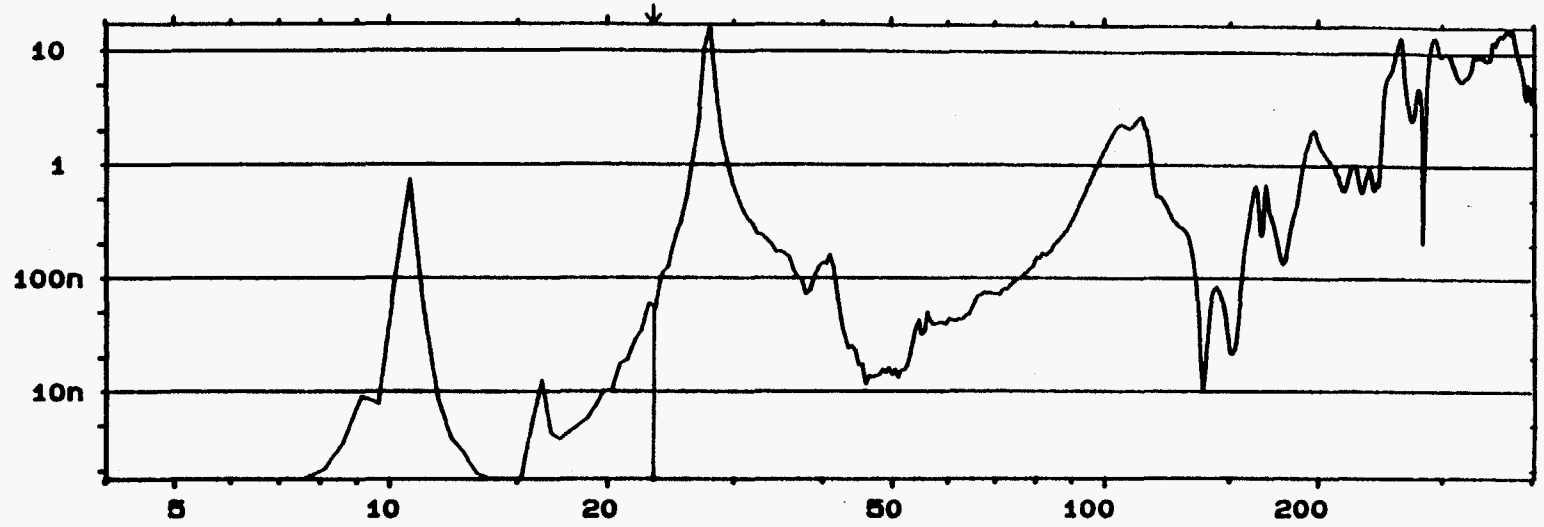

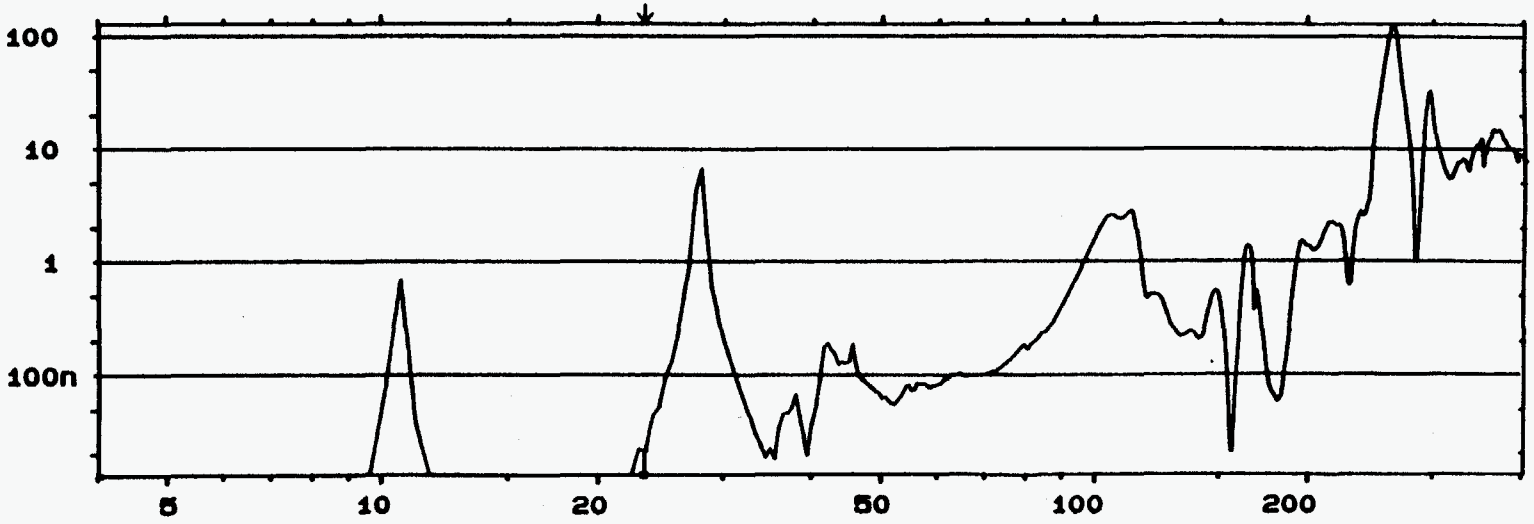

W2 AUTO SPEC CH.B
Y: 129 U /Hz PSD 40dB
X: 4Hz TO 400Hz LOG
SETUP W12 #A: 10

MAIN Y: 21.0E-9U /Hz
X: 23.0Hz

Bruel Kjær

Type 2034

Page No.
68

Sign.:

Meas.
Object:

Comments:

Test 7

W2 1/FREQ RESP H2 PHASE
Y: -200 TO +200 DEG
X: 4Hz TO 400Hz LOG
SETUP W12 #A: 10

MAIN Y:
X: 23.0Hz

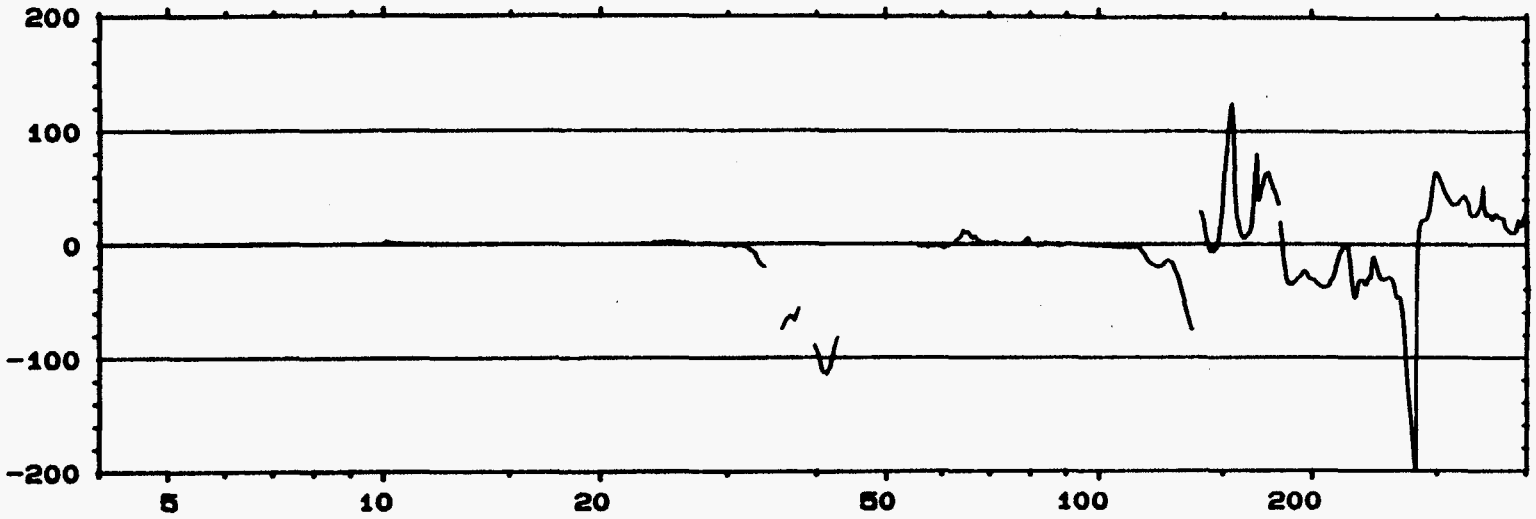

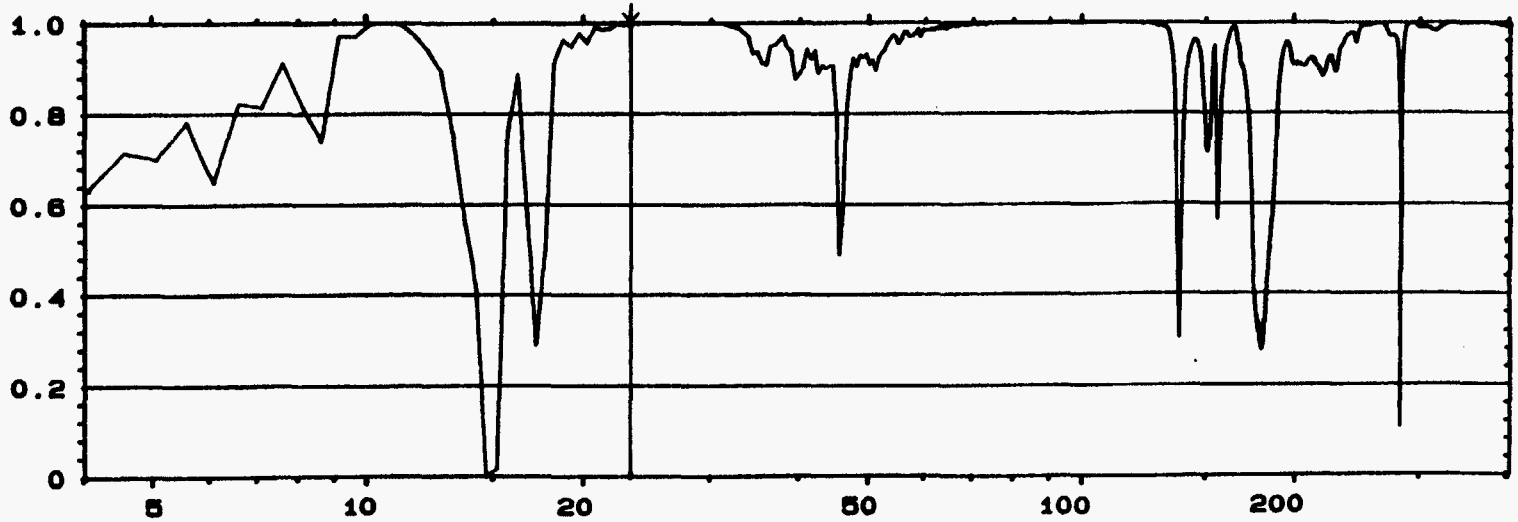

W2 COHERENCE
Y: 1.00
X: 4Hz TO 400Hz LOG
SETUP W12 #A: 10

INPUT

MAIN Y: 996m
X: 23.0Hz

Bruel Kjaer

Type 2034

Page No.
69

Sign.:

Meas.
Object:

Comments:

Test 8

W2 AUTO SPEC CH.A
Y: 3.31E-9U /Hz PSD 40dB
X: 4Hz TO 400Hz LOG
SETUP W12 #A: 20

MAIN Y: 38.3E-12U /Hz
X: 23.0Hz

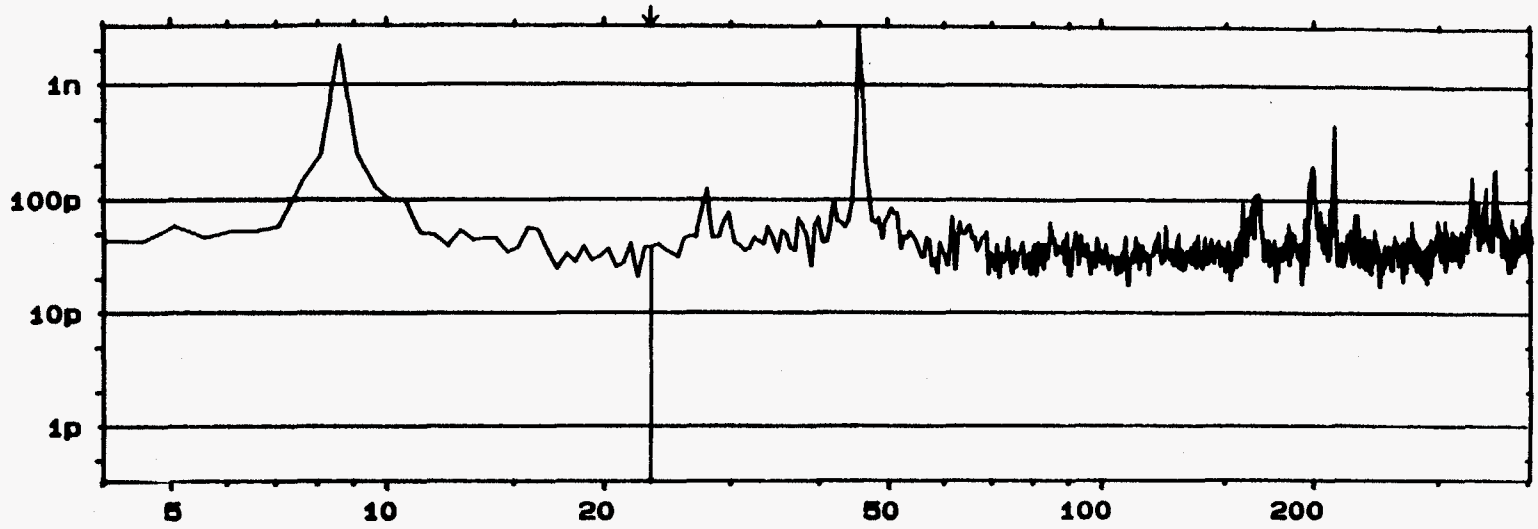

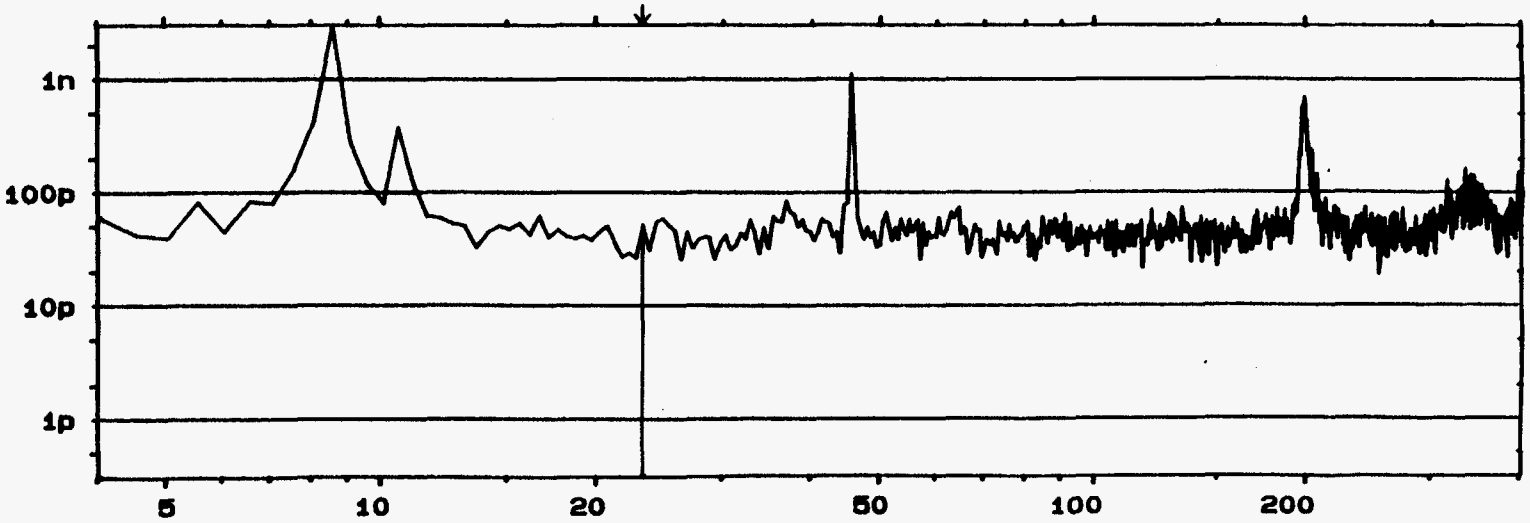

W2 AUTO SPEC CH.B
Y: 3.04E-9U /Hz PSD 40dB
X: 4Hz TO 400Hz LOG
SETUP W12 #A: 20

MAIN Y: 50.8E-12U /Hz
X: 23.0Hz

Bruel Kjær

Type 2034

Page No.
70

Sign.:

Meas.
Object:

Comments:

Test #9

W2 AUTO SPEC CH.A [ ] INPUT MAIN Y: 11.8E-9U /Hz
Y: 7.73 U /Hz PSD 40dB X: 23.0Hz
X: 4Hz TO 400Hz LOG
SETUP W12 #A: 10

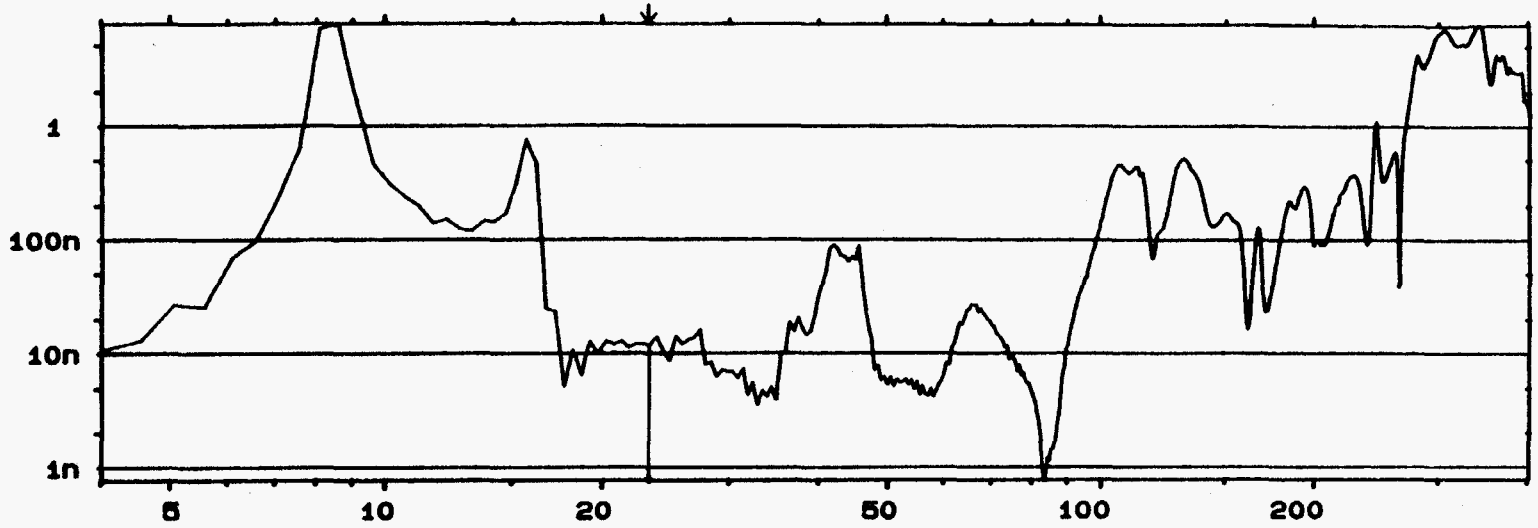

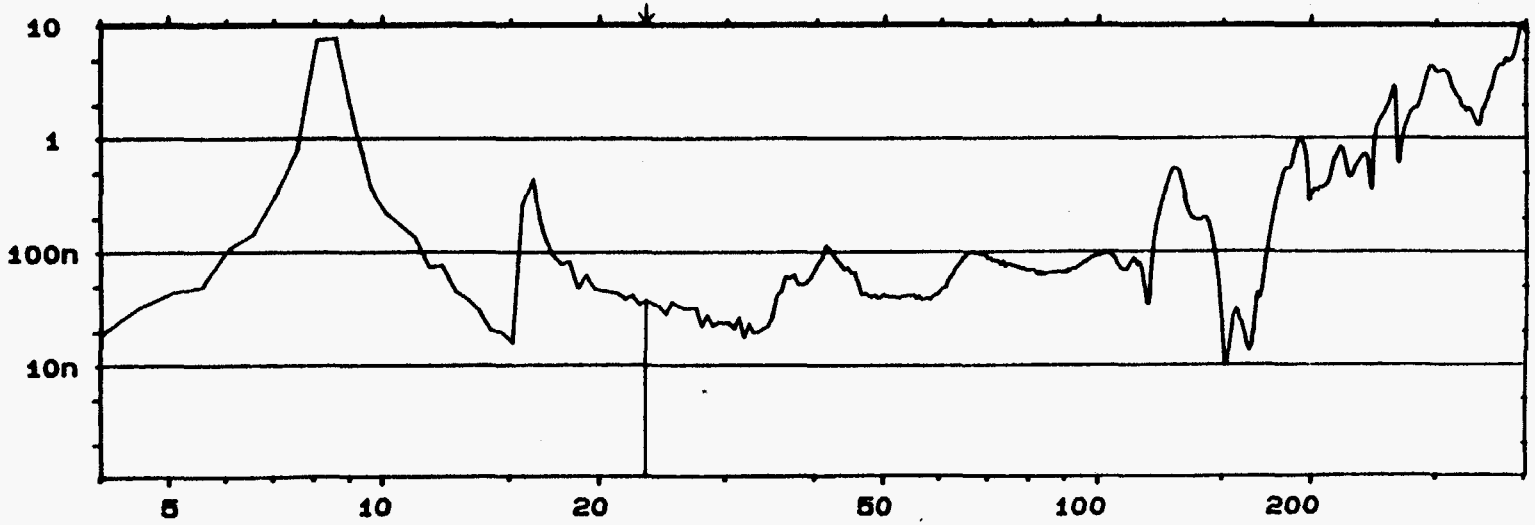

W2 AUTO SPEC CH.B
Y: 10.4 U /Hz PSD 40dB
X: 4Hz TO 400Hz LOG
SETUP W12 #A: 10

MAIN Y: 36.6E-9U /Hz
X: 23.0Hz

Bruel Kjaer

Type 2034

Page No.
71

Sign.:

Meas.
Object:

Comments:

Test 10

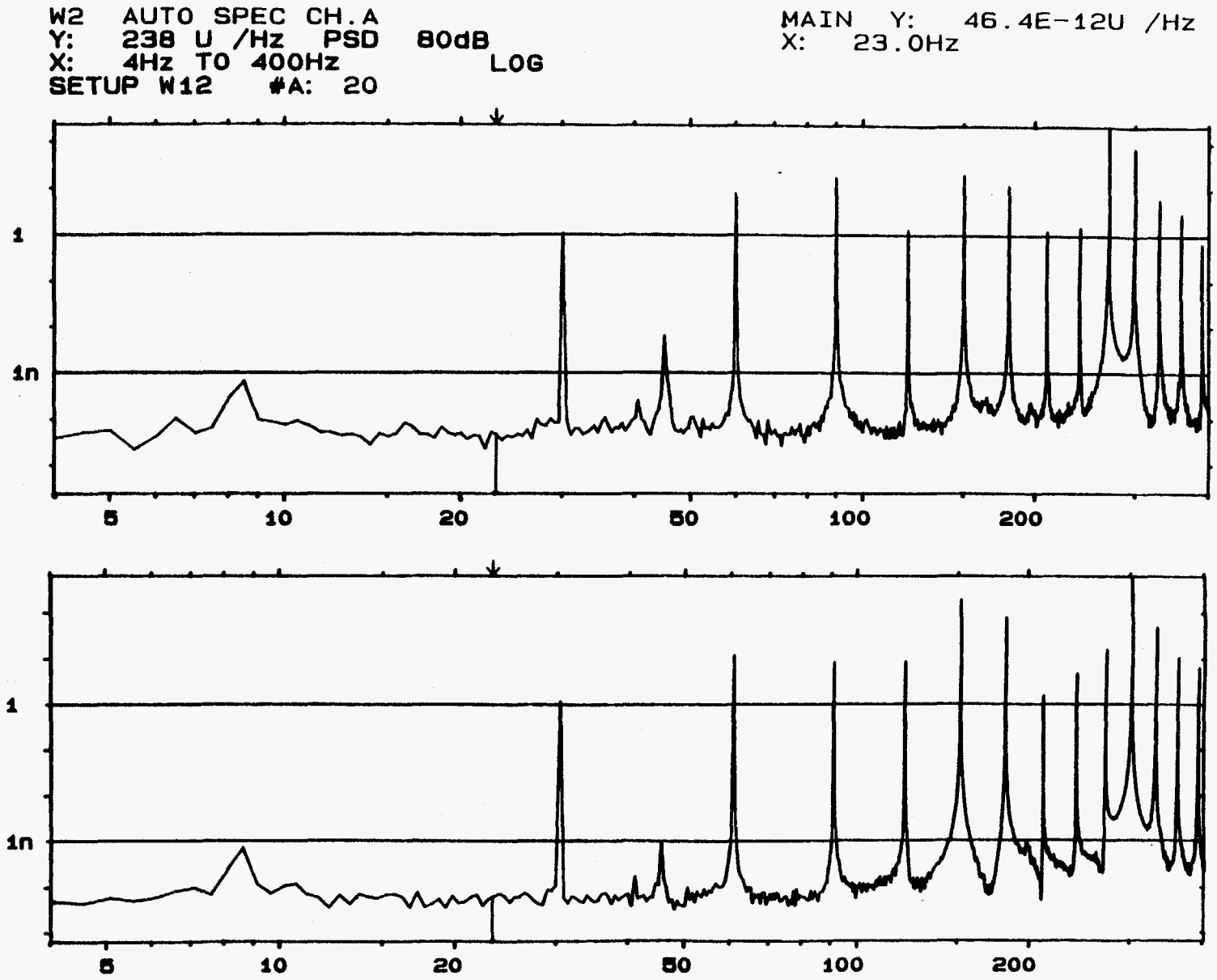

Bruel Kjær

)e 2034

Page No.
72

Sign.:

Meas.
Object:

Comments:

Test 11

W2 AUTO SPEC CH.A
Y: 298 U /Hz PSD 80dB
X: 4Hz TO 400Hz LOG
SETUP W12 #A: 20

MAIN Y: 1.01E-9U /Hz
X: 23.0Hz

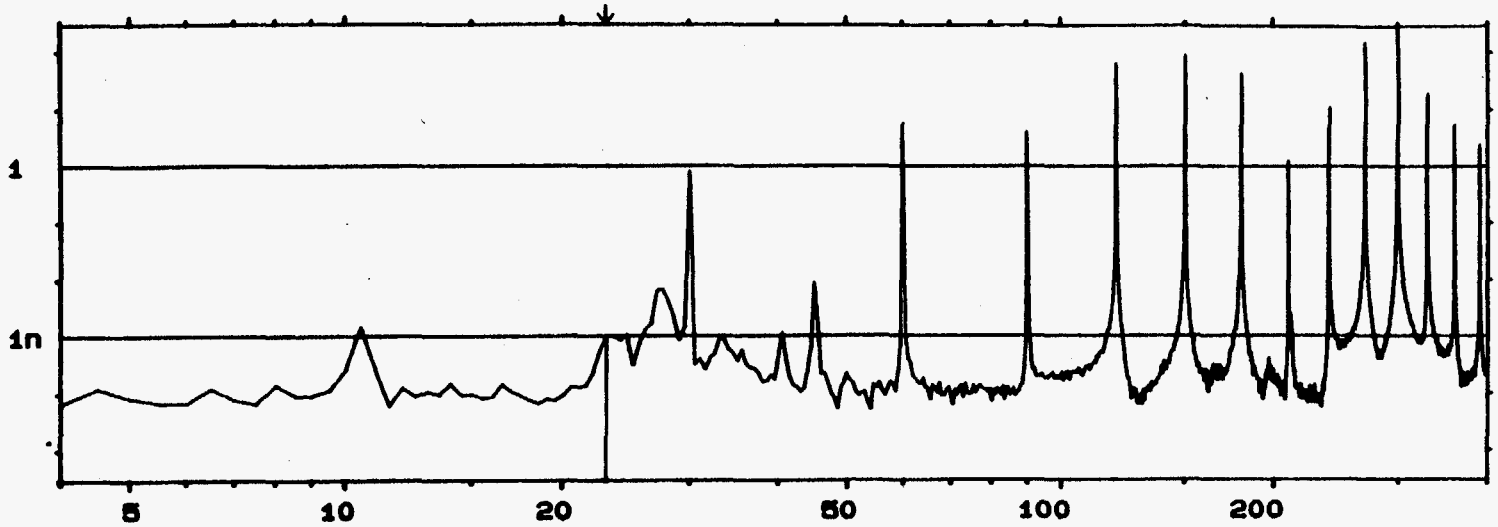

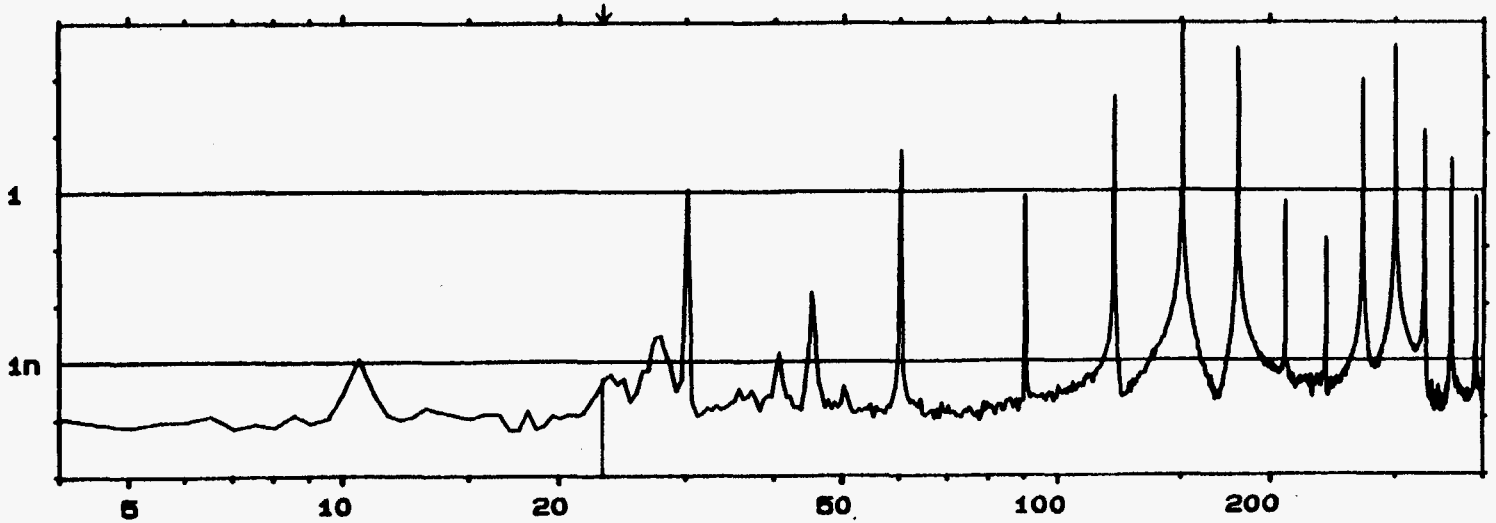

W2 AUTO SPEC CH.B
Y: 965 U /Hz PSD 80dB
X: 4Hz TO 400Hz LOG
SETUP W12 #A: 20

MAIN Y: 478E-12U /Hz
X: 23.0Hz

Bruel Kjaer

Type 2034

Page No.
73

Sign.:

Meas.
Object:

Comments:

Test 11

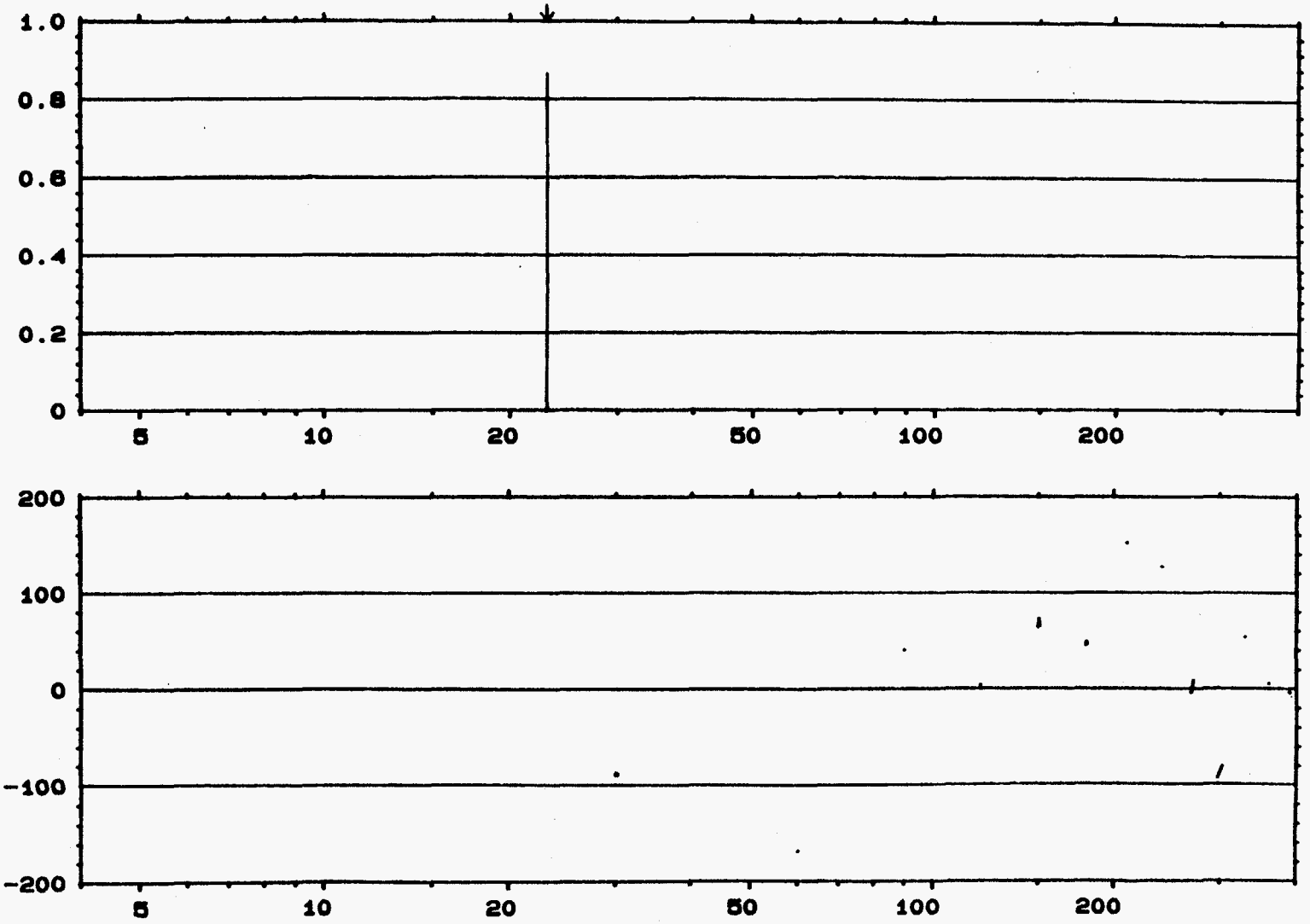

Bruel Kjær

Type 2034

Page No.
74

Sign.:

Meas.
Object:

Comments:

Test 12

W2 AUTO SPEC CH.A [ ] INPUT MAIN Y: 219E-12U /Hz
Y: 101 U /Hz PSD 80dB X: 23.0Hz
X: 4Hz TO 400Hz LOG
SETUP W12 #A: 20

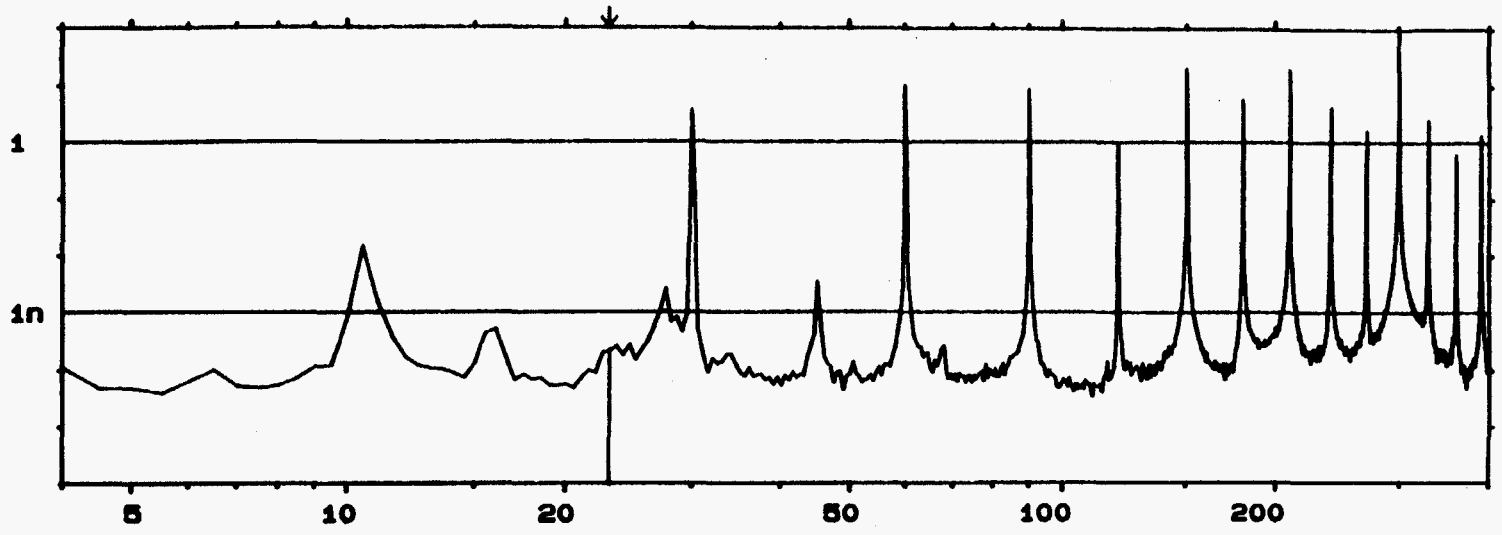

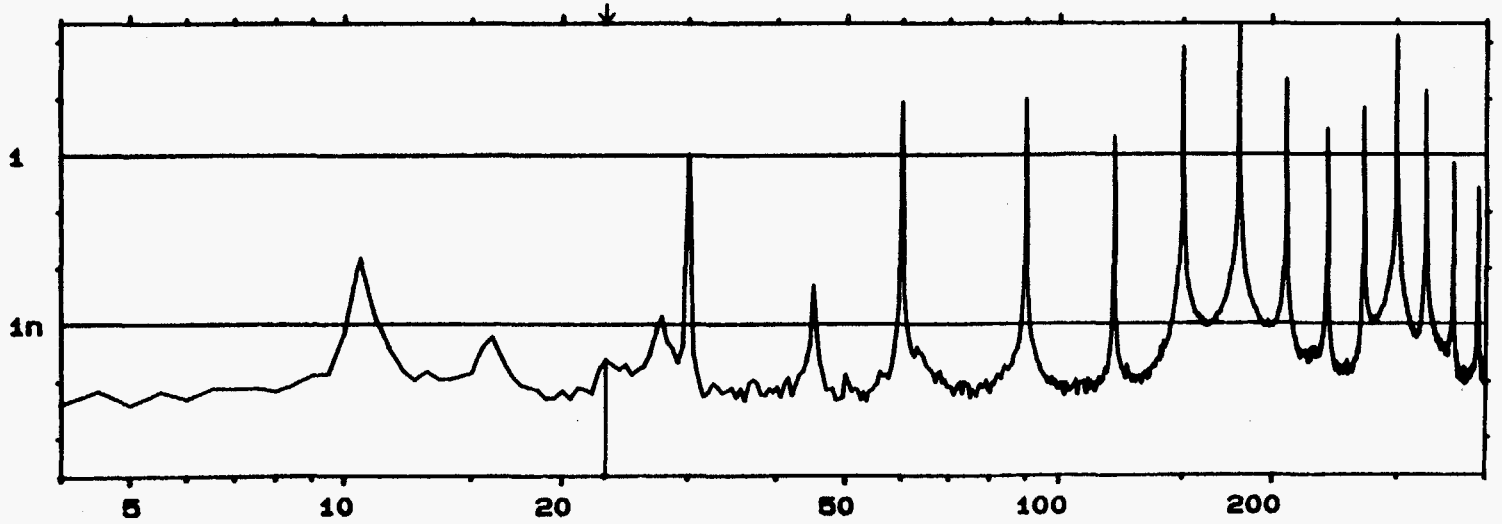

W2 AUTO SPEC CH.B
Y: 210 U /Hz PSD 80dB
X: 4Hz TO 400Hz LOG
SETUP W12 #A: 20

MAIN Y: 239E-12U /Hz
X: 23.0Hz

Bruel Kjaer

Type 2034

Page No.
75

Sign.:

Meas.
Object:

Comments:

Test 13

W2 AUTO SPEC CH.A
Y: 1.17mU /Hz PSD 80dB
X: 4Hz TO 400Hz LOG
SETUP W12 #A: 20

MAIN Y: 184E-12U /Hz
X: 23.0Hz

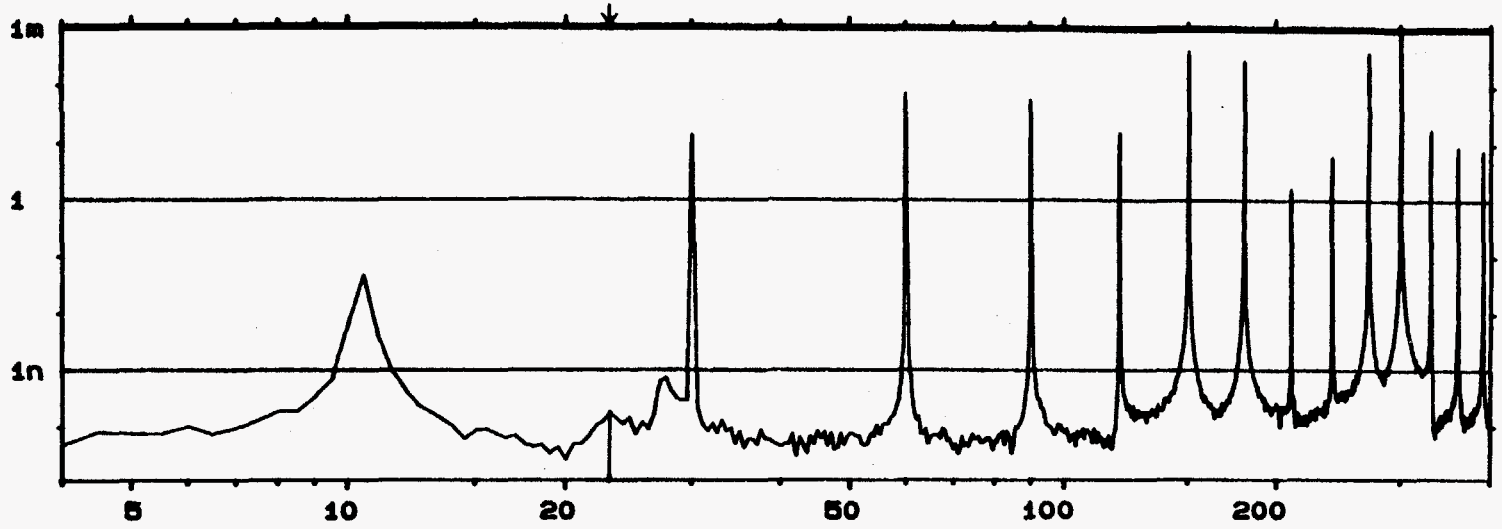

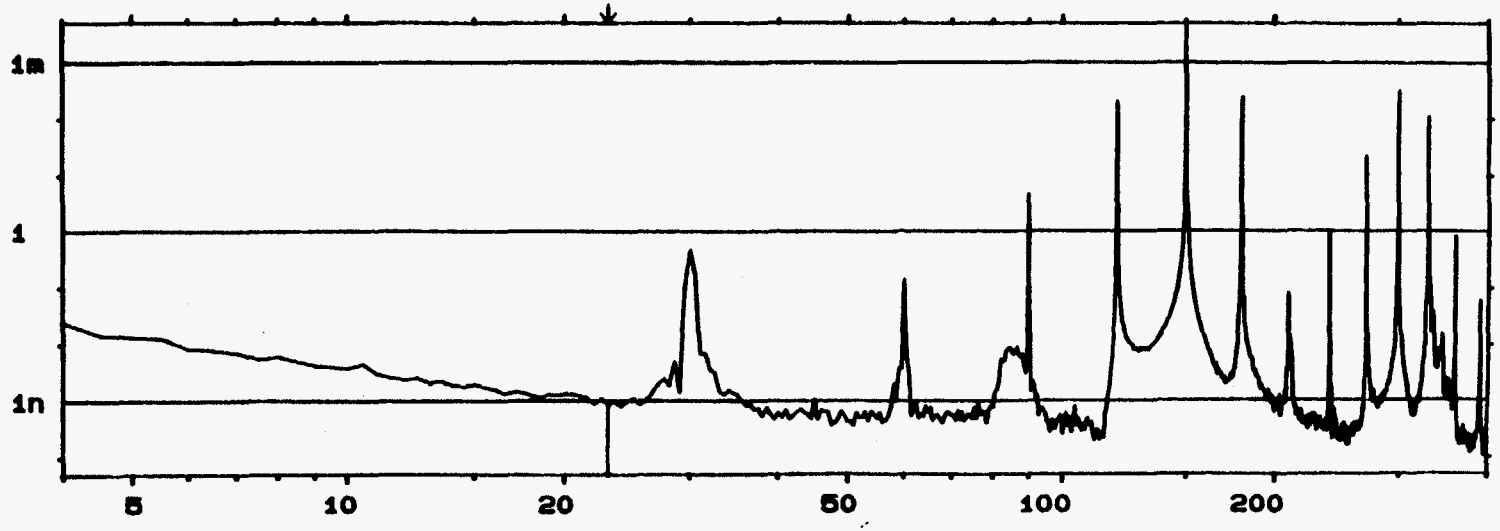

W2 AUTO SPEC CH.B
Y: 4.99mU /Hz PSD 80dB
X: 4Hz TO 400Hz LOG
SETUP W12 #A: 20

MAIN Y: 856E-12U /Hz
X: 23.0Hz

Bruel Kjær

Type 2034

Page No.
76

Sign.:

Meas.
Object:

Comments:

Test 14

W2 AUTO SPEC CH.A
Y: 233 U /Hz PSD 80dB
X: 4Hz TO 400Hz LOG
SETUP W12 #A: 20

MAIN Y: 1.42E-9U /Hz
X: 23.0Hz

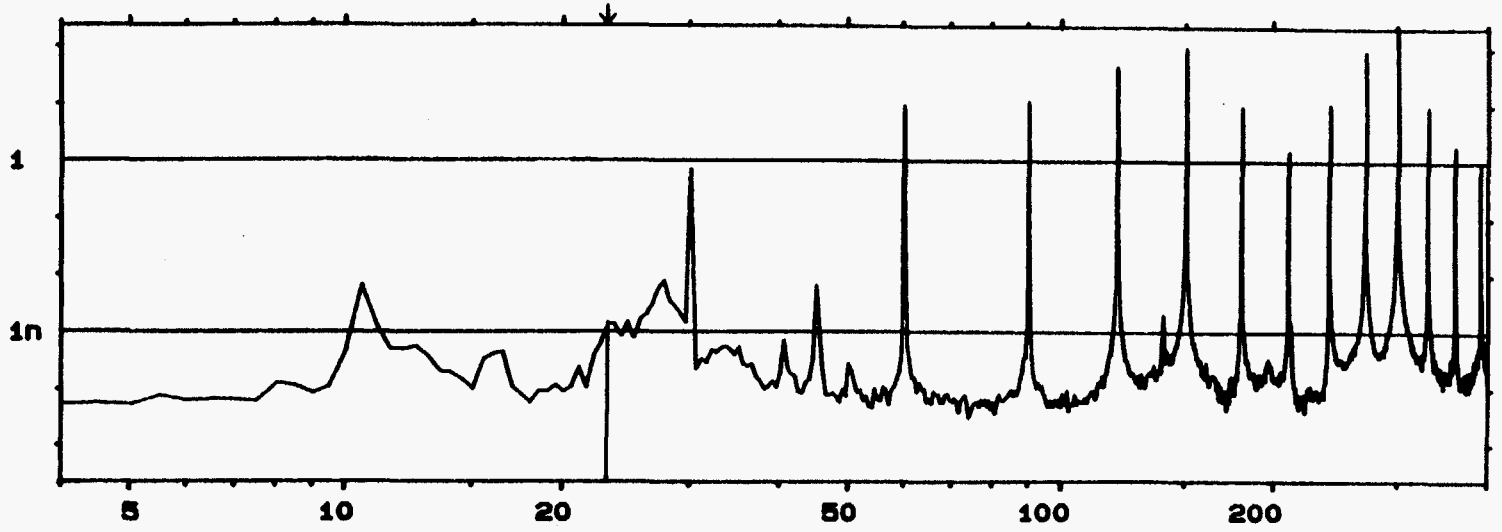

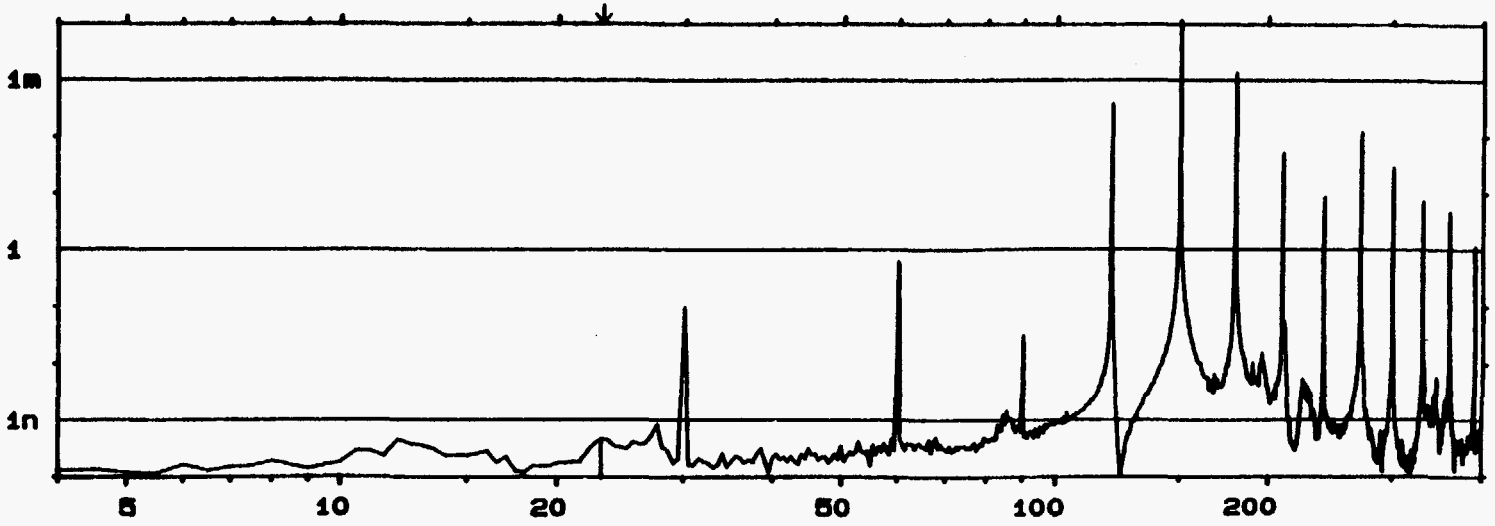

W2 AUTO SPEC CH.B
Y: 9.62mU /Hz PSD 80dB
X: 4Hz TO 400Hz LOG
SETUP W12 #A: 20

MAIN Y: 460E-12U /Hz
X: 23.0Hz

Bruel Kjær

Type 2034

Page No.
77

Sign.:

Meas.
Object:

Comments:

Test 15

W2 AUTO SPEC CH.A
Y: 1.45mU /Hz PSD 80dB
X: 4Hz TO 400Hz LOG
SETUP W12 #A: 20

MAIN Y: 70.0E-12U /Hz
X: 23.0Hz

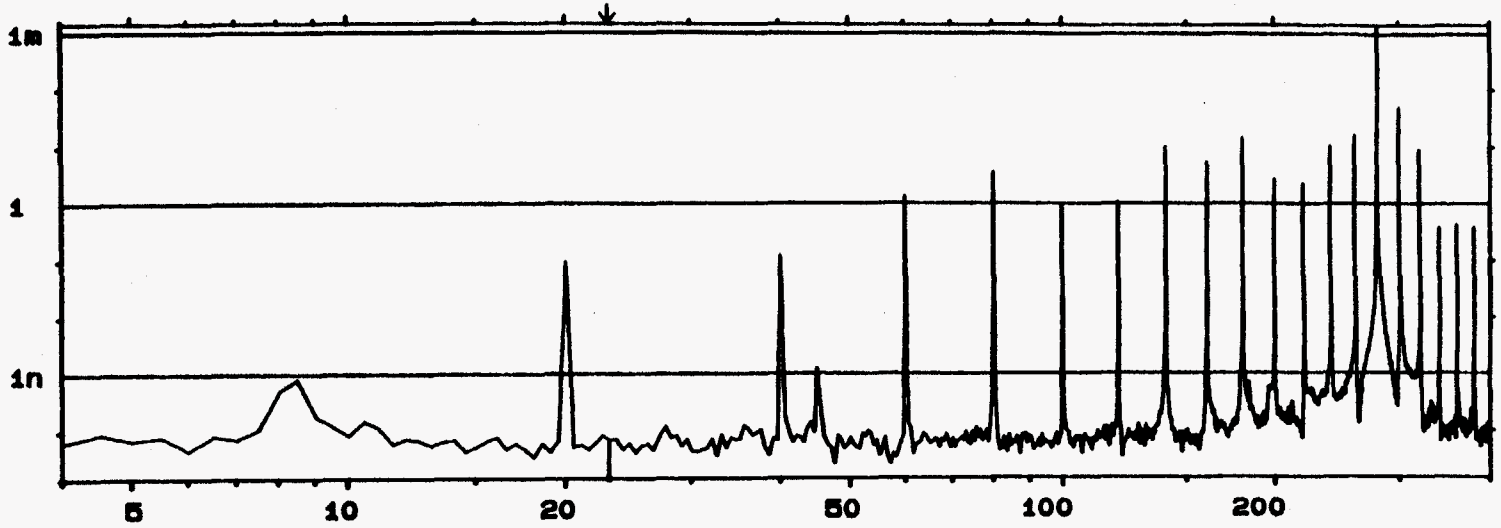

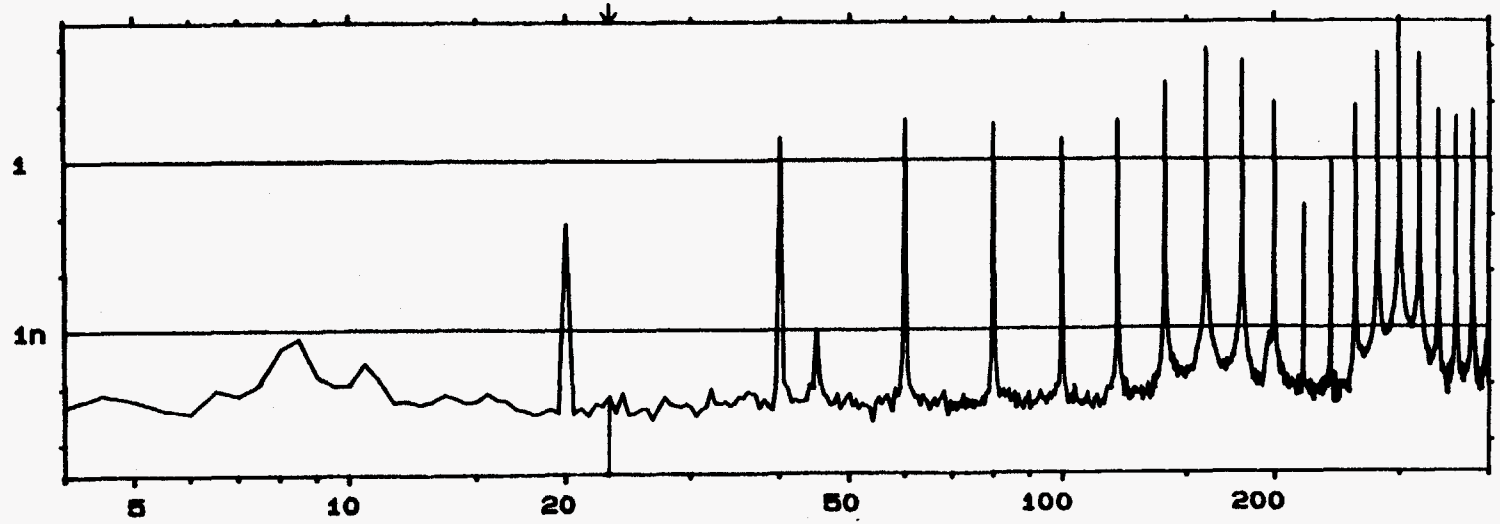

W2 AUTO SPEC CH.B
Y: 278 U /Hz PSD 80dB
X: 4Hz TO 400Hz LOG
SETUP W12 #A: 20

MAIN Y: 68.7E-12U /Hz
X: 23.0Hz

Bruel Kjær

Type 2034

Page No.
78

Sign.:

Meas.
Object:

Comments:

Ext 16

W2 AUTO SPEC CH.A
Y: 435 U /Hz PSD 80dB
X: 4Hz TO 400Hz LOG
SETUP W12 #A: 20

MAIN Y: 1.23E-9U /Hz
X: 23.0Hz

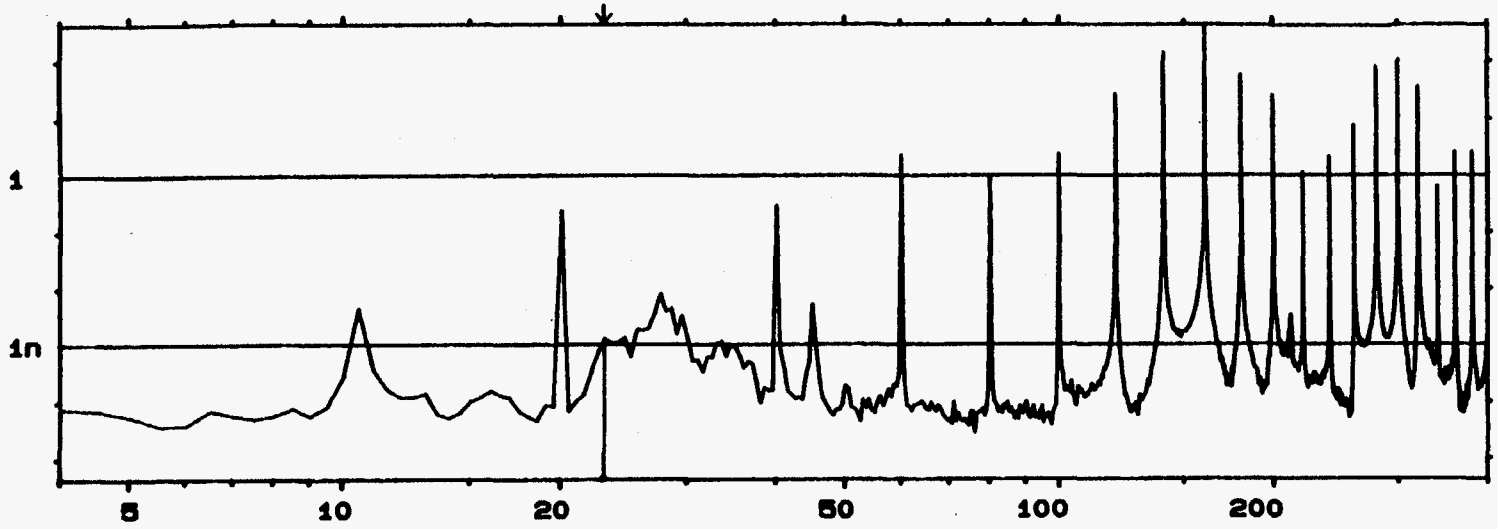

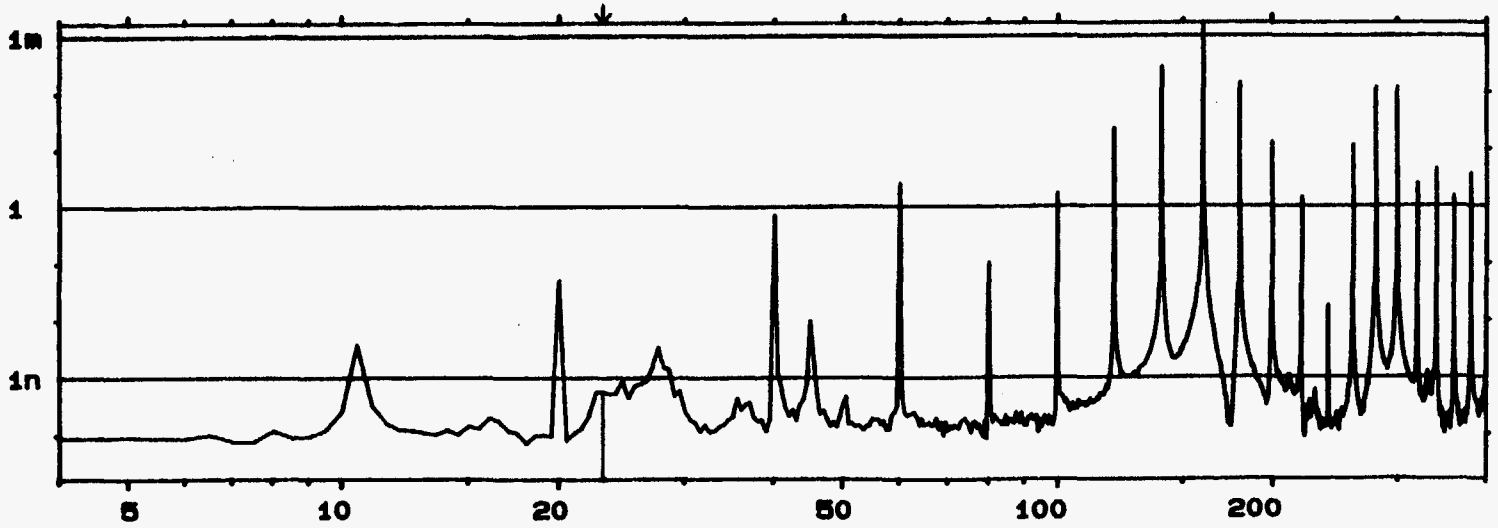

W2 AUTO SPEC CH.B
Y: 1.68mU /Hz PSD 80dB
X: 4Hz TO 400Hz LOG
SETUP W12 #A: 20

MAIN Y: 562E-12U /Hz
X: 23.0Hz

Bruel Kjaer

Type 2034

Page No.
79

Sign.:

Meas.
Object:

Comments:

Test 17

W2 AUTO SPEC CH.A
Y: 66.0 U /Hz PSD 80dB
X: 4Hz TO 400Hz LOG
SETUP W12 #A: 20

MAIN Y: 237E-12U /Hz
X: 23.0Hz

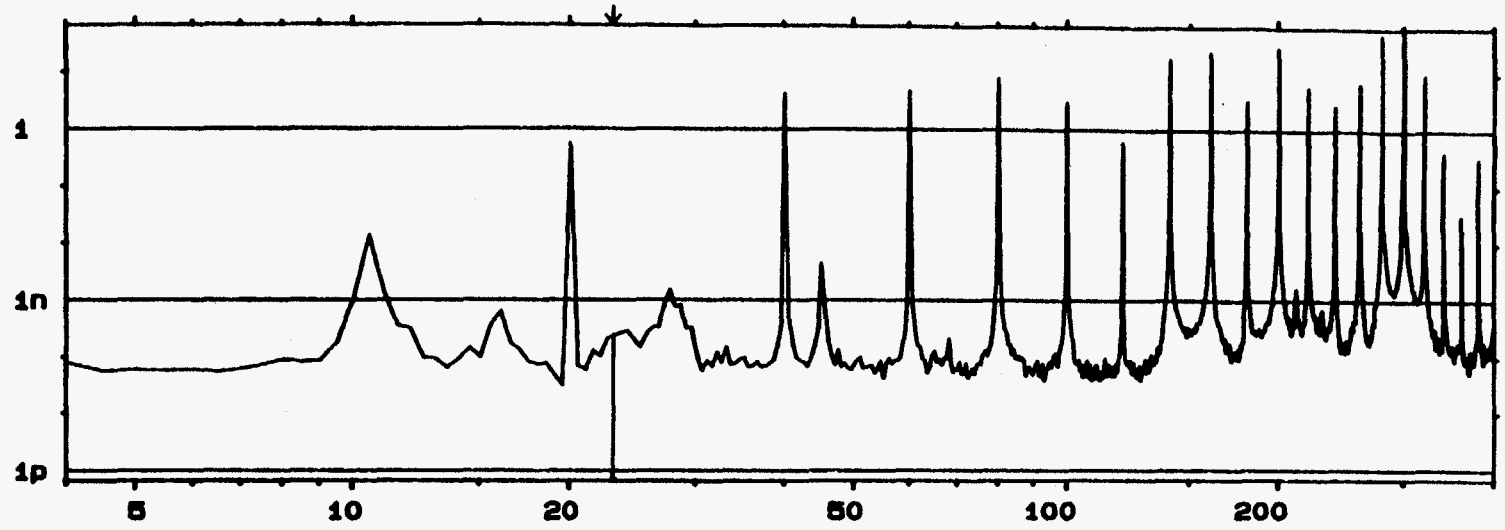

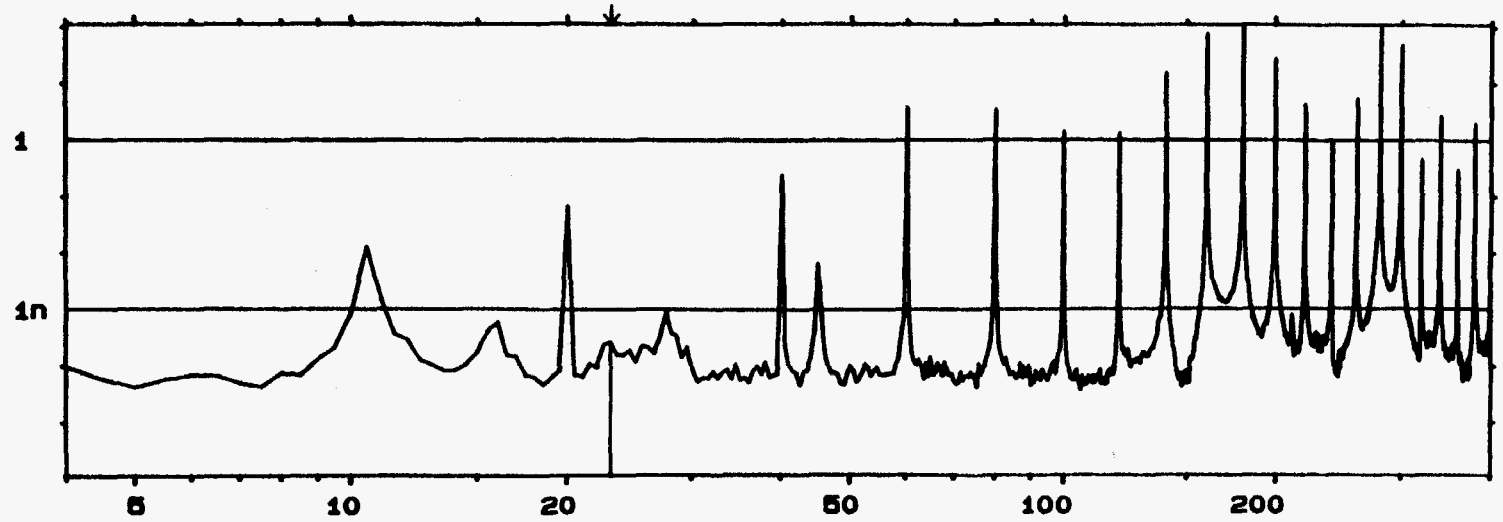

W2 AUTO SPEC CH.B
Y: 113 U /Hz PSD 80dB
X: 4Hz TO 400Hz LOG
SETUP W12 #A: 20

MAIN Y: 266E-12U /Hz
X: 23.0Hz

Bruel Kjaer

Type 2034

Page No.
80.

Sign.:

Meas.
Object:

Comments:

Test 18

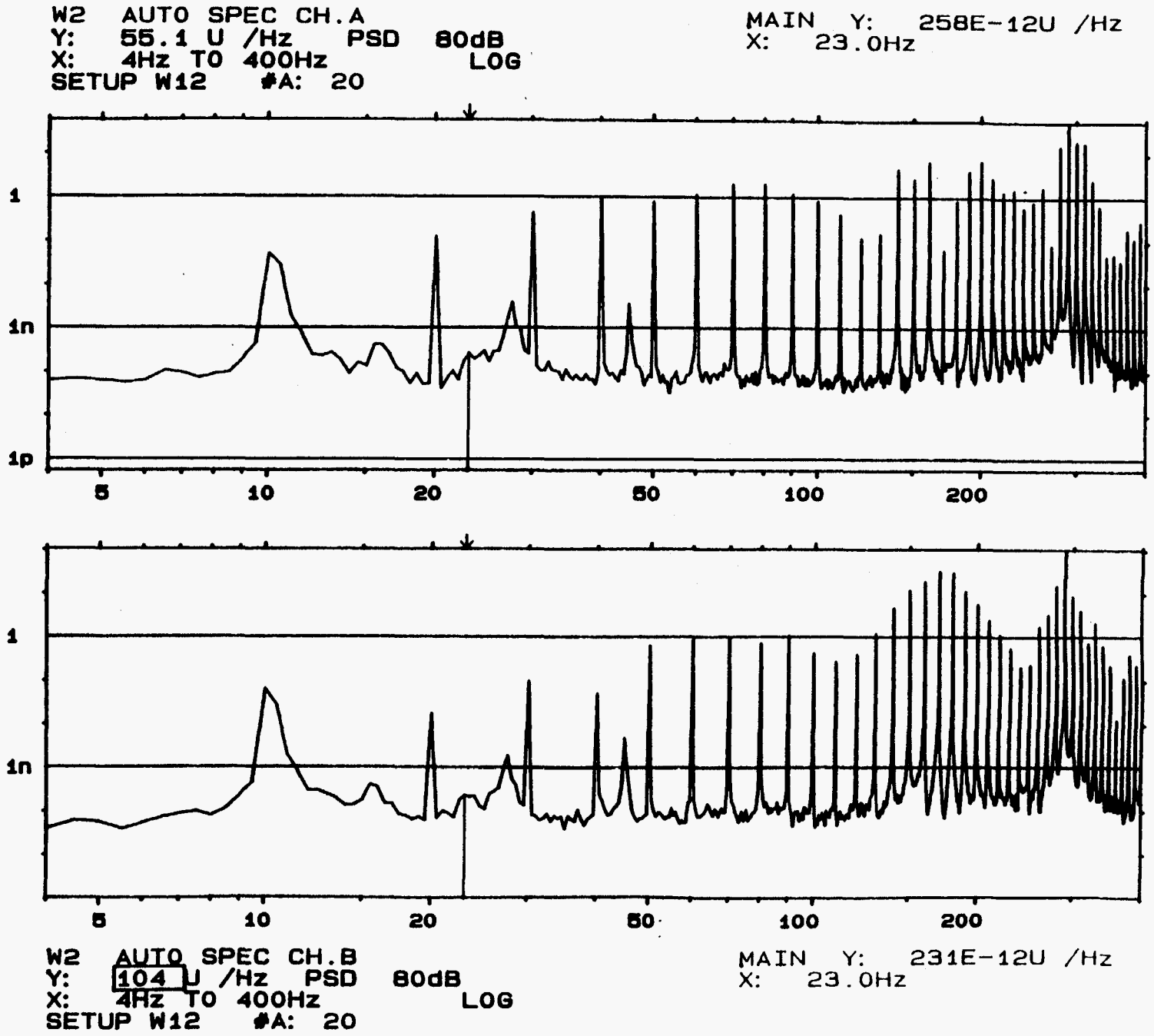

Brüel Kjær

Type 2034

Page No.
81

Sign.:

Meas.
Object:

Comments:

Test 18

W2 FREQ RESP H1 PHASE INPUT MAIN Y:
Y: -200 TO +200 DEG X: 23.0Hz
X: 4Hz TO 400Hz LOG
SETUP W12 #A: 20

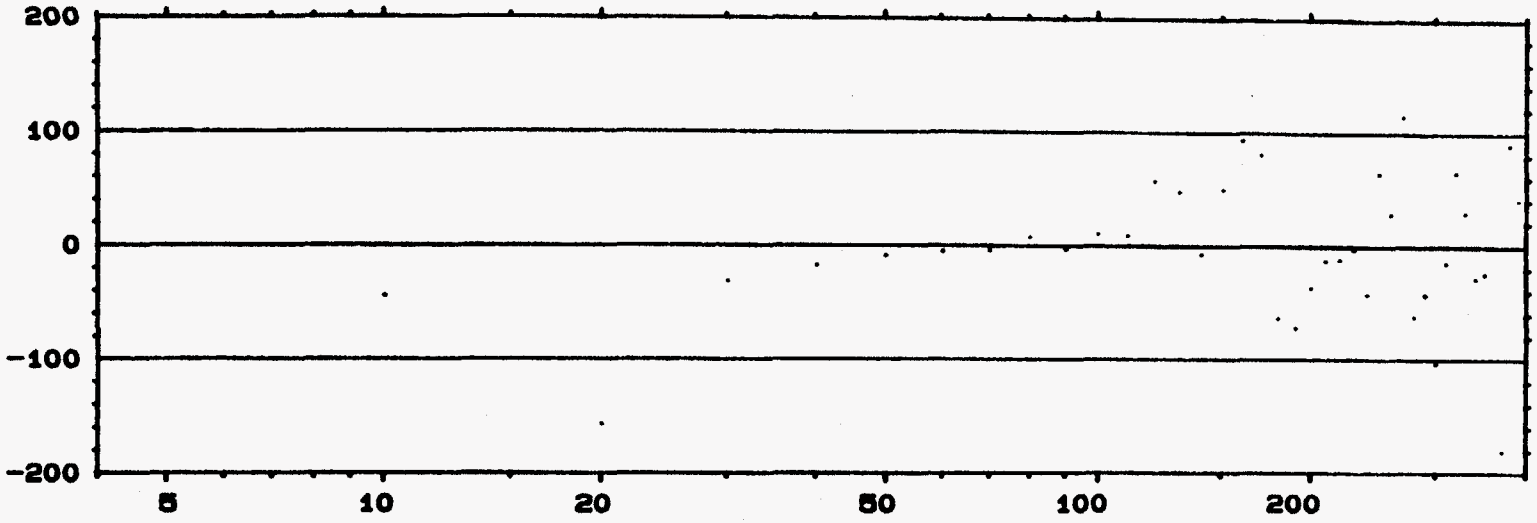

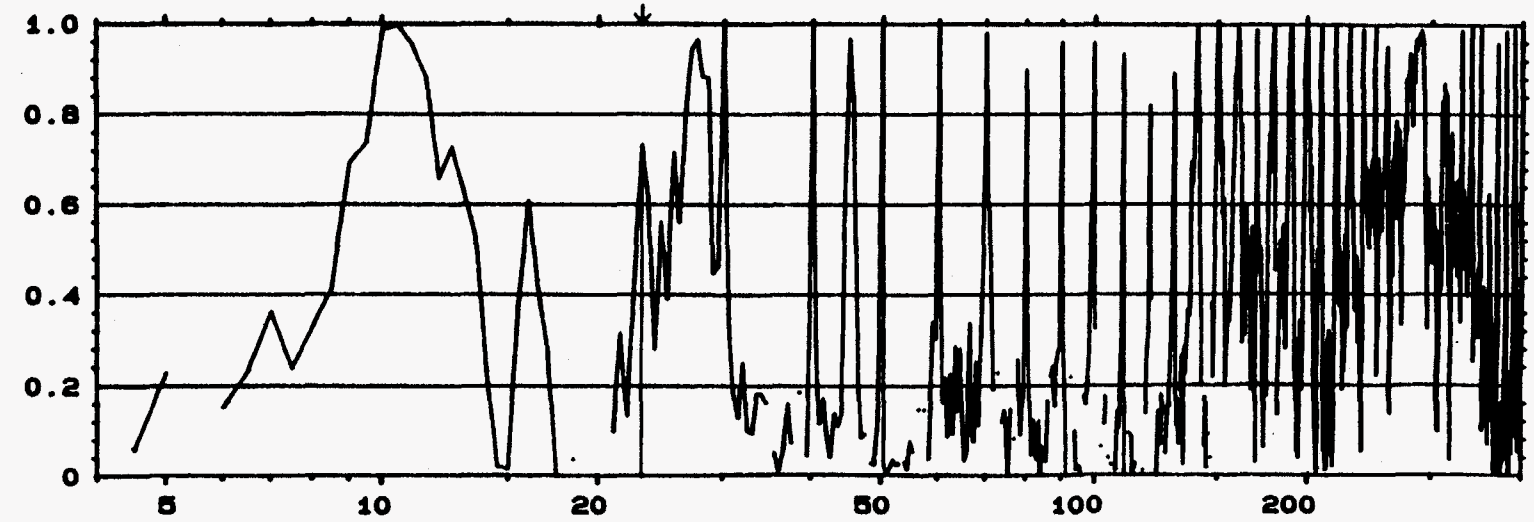

W2 COHERENCE MAIN Y: 734m
Y: 1.00 X: 23.0Hz
X: 4Hz TO 400Hz LOG
SETUP W12 #A: 20

Bruel Kjaer

Type 2034

Page No.
84

Sign.:

Meas.
Object:

Comments:

Test 17

W2 AUTO SPEC CH.A
Y: 109 U /Hz PSD 80dB
X: 4Hz TO 400Hz LOG
SETUP W12 #A: 20

MAIN Y: 1.50E-9U /Hz
X: 23.0Hz

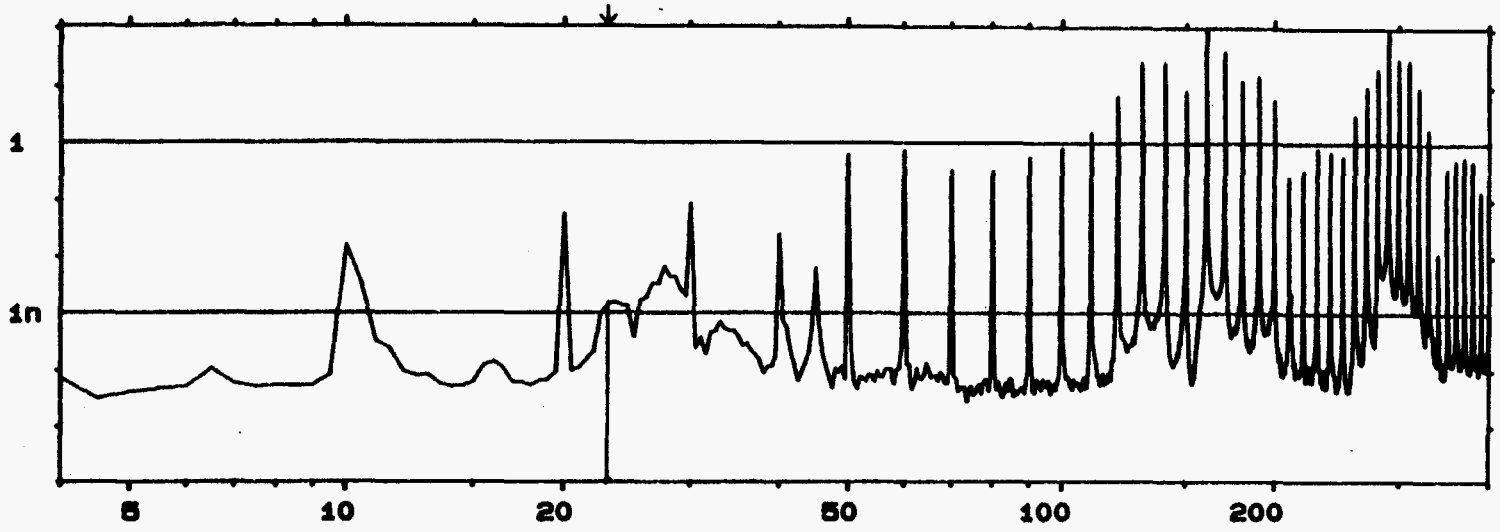

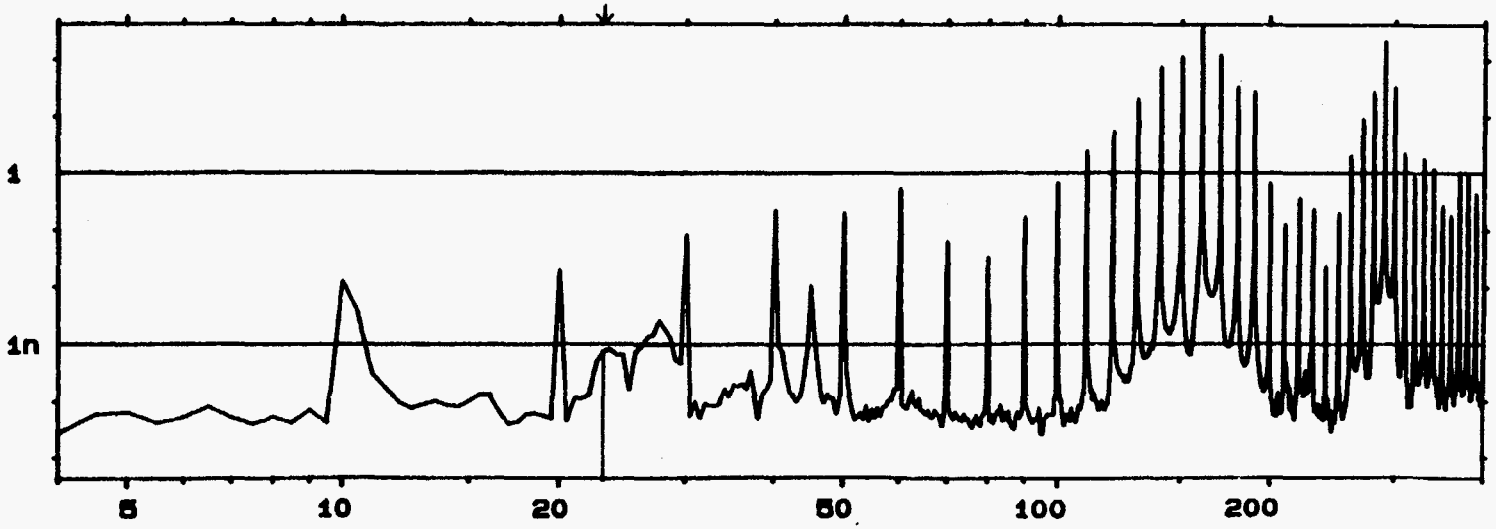

W2 AUTO SPEC CH.B
Y: 425 U /Hz PSD 80dB
X: 4Hz TO 400Hz LOG
SETUP W12 #A: 20

MAIN Y: 750E-12U /Hz
X: 23.0Hz

Bruel Kjaer

Type 2034

Page No.
85

Sign.:

Meas.
Object:

Comments:

Test 19

W2 FREQ RESP H1 PHASE INPUT MAIN Y:
Y: -200 TO +200 DEG X: 23.0Hz
X: 4Hz TO 400Hz LOG
SETUP W12 #A: 20

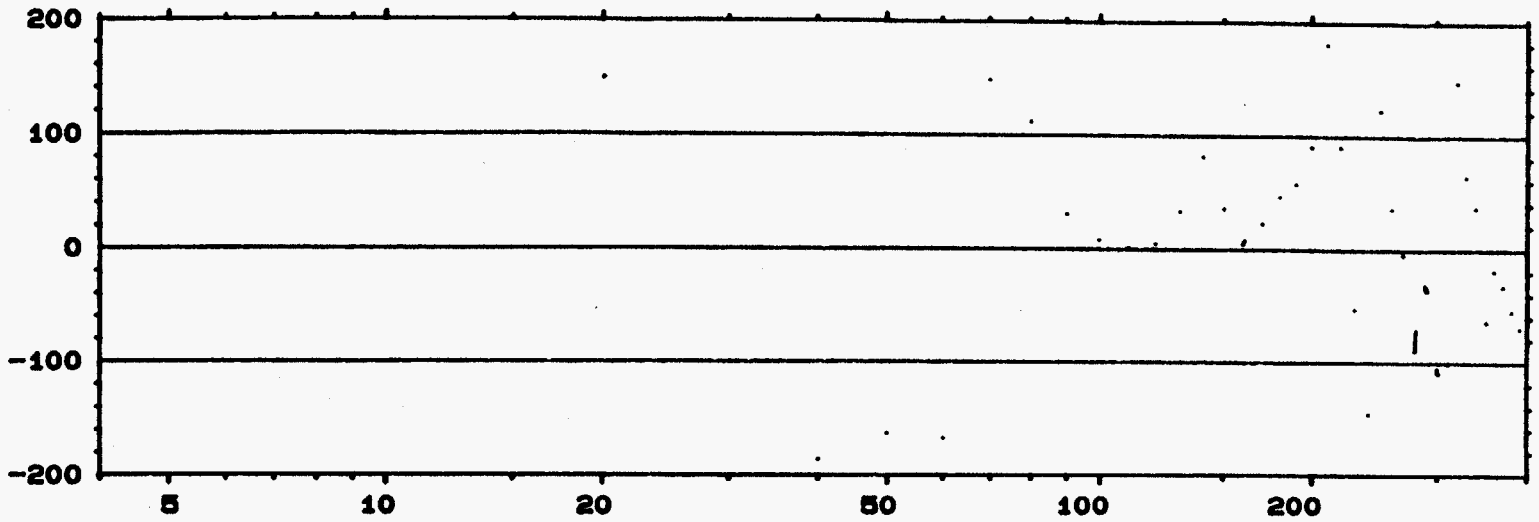

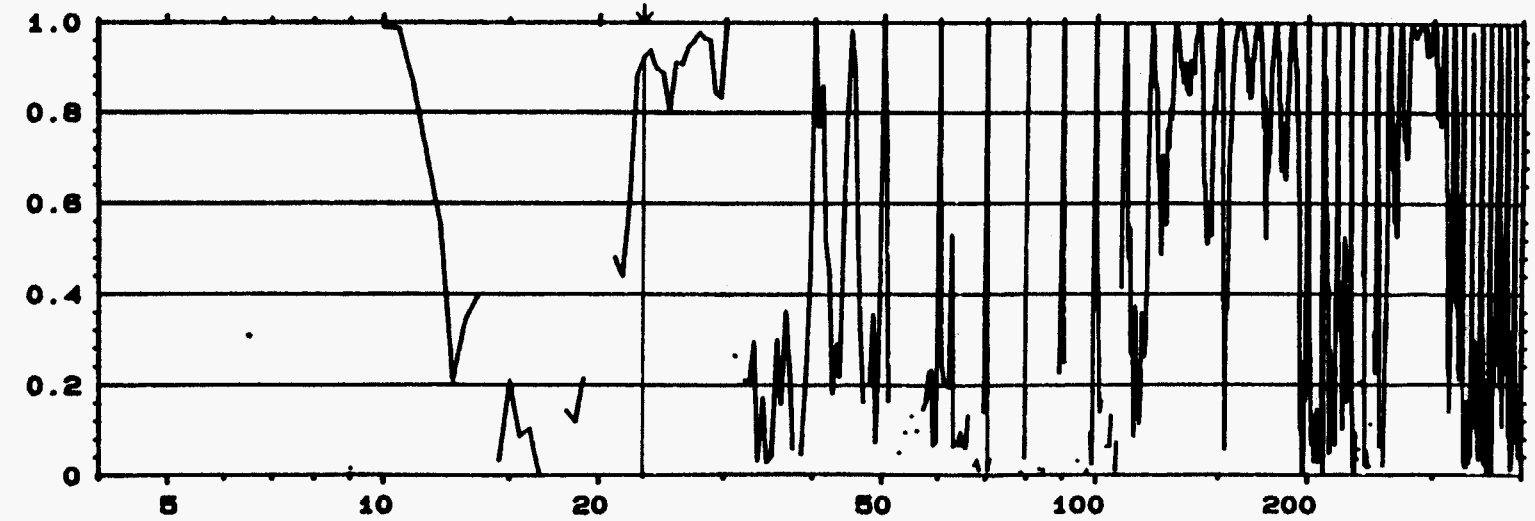

W2 COHERENCE MAIN Y: 923m
Y: 1.00 X: 23.0Hz
X: 4Hz TO 400Hz LOG
SETUP W12 #A: 20

Bruel Kjær

Type 2034

Page No.
86

Sign.:

Meas.
Object:

Comments:

Test 19

W2 AUTO SPEC CH.A
Y: 7.36mU RMS 80dB
X: 4Hz TO 400Hz LOG
SETUP W12 #A: 20

MAIN Y: 27.3 U
X: 23.0Hz

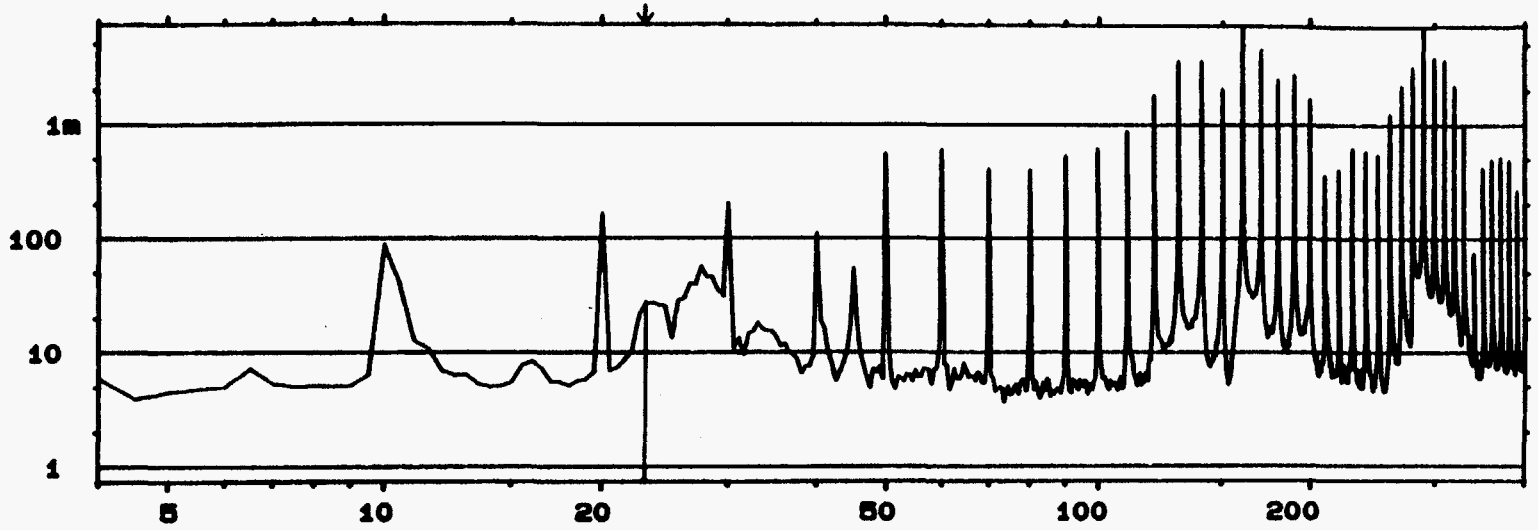

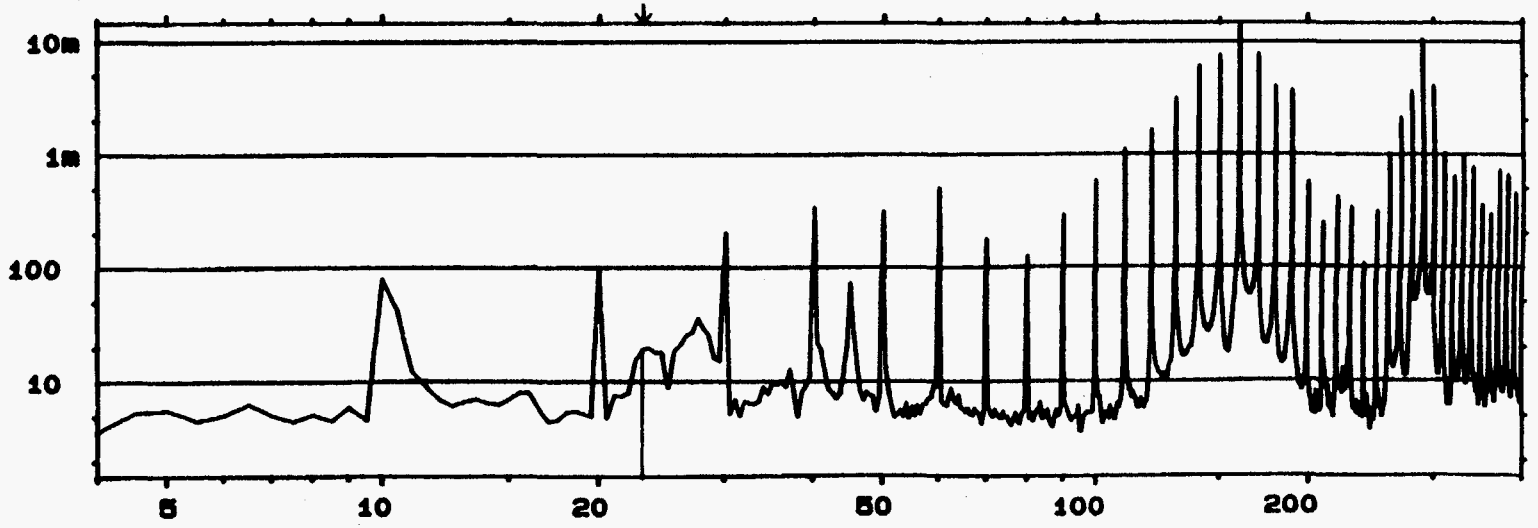

W2 AUTO SPEC CH.B
Y: 14.6mU RMS 80dB
X: 4Hz TO 400Hz LOG
SETUP W12 #A: 20

MAIN Y: 19.3 U
X: 23.0Hz

Bruel Kjaer

Type 2034

Page No.
87

Sign.:

Meas.
Object:

Comments:

Test 20

W2 AUTO SPEC CH.A
Y: 6.20mU RMS 80dB
X: 4Hz TO 400Hz LOG
SETUP W12 #A: 20

MAIN Y: 5.29 U
X: 23.0Hz

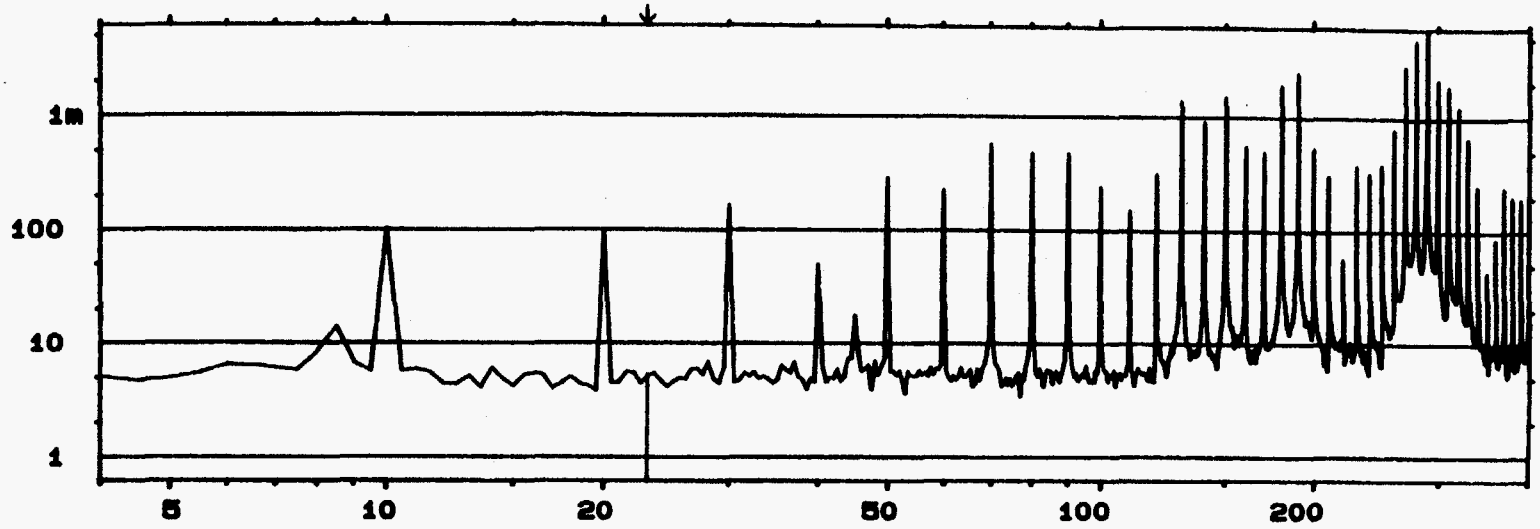

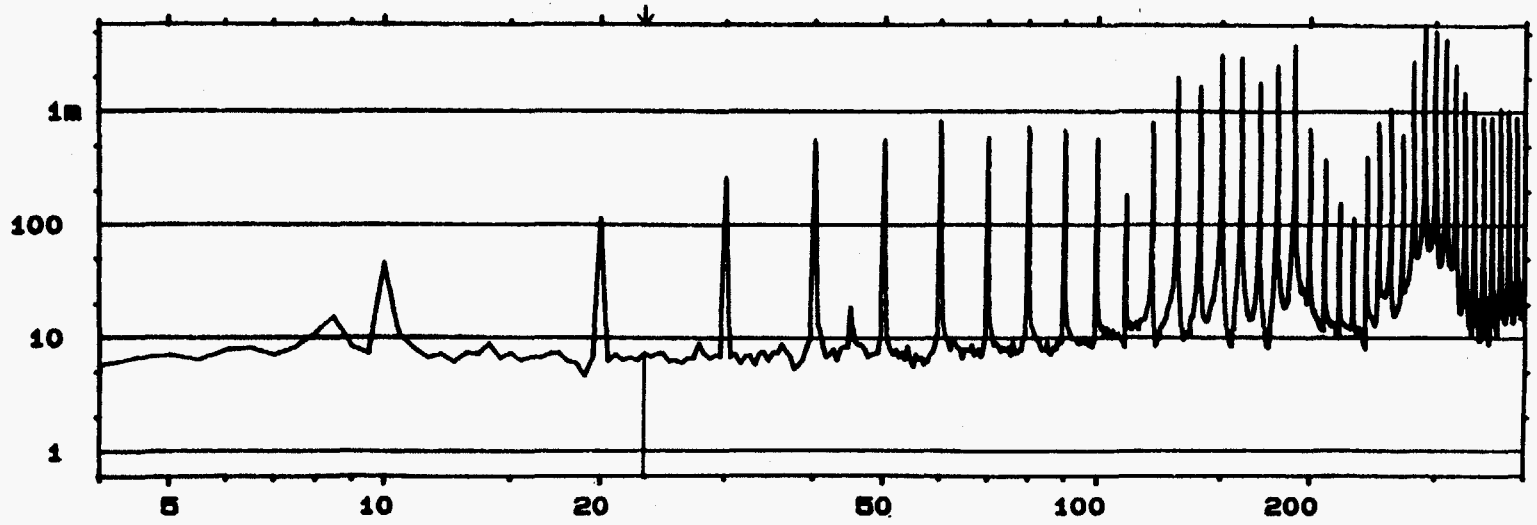

W2 AUTO SPEC CH.B
Y: 5.96mU RMS 80dB
X: 4Hz TO 400Hz LOG
SETUP W12 #A: 20

MAIN Y: 7.31 U
X: 23.0Hz

Bruel Kjær

Type 2034

Page No.
88

Sign.:

Meas.
Object:

Comments:

Test 20

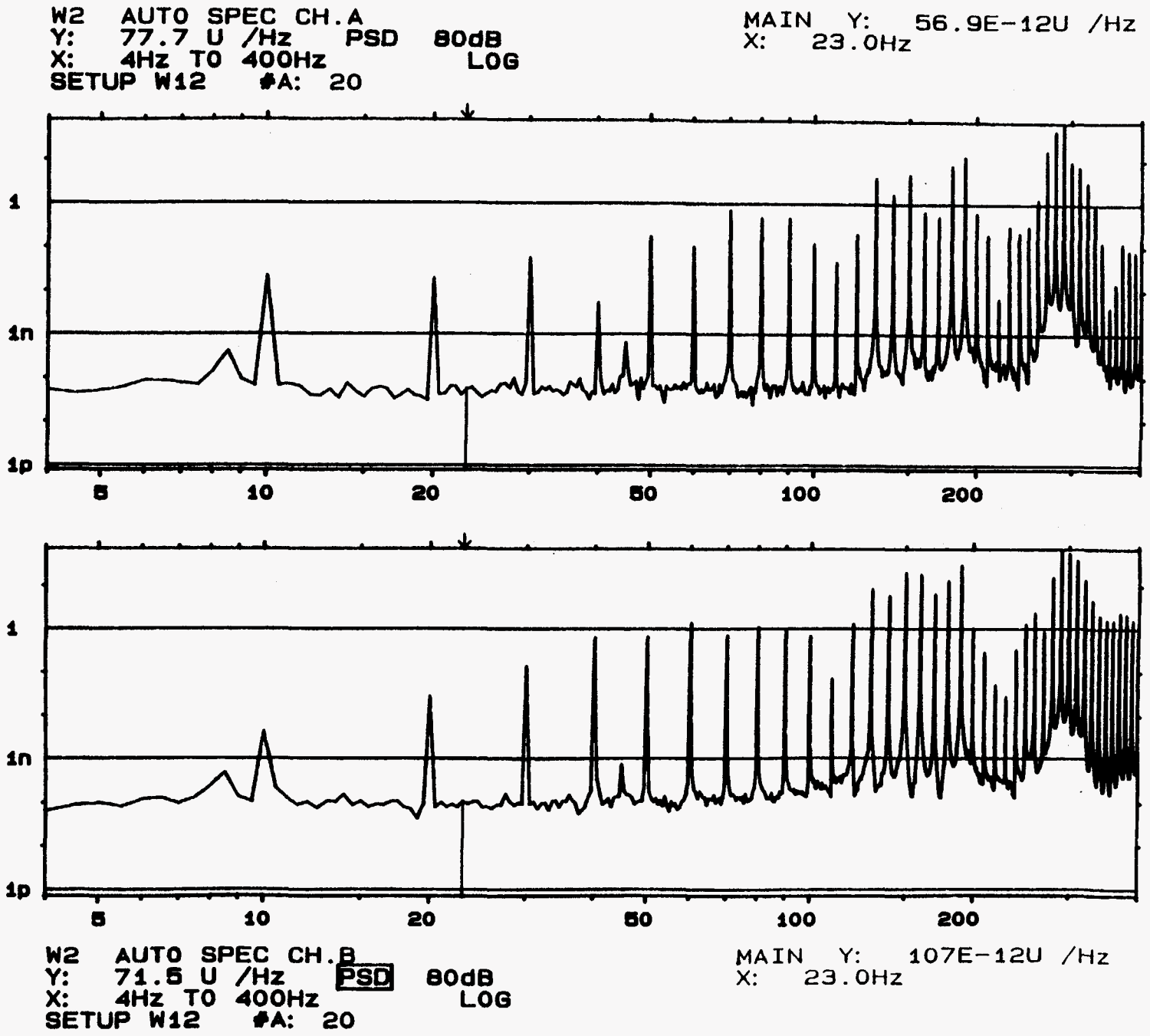

Bruel Kjaer

Type 2034

Page No.
89

Sign.:

Meas.
Object:

Comments:
Test 20

W2 FREQ RESP H1 PHASE INPUT MAIN Y:
Y: -200 TO +200 DEG X: 23.0Hz
X: 4Hz TO 400Hz LOG
SETUP W12 #A: 20

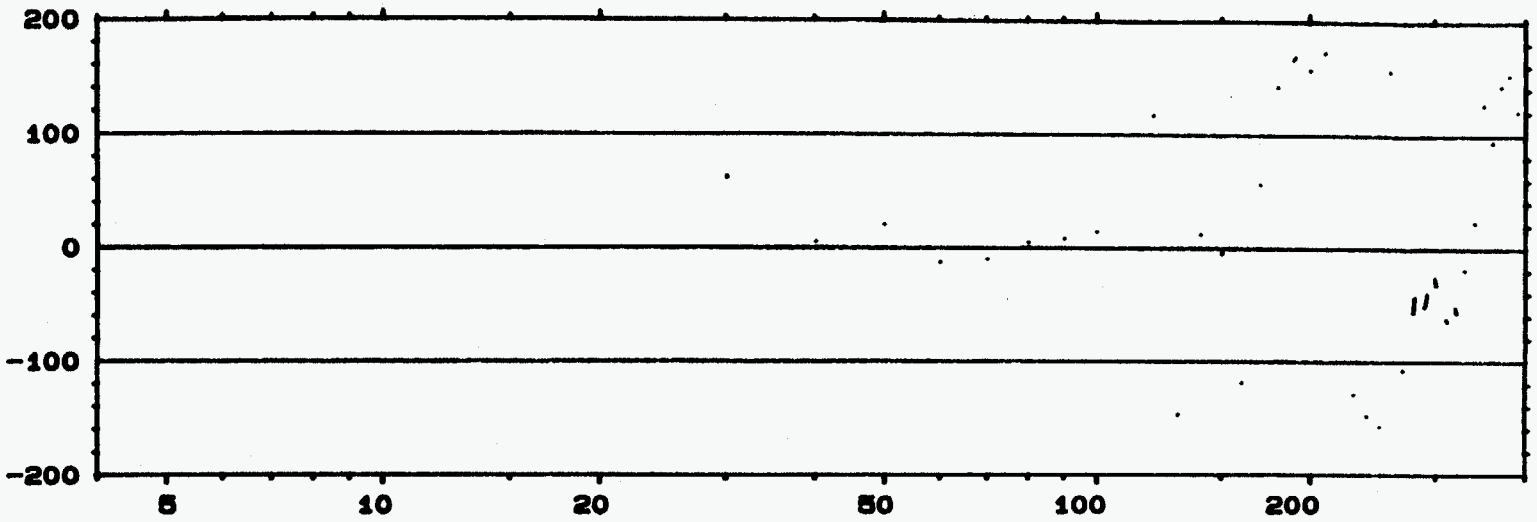

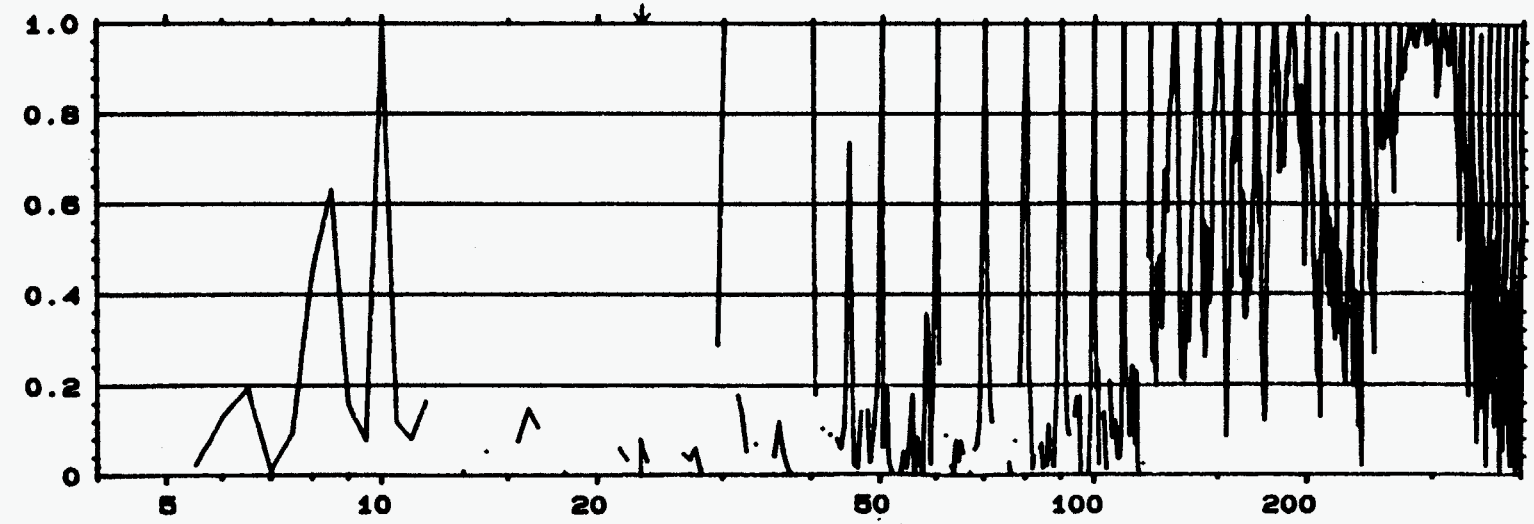

W2 COHERENCE MAIN Y: 78.9m
Y: 1.00 X: 23.0Hz
X: 4Hz TO 400Hz LOG
SETUP W12 #A: 20

Bruel Kjær

Type 2034

Page No.
91

Sign.:

Meas.
Object:

Comments:

Test 21

W2 AUTO SPEC CH.A
Y: 8.56 U /Hz PSD 20dB
X: 4Hz TO 400Hz LOG
SETUP W12 #A: 10

MAIN Y: 119E-9U /Hz
X: 20.0Hz

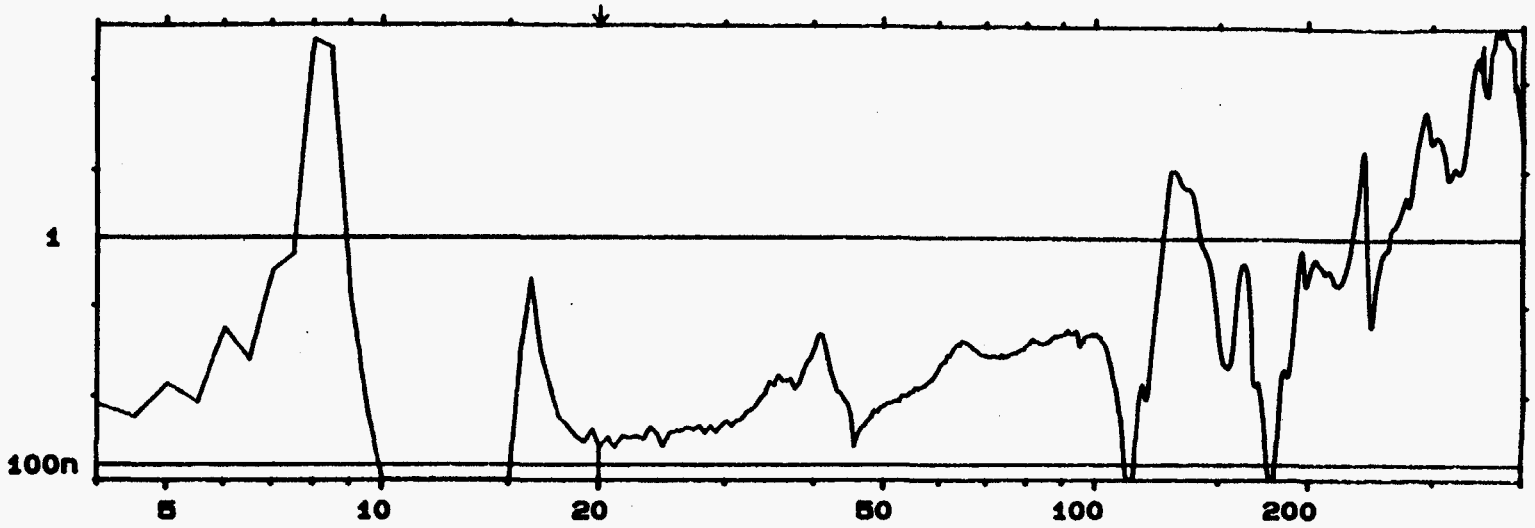

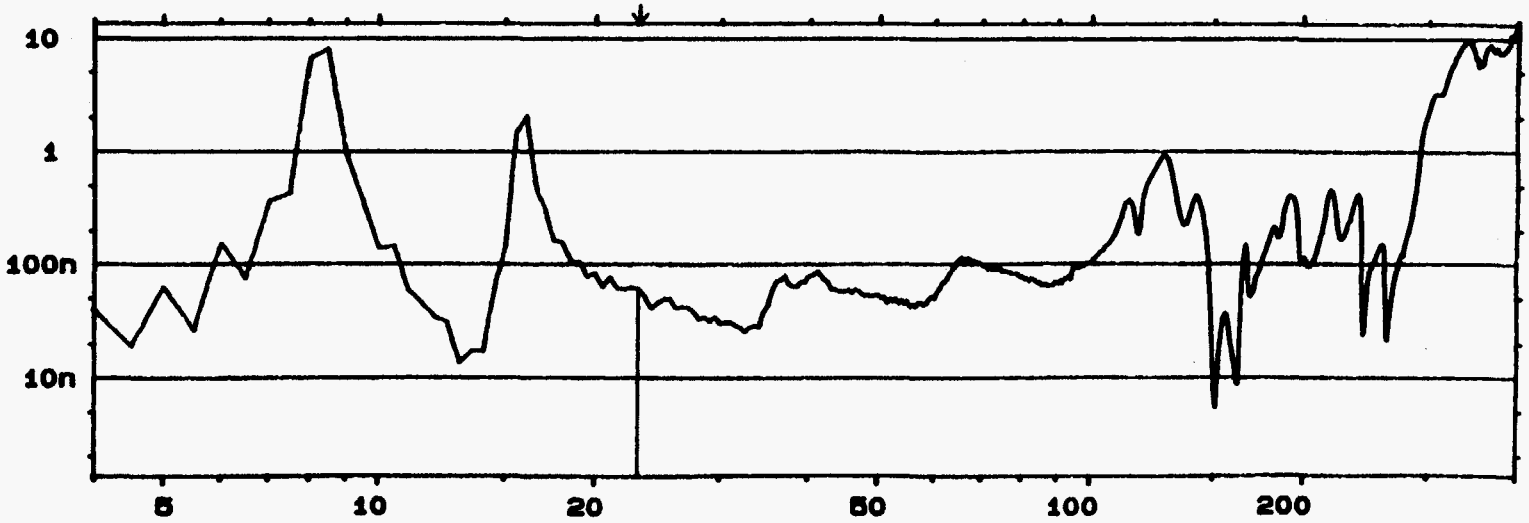

W2 AUTO SPEC CH.B
Y: 13.5 U /Hz PSD 40dB
X: 4Hz TO 400Hz LOG
SETUP W12 #A: 10

MAIN Y: 60.7E-9U /Hz
X: 23.0Hz

Bruel Kjaer

Type 2034

Page No.
92

Sign.:

Meas.
Object:

Comments:

IC3621

W2 FREQ RESP H1 PHASE INPUT MAIN Y: -141.4DEG
Y: -200 TO +200 DEG X: 20.0Hz
X: 4Hz TO 400Hz LOG
SETUP W12 #A: 10

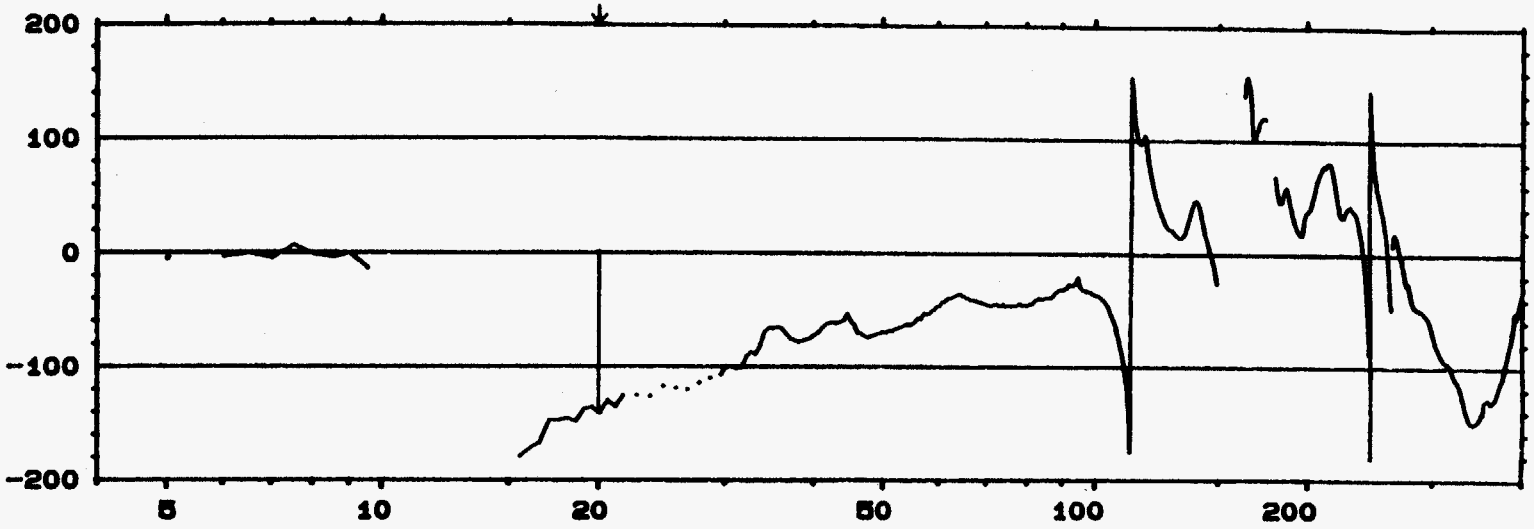

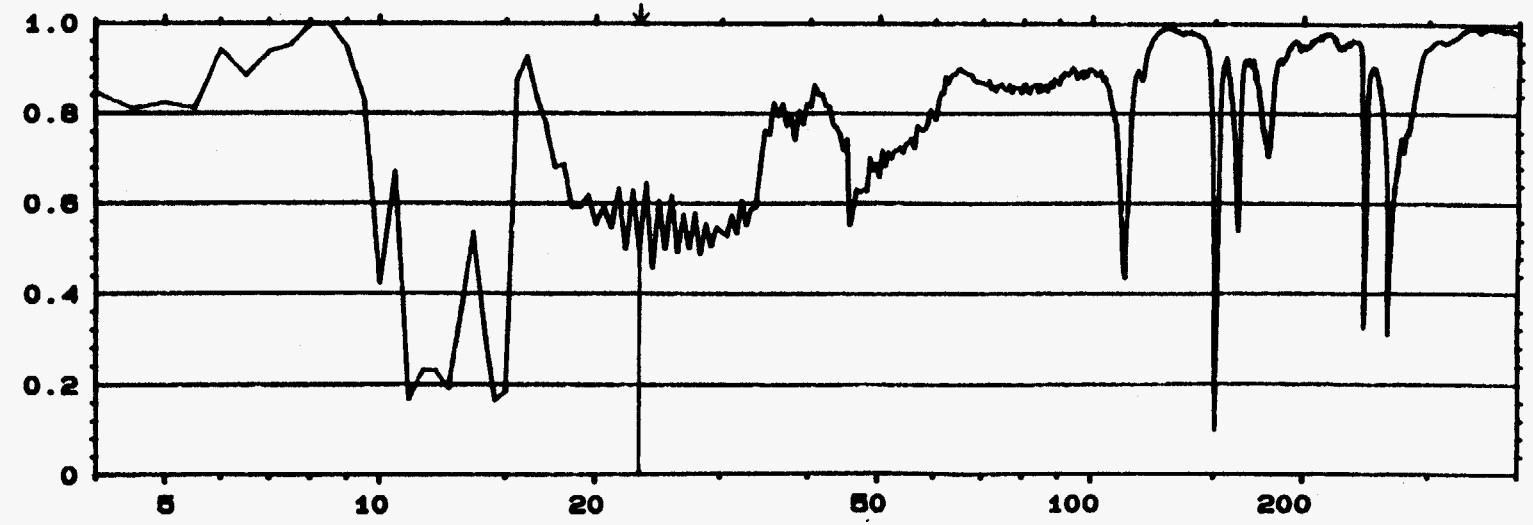

W2 COHERENCE MAIN Y: 499m
Y: 1.00 X: 23.0Hz
X: 4Hz TO 400Hz LOG
SETUP W12 #A: 10

Bruel Kjær

Type 2034

Page No.
93

Sign.:

Meas.
Object:

Comments:

Test 22

W2 AUTO SPEC CH.A
Y: 30.5 U /Hz PSD 20dB
X: 4Hz TO 400Hz LOG
SETUP W12 #A: 10

MAIN Y: 19.8E-9U /Hz
X: 20.0Hz

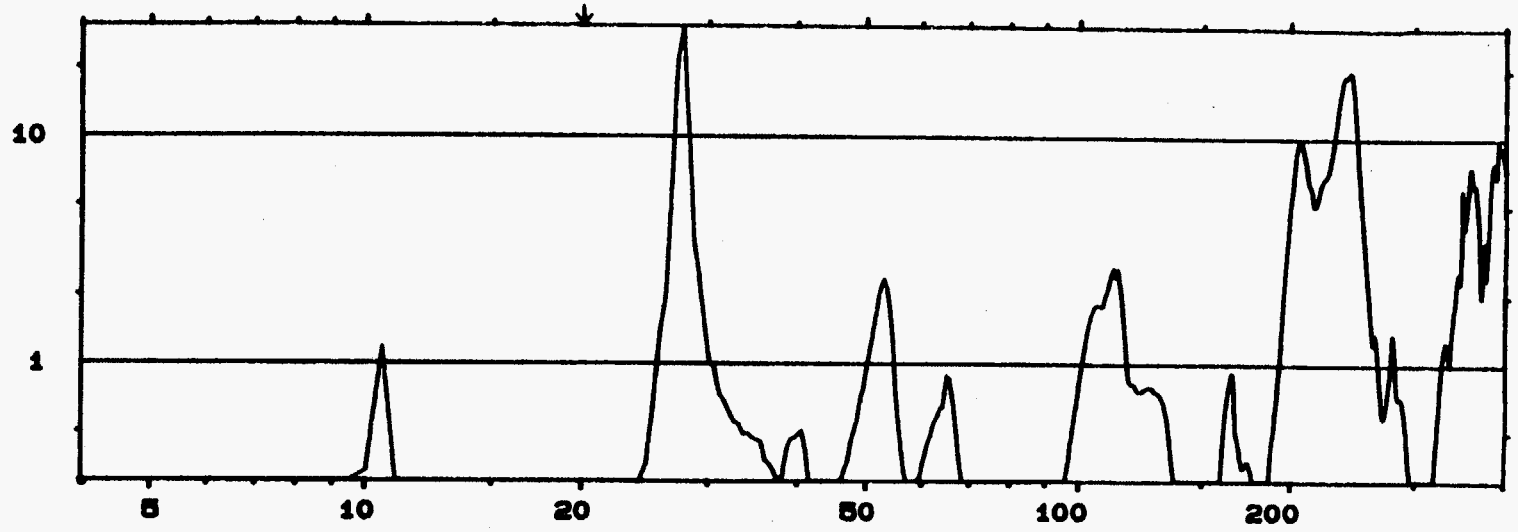

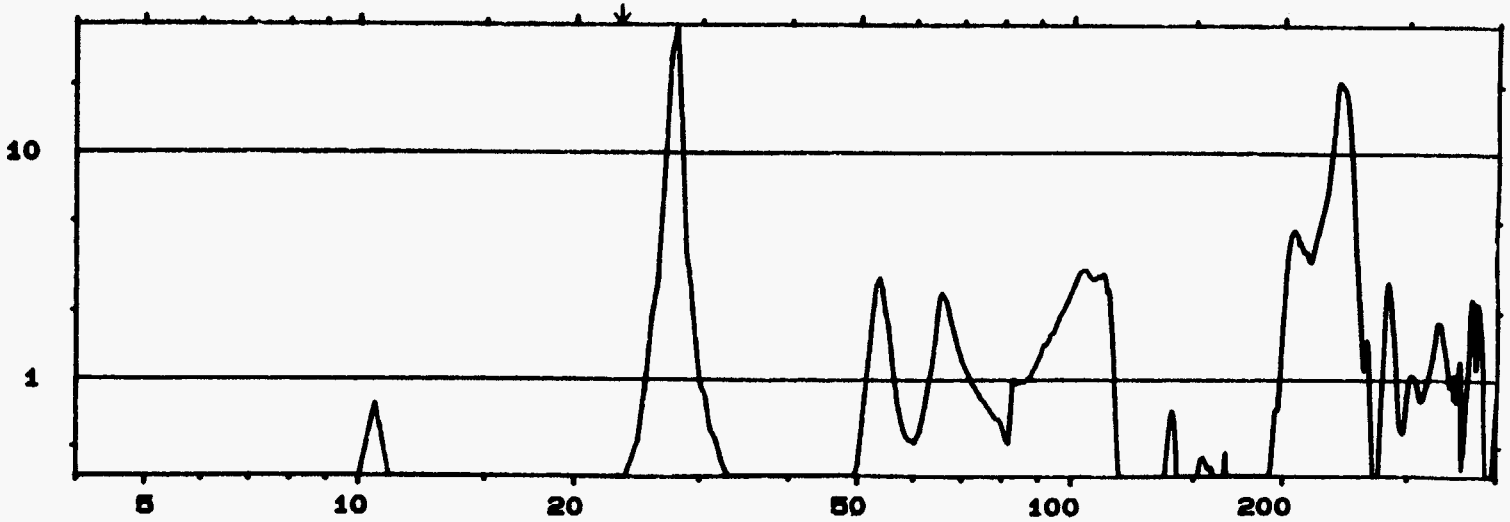

W2 AUTO SPEC CH.B
Y: 37.1 U /Hz PSD 20dB
X: 4Hz TO 400Hz LOG
SETUP W12 #A: 10

MAIN Y: 230E-9U /Hz
X: 23.0Hz

Bruel Kjær

Type 2034

Page No.
94

Sign.:

Meas.
Object:

Comments:

Ex 22

W2 FREQ RESP H1 PHASE INPUT MAIN Y:
Y: -200 TO +200 DEG X: 20.0Hz
X: 4Hz TO 400Hz LOG
SETUP W12 #A: 10

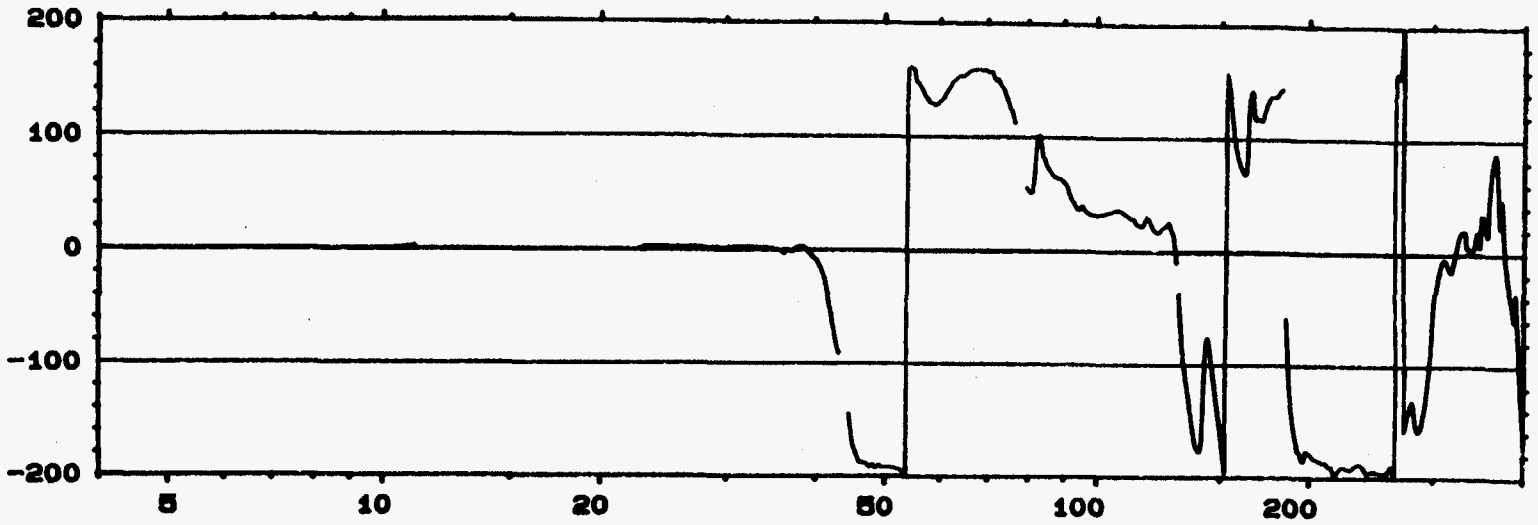

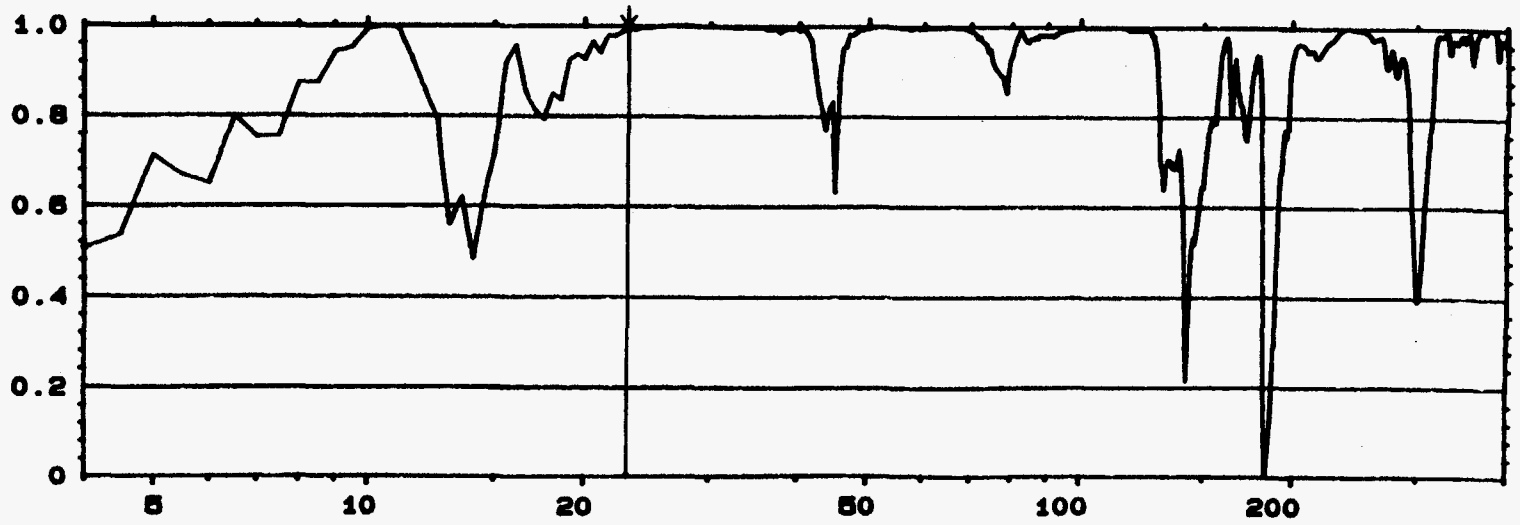

W2 COHERENCE MAIN Y: 992m
Y: 1.00 X: 23.0Hz
X: 4Hz TO 400Hz LOG
SETUP W12 #A: 10

Bruel Kjaer

Type 2034

Page No.
95

Sign.:

Meas.
Object:

Comments:

Test23

W2 AUTO SPEC CH.A
Y: 25.7 U /Hz PSD 40dB
X: 4Hz TO 400Hz LOG
SETUP W12 #A: 10

MAIN Y: 2.06 U /Hz
X: 27.5Hz

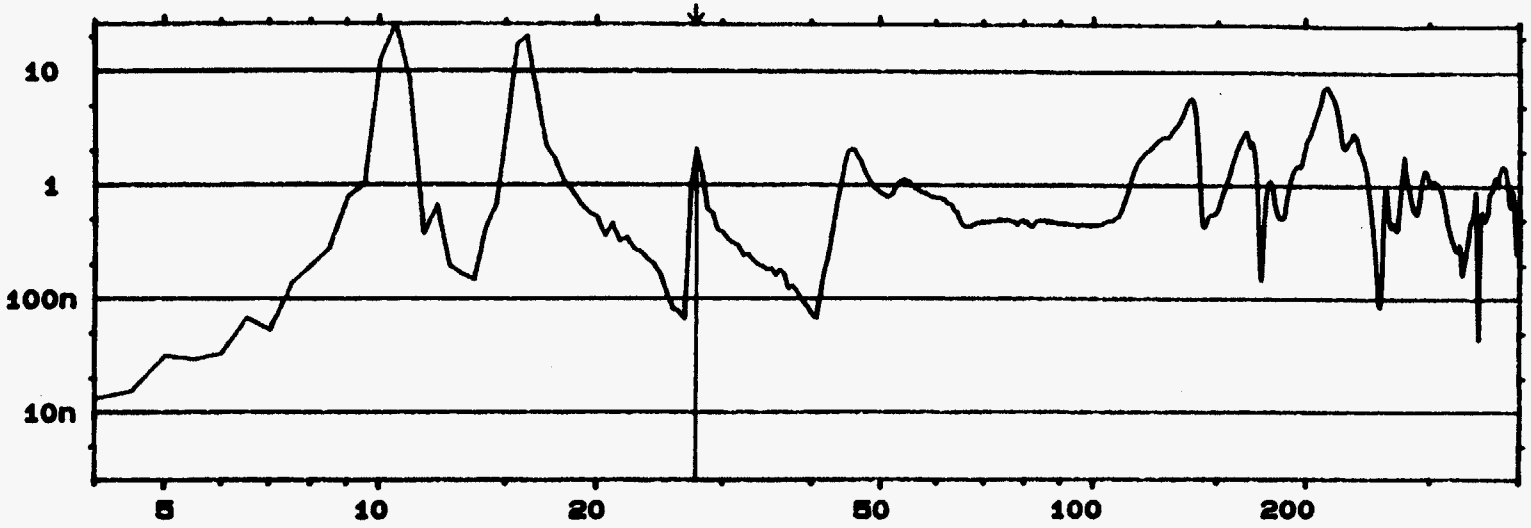

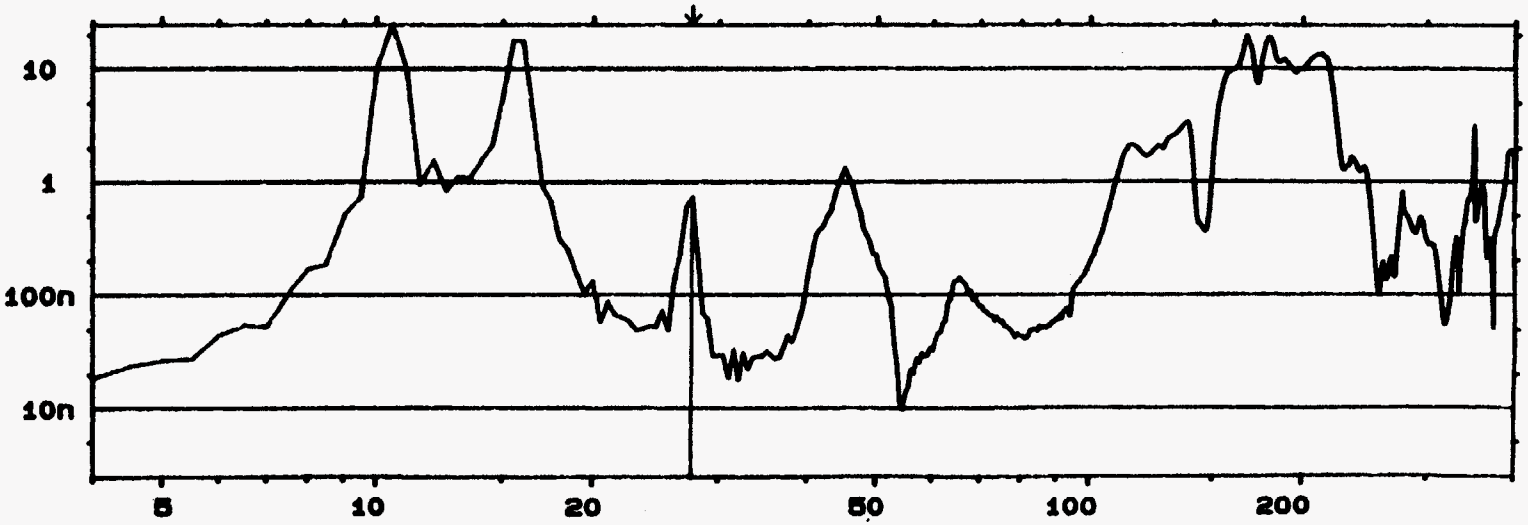

W2 AUTO SPEC CH.B
Y: 24.7 U /Hz PSD 40dB
X: 4Hz TO 400Hz LOG
SETUP W12 #A: 10

MAIN Y: 730E-9U /Hz
X: 27.5Hz

Bruel Kjær

Type 2034

Page No.
96

Sign.:

Meas.
Object:

Comments:

W2 FREQ RESP H1 PHASE INPUT MAIN Y: 16.8DEG
Y: -200 TO +200 DEG X: 27.5Hz
X: 4Hz TO 400Hz LOG
SETUP W12 #A: 10

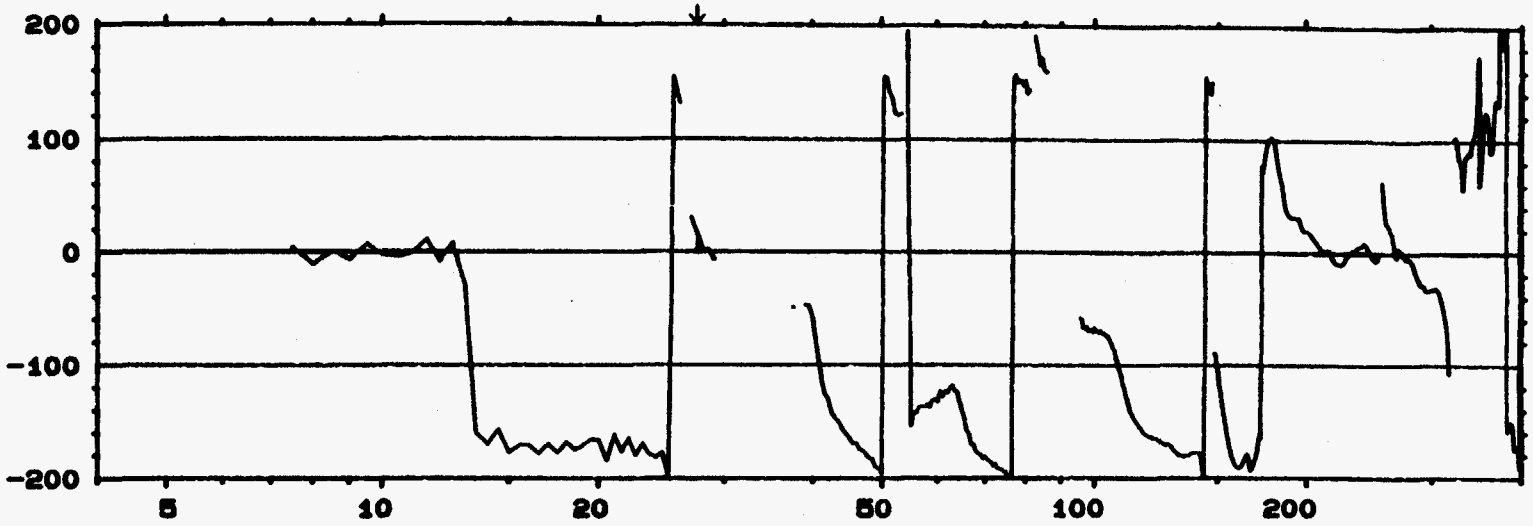

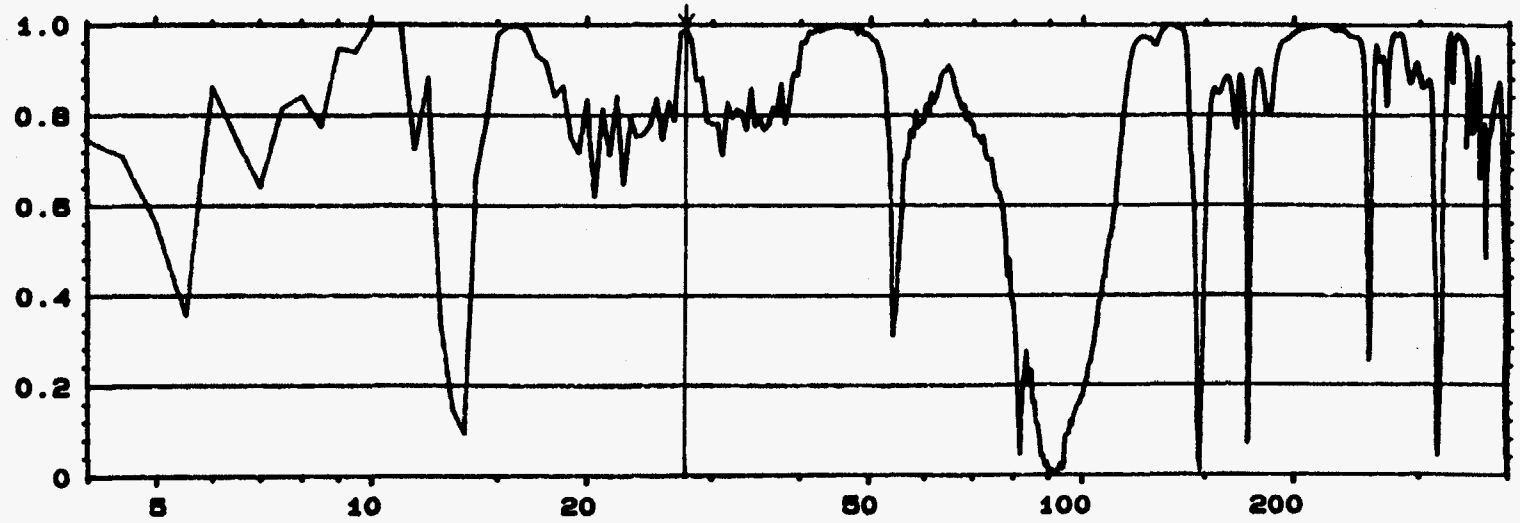

W2 COHERENCE MAIN Y: 987m
Y: 1.00 X: 27.5Hz
X: 4Hz TO 400Hz LOG
SETUP W12 #A: 10

Bruel Kjaer

Type 2034

Page No.
97

Sign.:

Meas.
Object:

Comments:

Test 24

W2 AUTO SPEC CH.A
Y: 10.7mU /Hz PSD 80dB
X: 4Hz TO 400Hz LOG
SETUP W12 #A: 20

MAIN Y: 42.3E-9U /Hz
X: 29.5Hz

TOTAL : 16.2mU

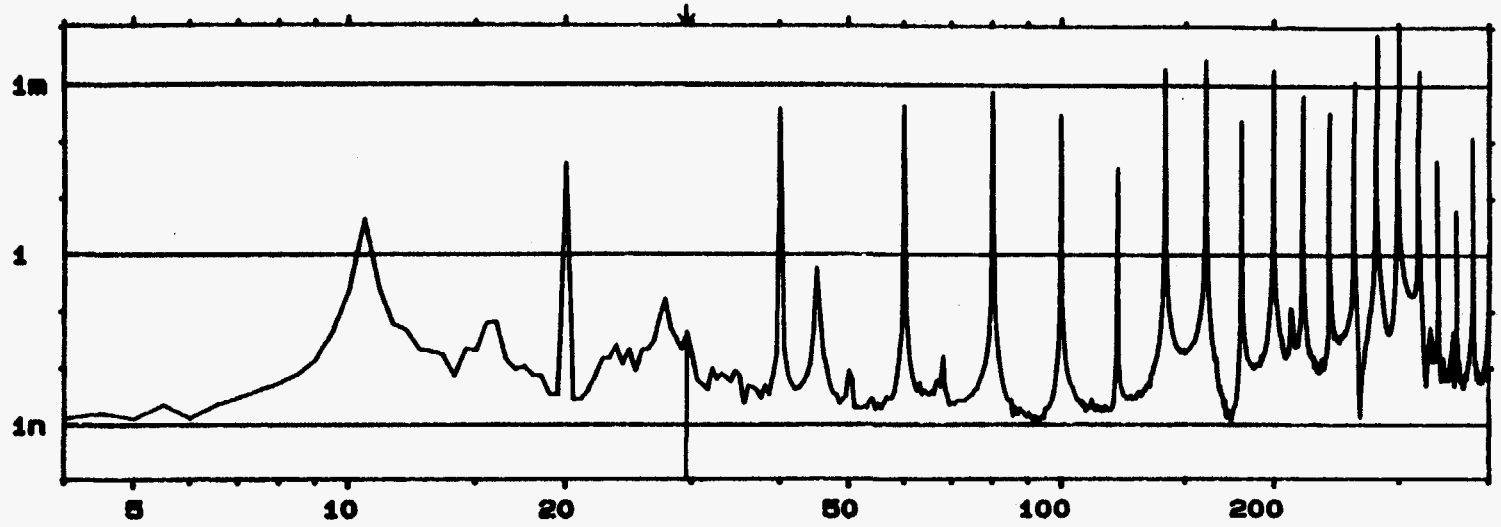

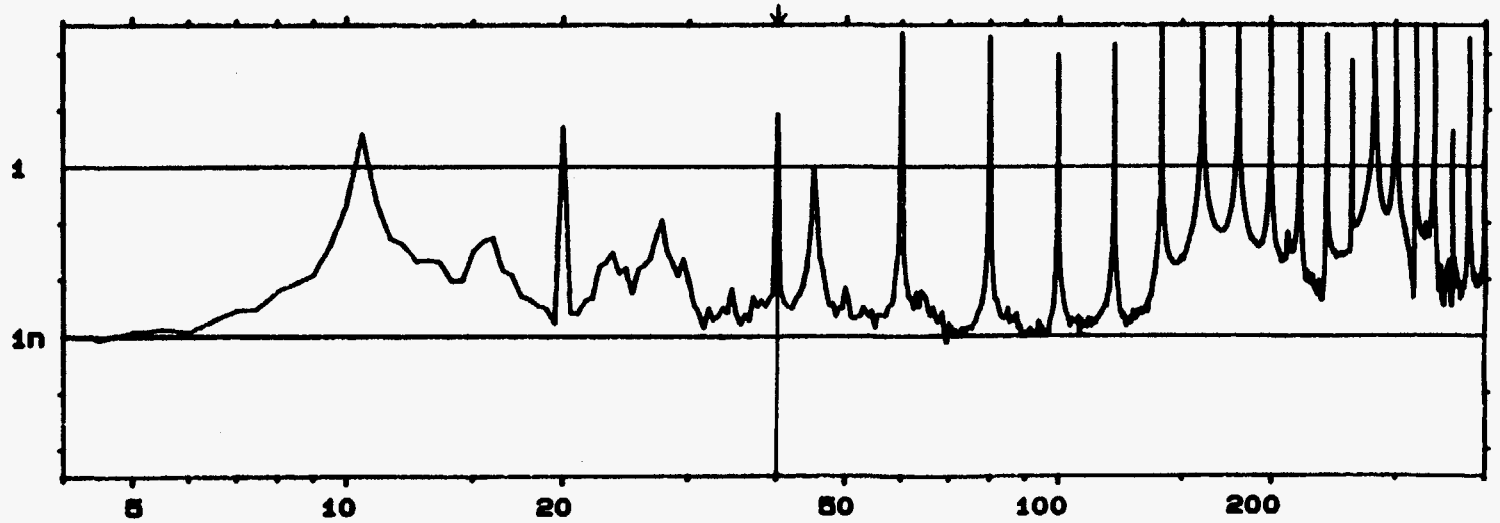

W2 AUTO SPEC CH.B
Y: 325 U /Hz PSD 80dB
X: 4Hz TO 400Hz LOG
SETUP W12 #A: 20

MAIN Y: 8.16 U /Hz
X: 40.0Hz

TOTAL : 30.3mU

Bruel Kjær

Type 2034

Page No.
98

Sign.:

Meas.
Object:

Comments:

Test 24

W2 AUTO SPEC CH.A
Y: 6.13E-9U /Hz PSD 80dB
X: 4Hz TO 400Hz LOG
SETUP W12 #A: 20 $1/j\omega^2$

MAIN Y: 1.23E-12U /Hz
X: 29.5Hz

TOTAL : 15.9E-9U

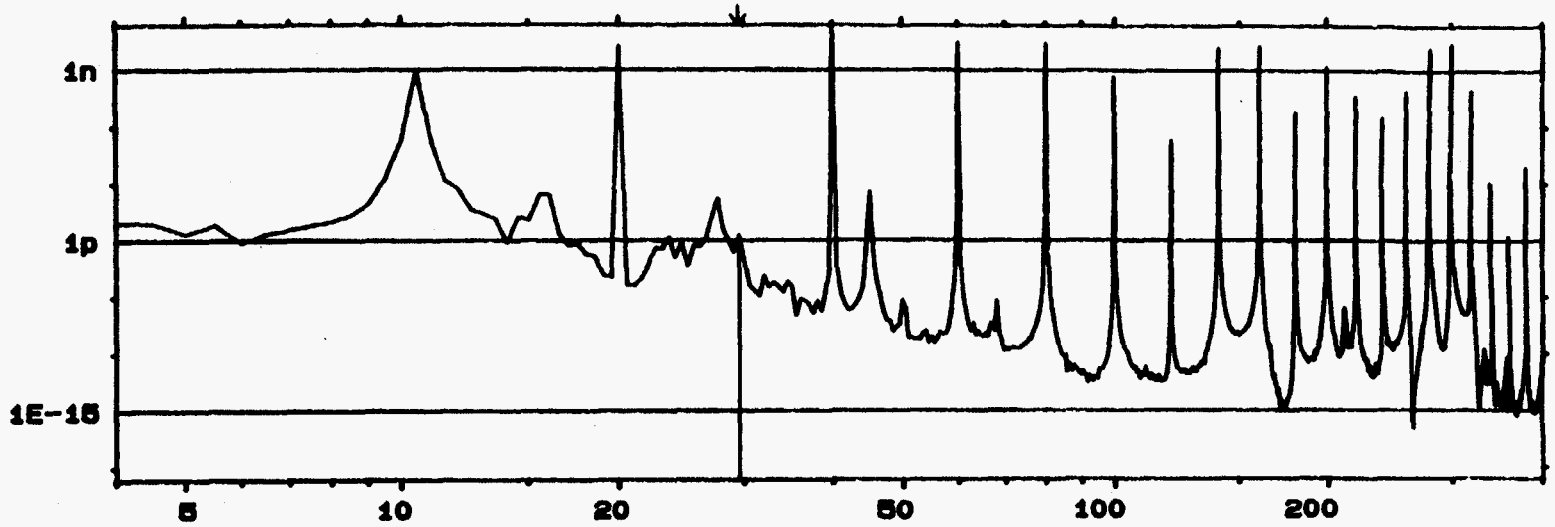

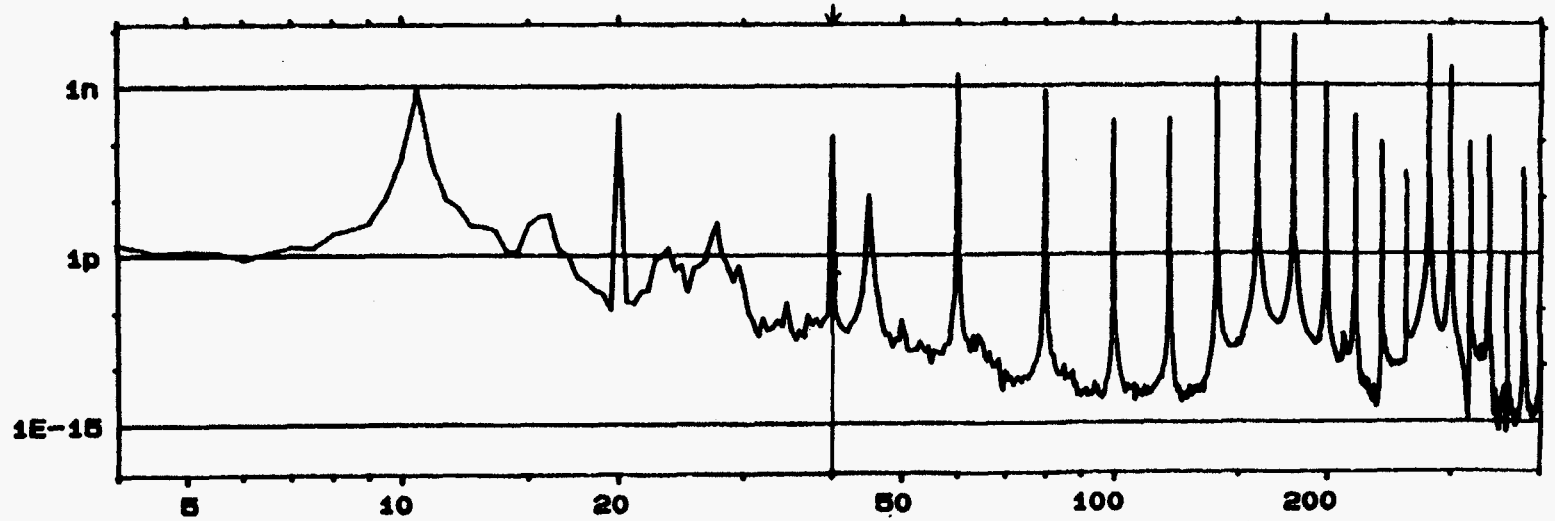

W2 AUTO SPEC CH.B
Y: 12.7E-9U /Hz PSD 80dB
X: 4Hz TO 400Hz LOG
SETUP W12 #A: 20 $1/j\omega^2$

MAIN Y: 129E-12U /Hz
X: 40.0Hz

TOTAL : 19.2E-9U

Bruel Kjaer

Type 2034

Page No.
99

Sign.:

Meas.
Object:

Commente:

Test24

W2 AUTO SPEC CH.A
Y: 335E-9U RMS 80dB
X: 4Hz TO 400Hz LOG
SETUP W12 #A: 20 1/jω²

MAIN Y: 4.21E-9U
X: 29.5Hz

TOTAL : 5.32 U

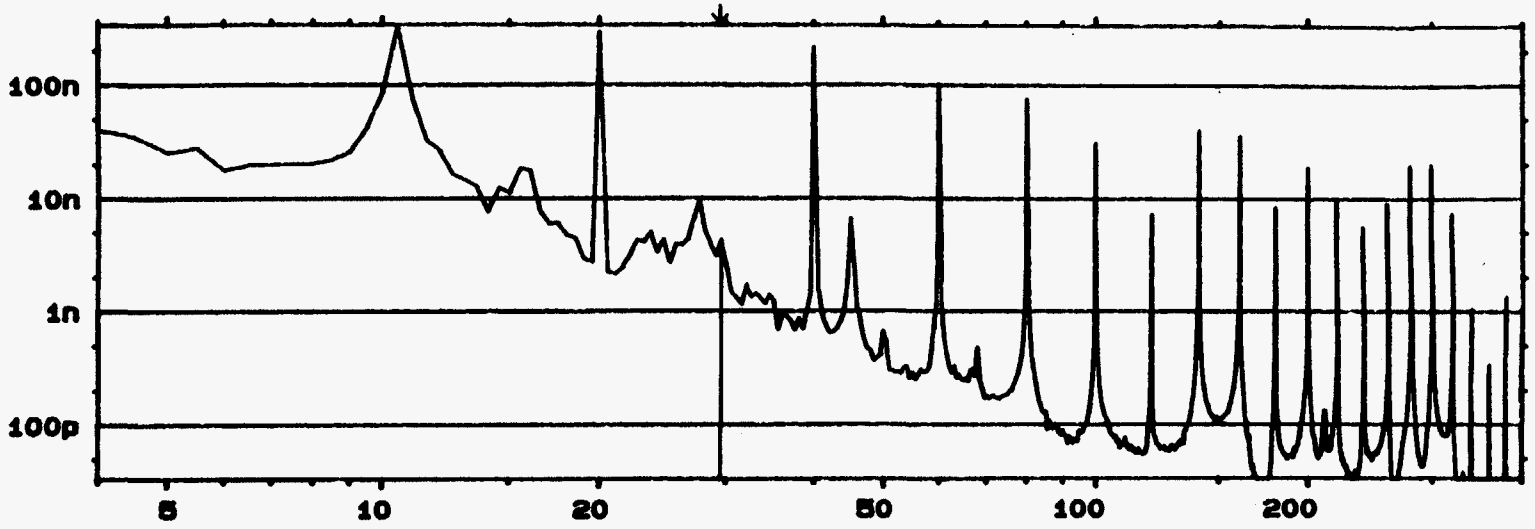

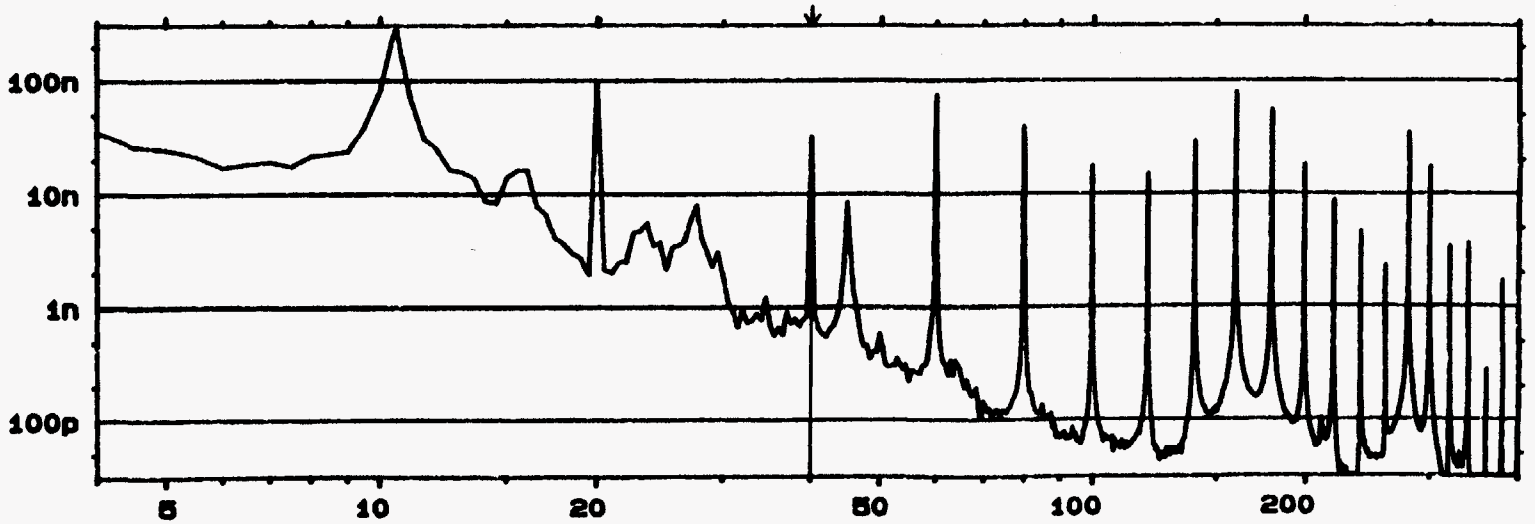

W2 AUTO SPEC CH.B
Y: 313E-9U RMS 80dB
X: 4Hz TO 400Hz LOG
SETUP W12 #A: 20 1/jω²

MAIN Y: 31.9E-9U
X: 40.0Hz

TOTAL : 2.56 U

Bruel Kjaer

Type 2034

Page No.
100

Sign.:

Meas.
Object:

Comments:

Test 24

W2 AUTO SPEC CH.A
Y: 6.13E-9U /Hz PSD 80dB
X: 4Hz TO 400Hz LOG
SETUP W12 #A: 20 1/j

MAIN Y: 1.23E-12U /Hz
X: 29.5Hz

TOTAL : 15.9E-9U

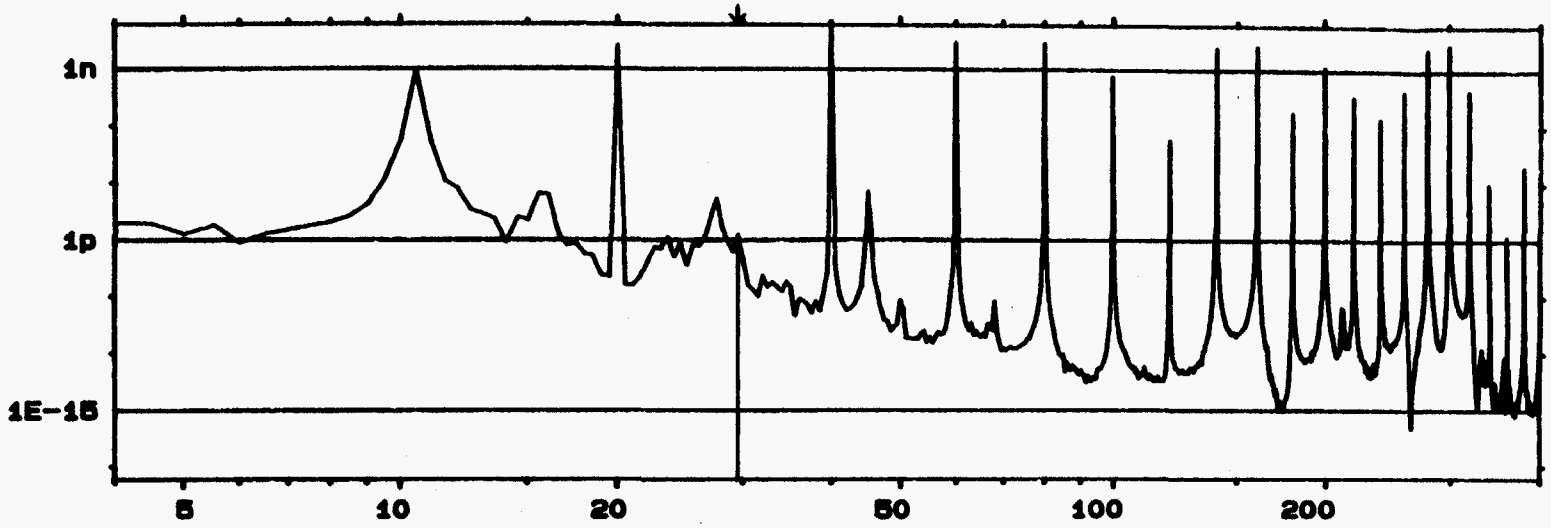

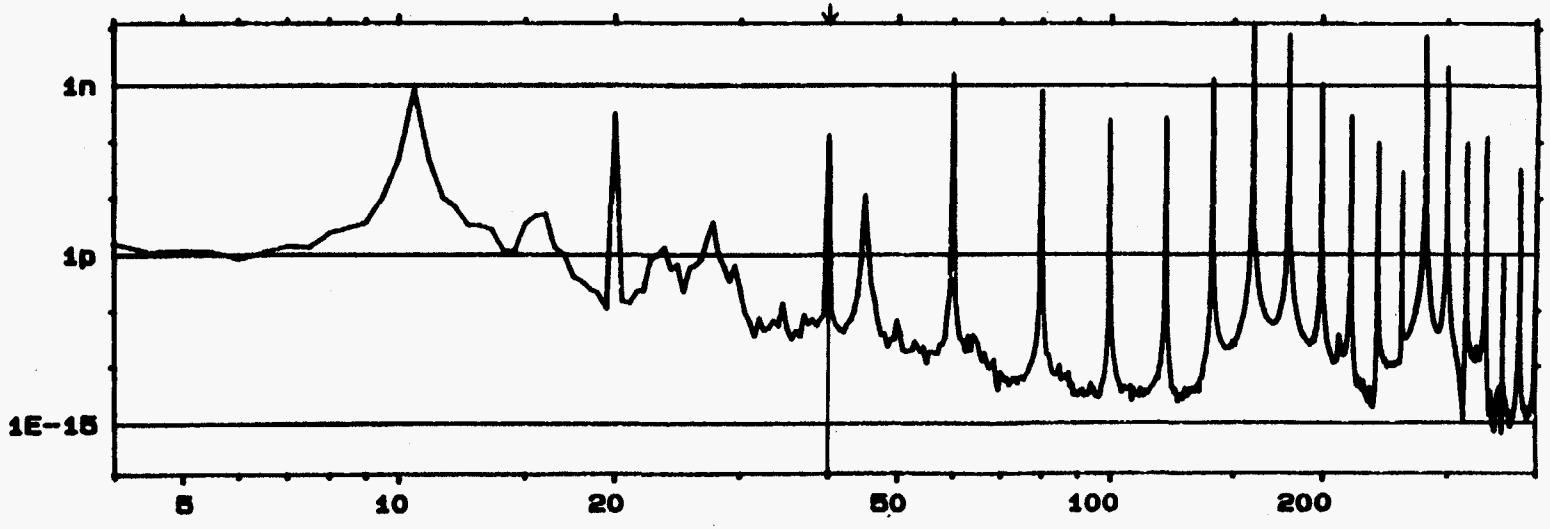

W2 AUTO SPEC CH.B
Y: 12.7E-9U /Hz PSD 80dB
X: 4Hz TO 400Hz LOG
SETUP W12 #A: 20 1/j

MAIN Y: 129E-12U /Hz
X: 40.0Hz

TOTAL : 19.2E-9U

Appendix E - COSMOS model and Von Mises Stress Plots for RI-BM-01

GeoStar 1.75: BM016

Main Jack Body Stress Plot for $\frac{1}{4}$" weld

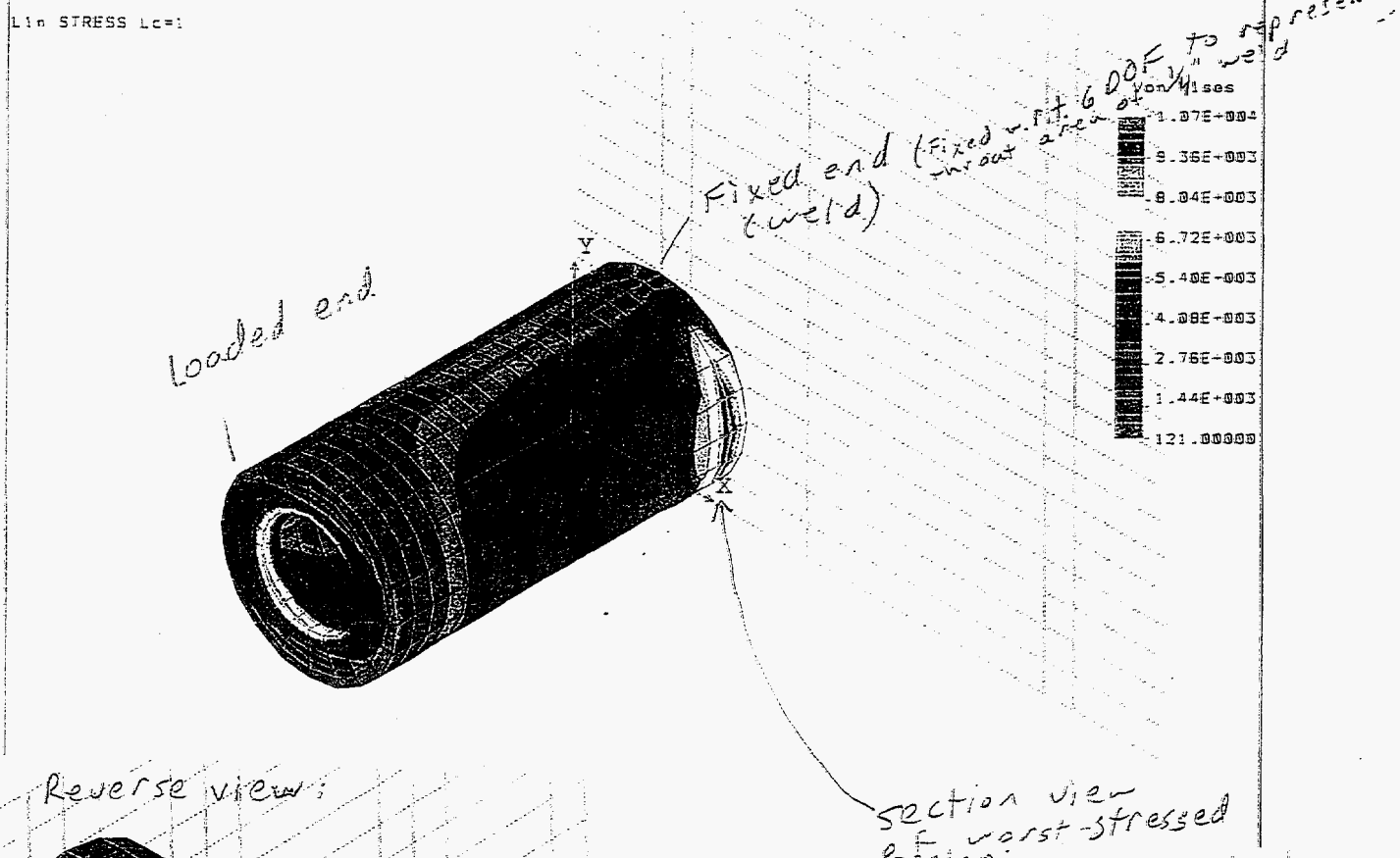

Reverse view:

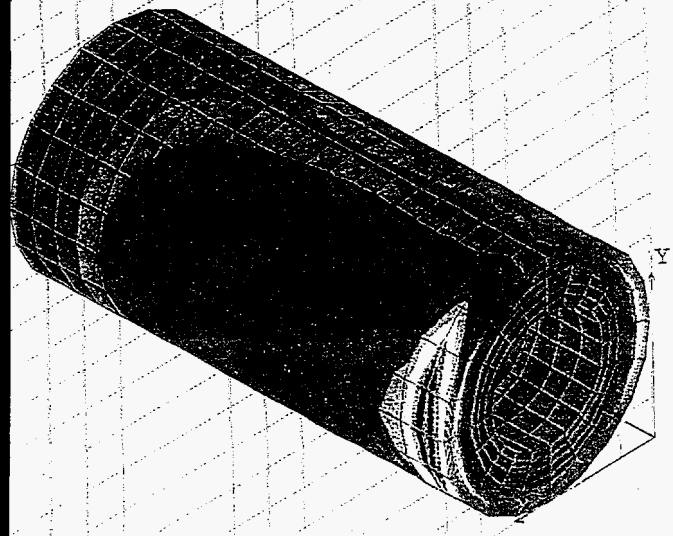

Section view of worst-stressed region:

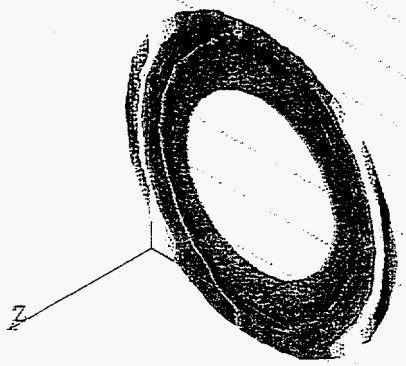

GeoStar 1.75 : BM011

Collar Plate Stress Plot

cosmos file RIBM011.gen

Lin STRESS Lc=1

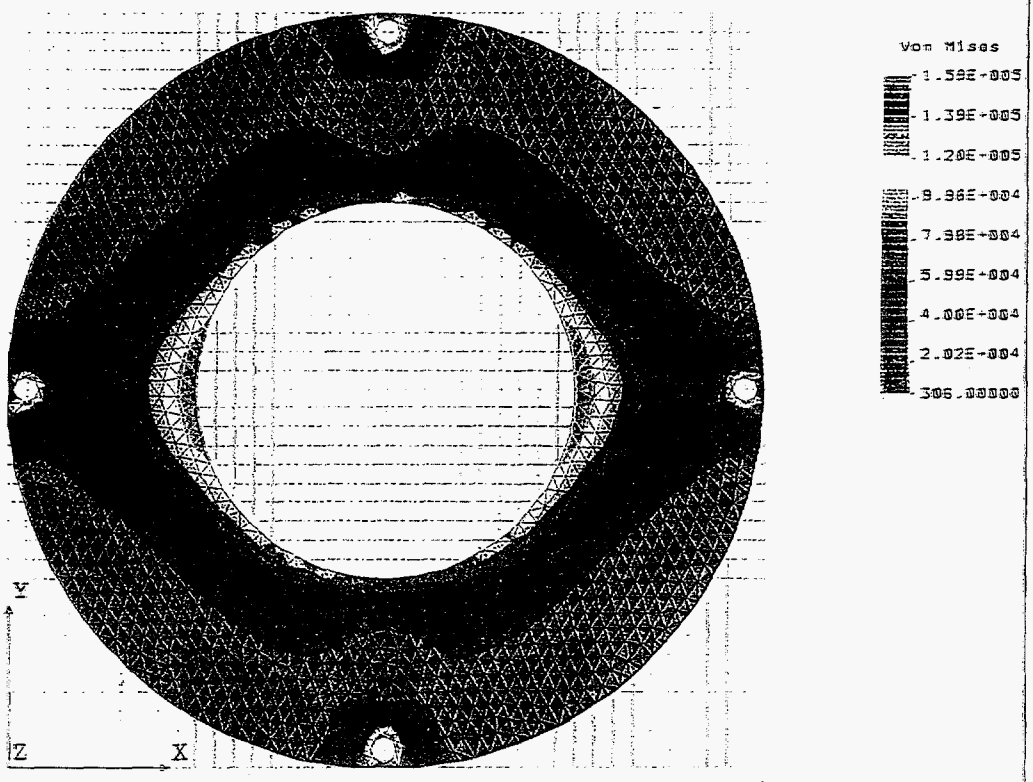

Plate thickness = 0.25"

Comments:

Majority of plate is failing — way beyond yield strength.

must thicken plate

GeoStar 1.75 : BM012

Collar Plate Stress Plot

Cosmos file RIBM012.gen

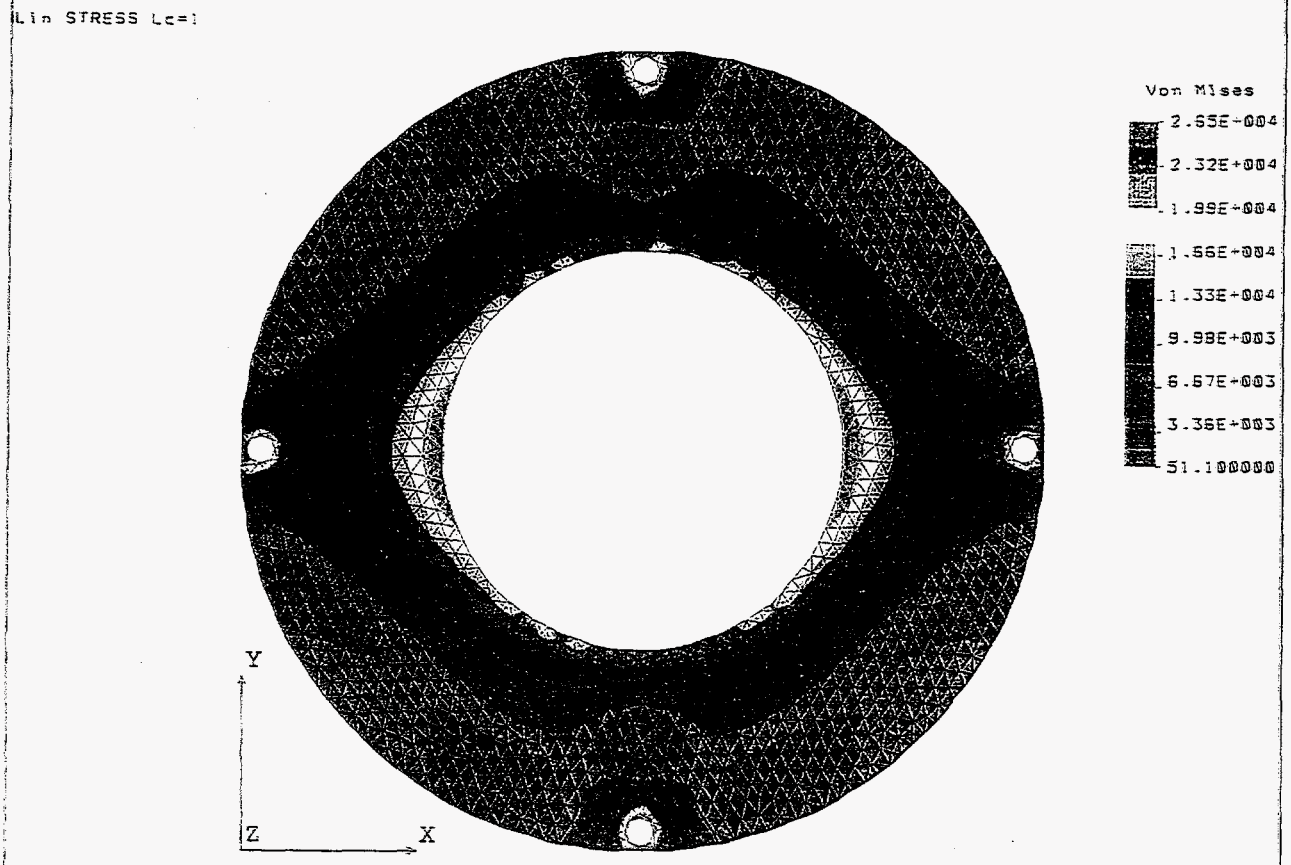

Plate thickness = 0.5"

Comments

All stresses are below yield strength, and majority (> 90%) of plate has a safety factor > 2. And since this corresponds to the worst-case loaded jack stand, the design is acceptable.

GeoStar 1.75: jbi

Collar Plate stress Plot

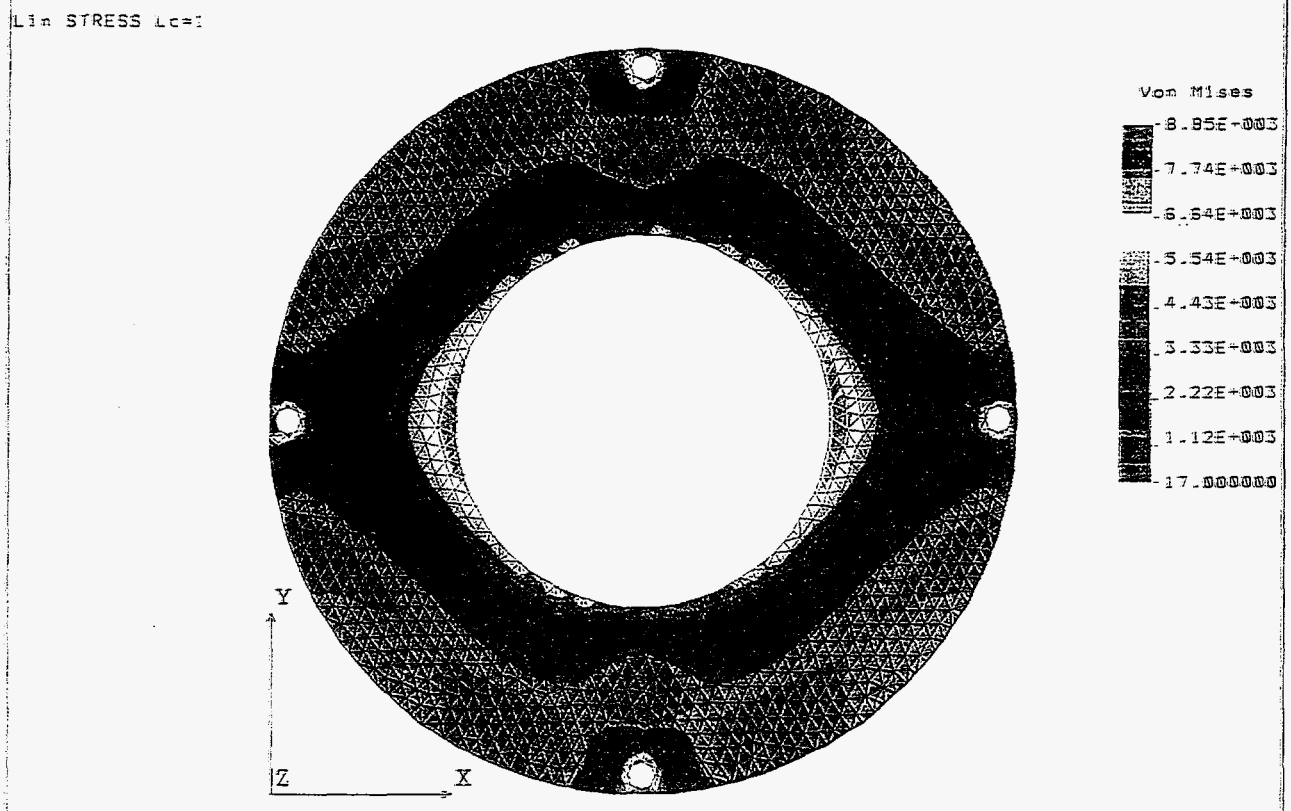

Plate thickness = 0.75"

comment S.F. > 3 for 100% of Plate

Base Plate $TRESS PLOT

Cosmos File BM013.gen

Loading (1)

$g_x = 2$ lbs (into page)

$\rightarrow$ 2470 lbs

$M_y = 88697$ in.lbs

} applied to contour G (distributed among nodes)

Lin STRESS Lc=1

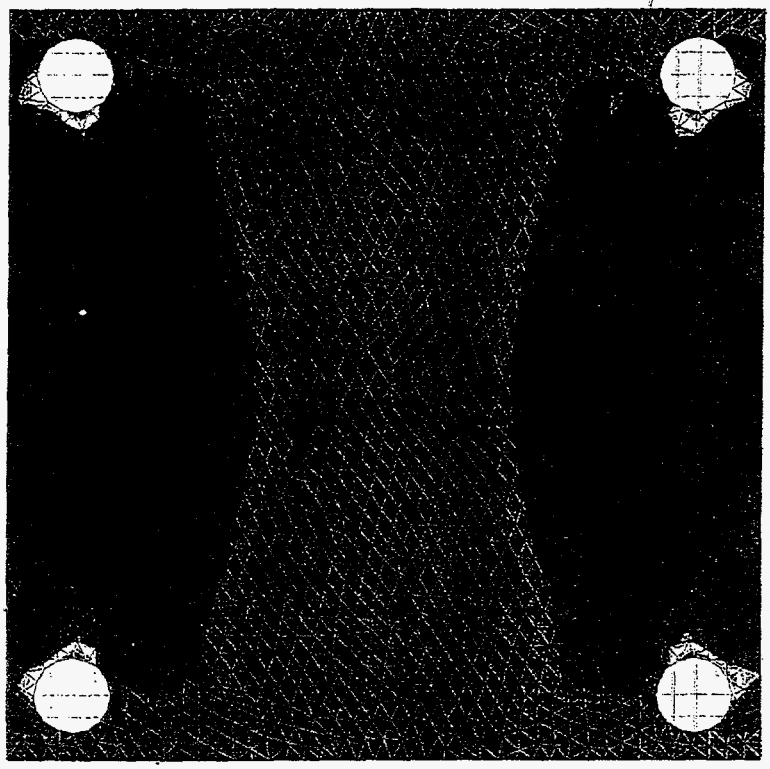

Von Mises
5.20E+004
5.43E+004
4.65E+004
3.88E+004
3.11E+004
2.33E+004
1.56E+004
7.87E+003
137.00000

plate thickness = 0.75"

Comment

Too high of stresses in green yellow & red areas. Must strengthen plate — thickness = 1.00"?

GeoStar 1.75: BM013

Base Plate Stress Plot

Cosmos file: BM013.gen

Loading (2)

x 892 lbs (into page)

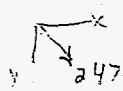

$\Rightarrow$ $F_x = 1,746.6$ lbs
$F_y = 1,746.6$ lbs
$M_x = 68,005$ in-lbs
$M_y = 68,005$ in-lbs
} applied to contour 6 distributed among nodes

Lin STRESS Lc=1

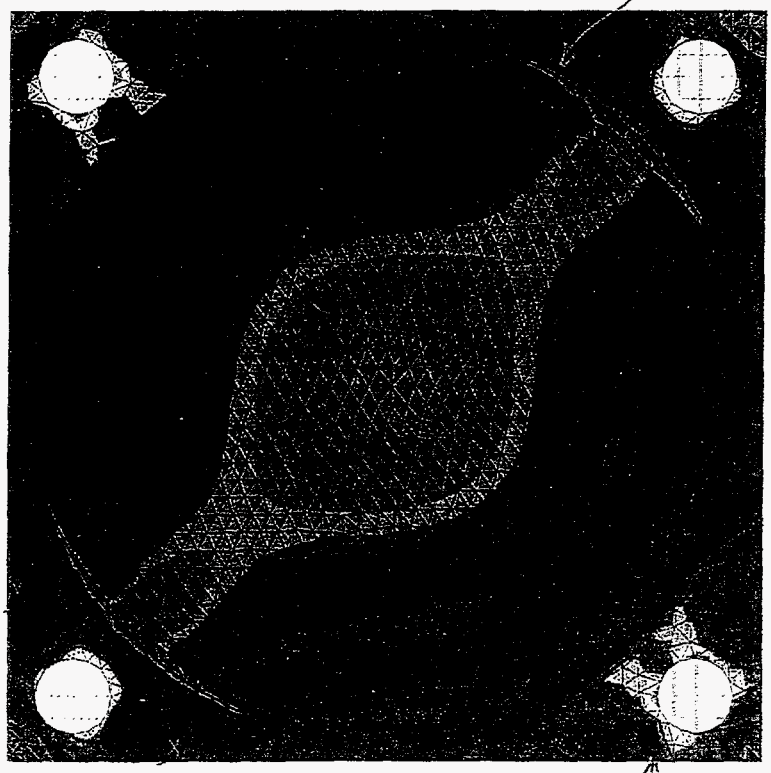

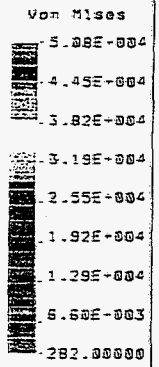

area of highest stress

Plate thickness = 0.75"

Comments

Stress too high - increase plate thickness to 1.00".

GeoStar 1.75: BM013

Base Plate Stress Plot

Cosmos file BM013.ges

Loading (2)

× 892 lbs (into page)

2470 lbs ⇒ F_x = 1746.6 lbs

F_y = 1746.6 lbs

M_x = 65,005 in-lbs

M_y = 65,005 in-lbs

applied to contour 6 distributed among nodes

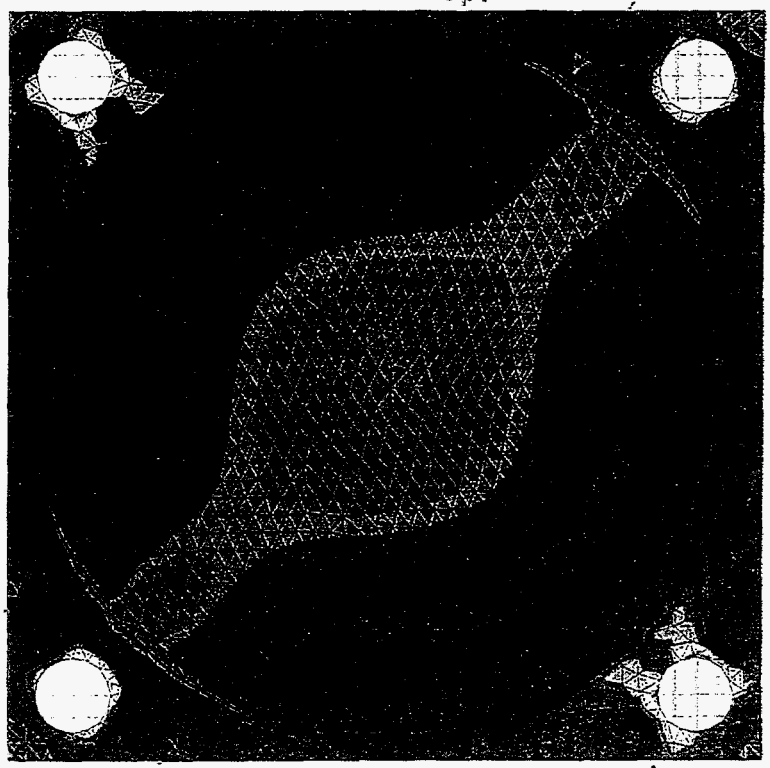

area of highest stress (see next page)

Plate Thickness = 1.00"

Comments:

stress level is acceptable SF > 2.7 for more than 95% of plate. (High local stresses will be smoothed out by washers - giving S.F ≈ 3)

Base Plate Stress Plot with deformation.

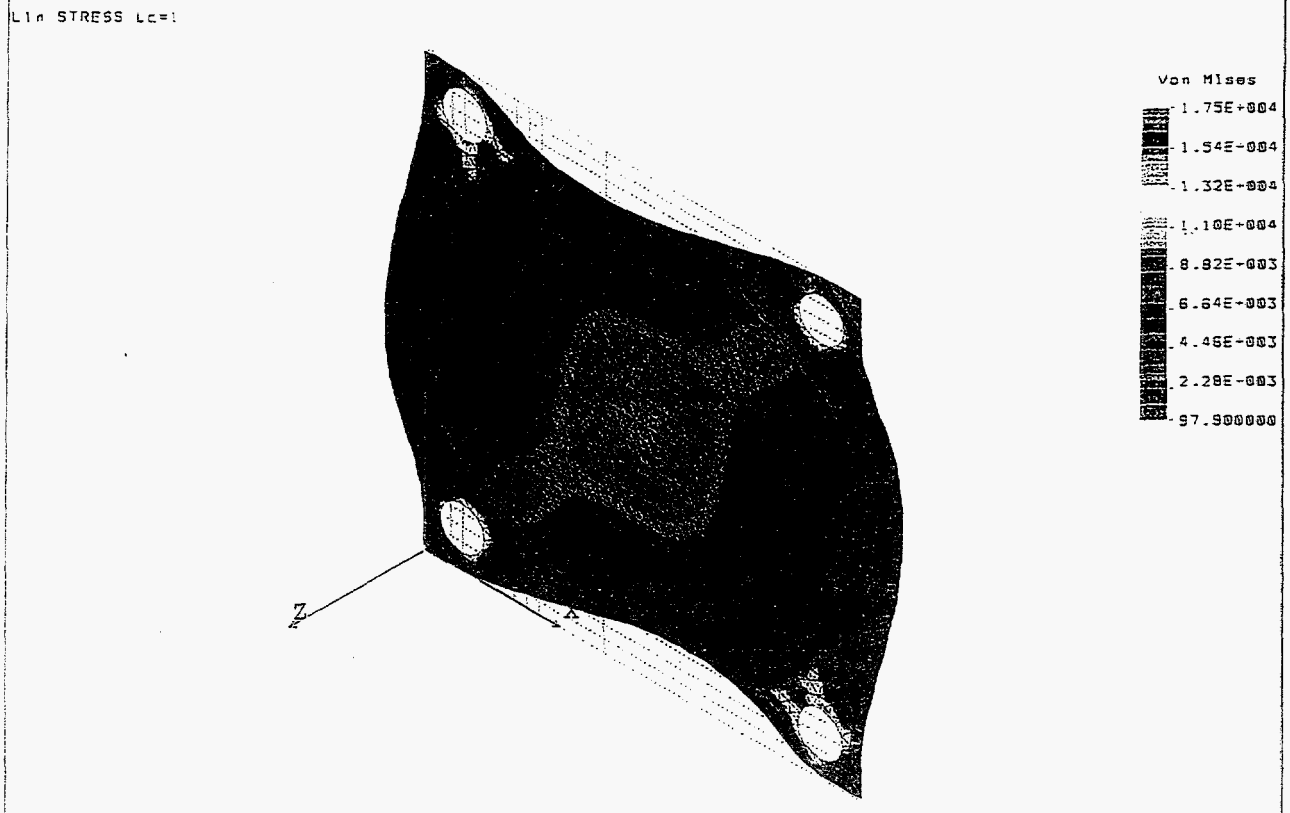

GeoStar 1.75: BM013

Base Plate

Stress Plot
cosmos file BM013.gen

bolt site a

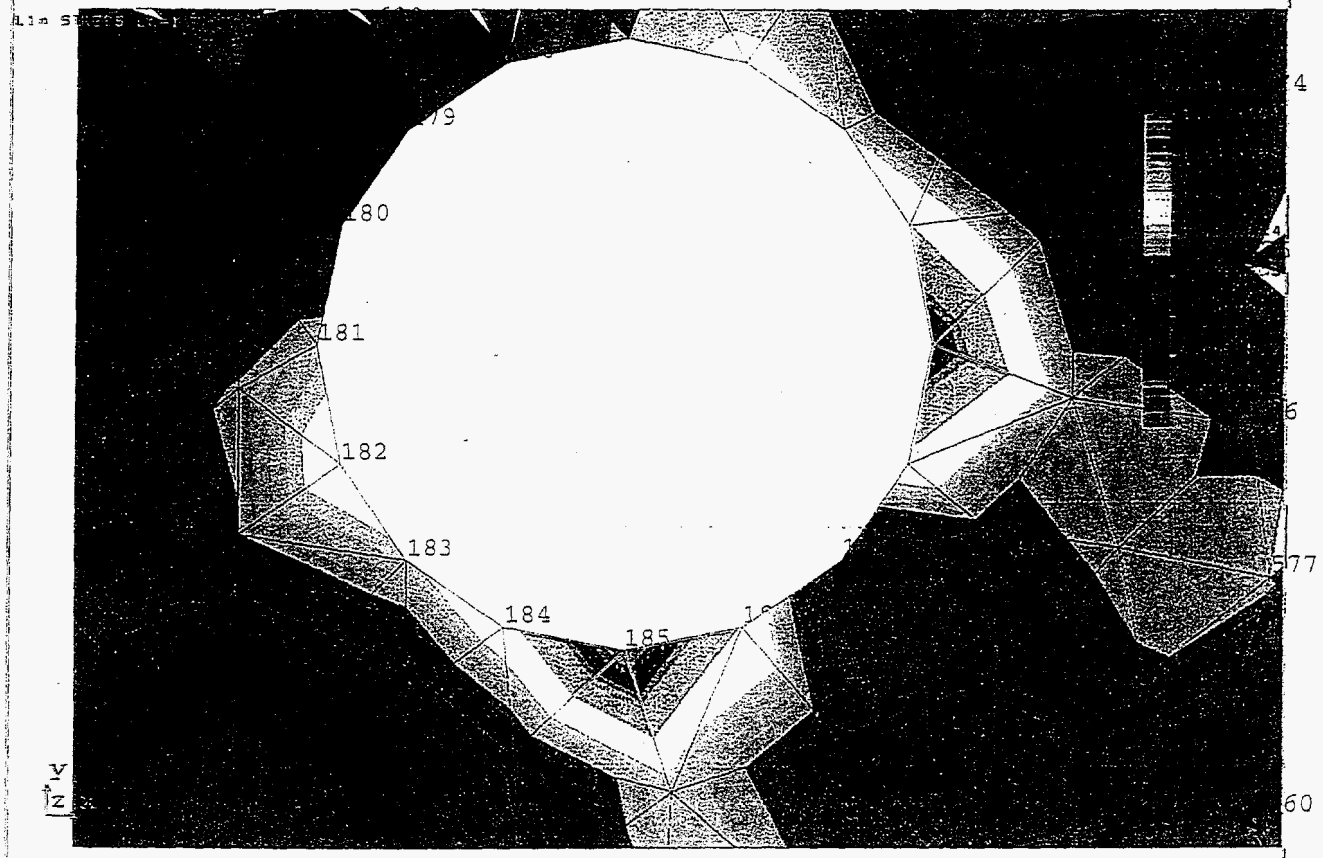

GeoStar 1.75: BM013

Base Plate stress Plot
cosmos file BM013.ges

bolt site C ⇒ see next few pages for reaction forces at nodes

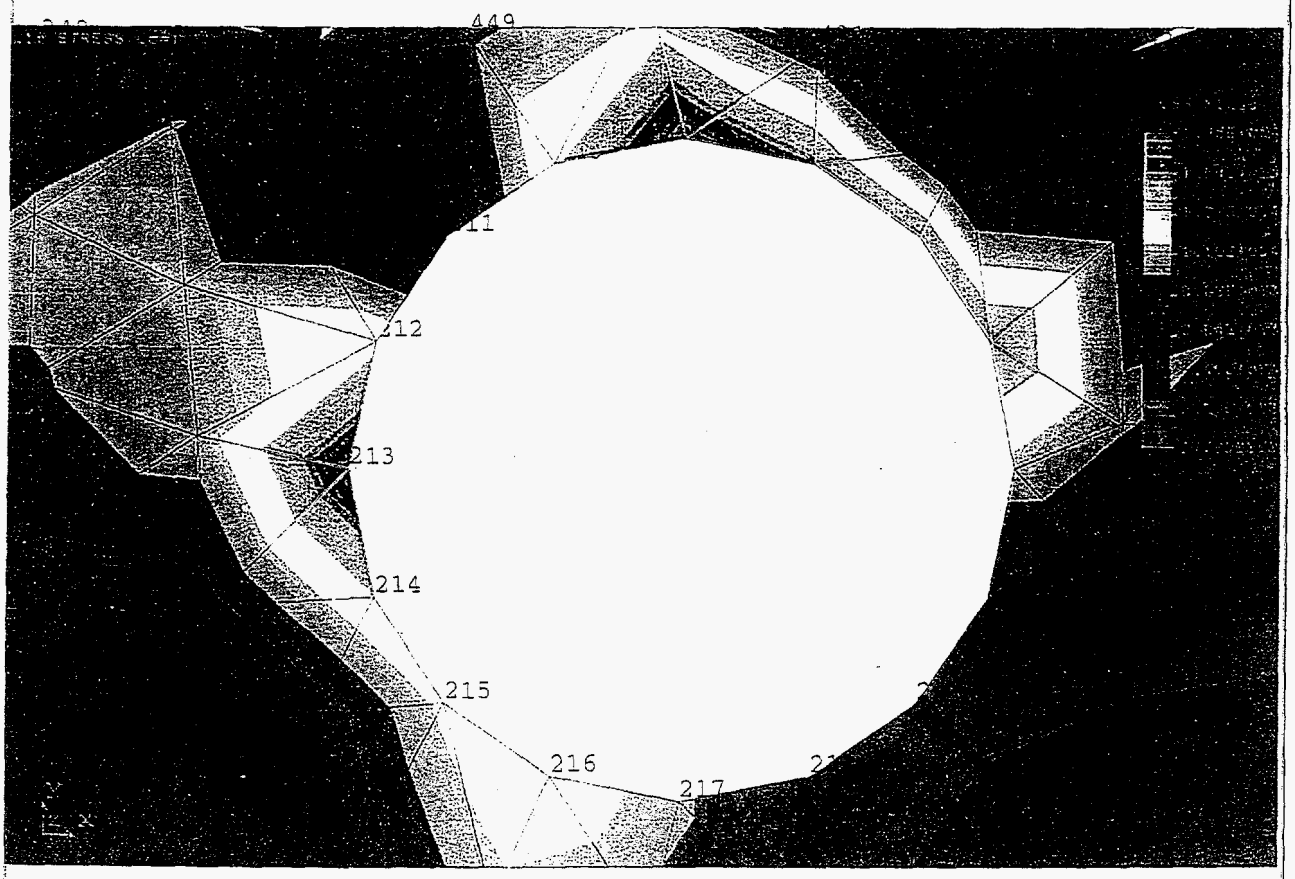

GeoStar 1.75: BM019

Riser Tube in Pedestal

Stress plot

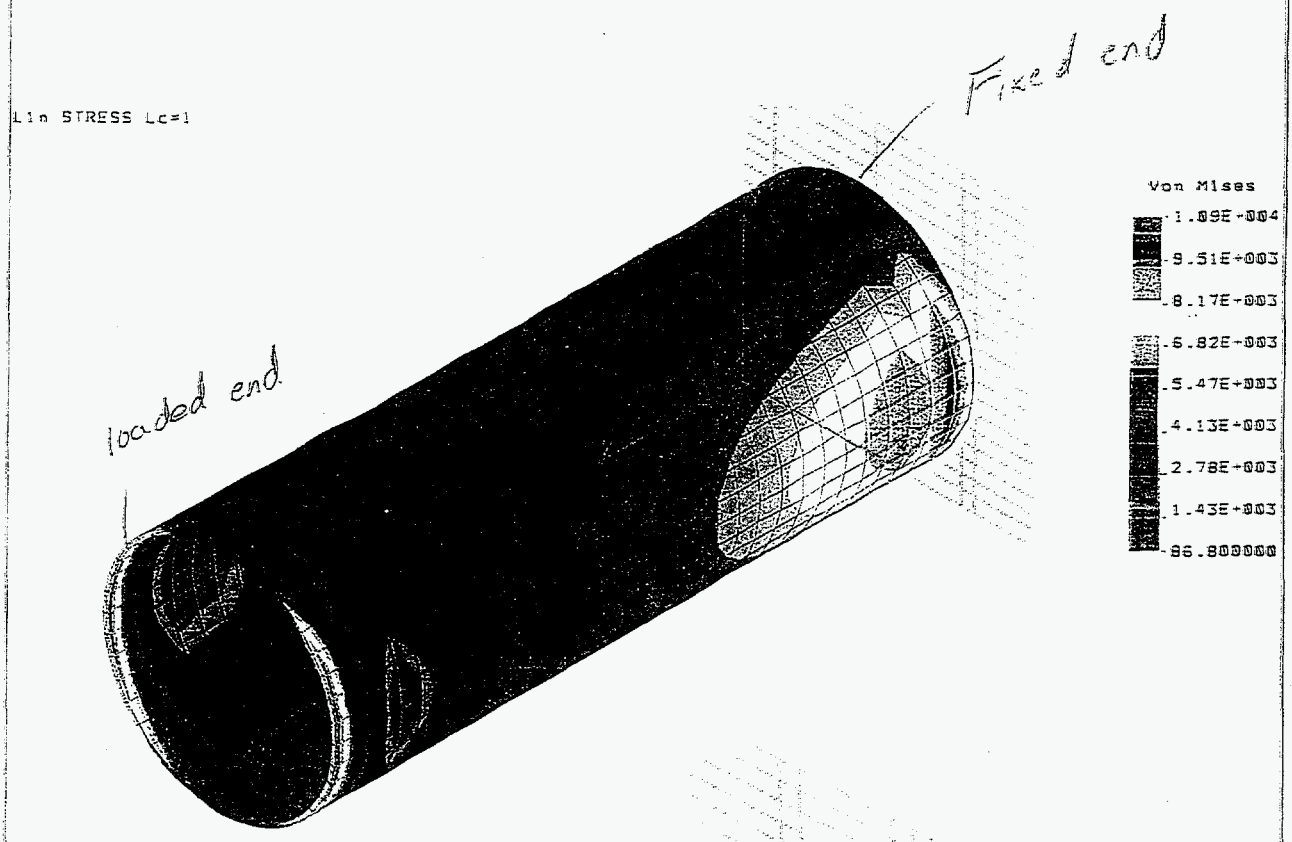

Section Plot of highest Stressed region

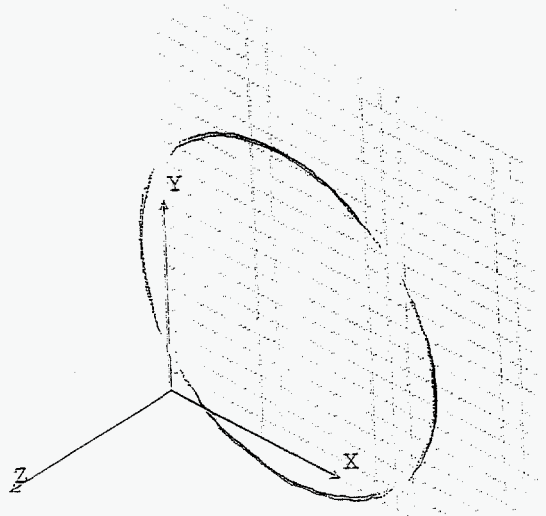

S.F. $= \frac{35}{11} = 3.2$

Appendix F - COSMOS model and Von Mises Stress Plots for RI-QF-02

GeoStar 1.75: QF021

Deformed stress flat ceiling plate.

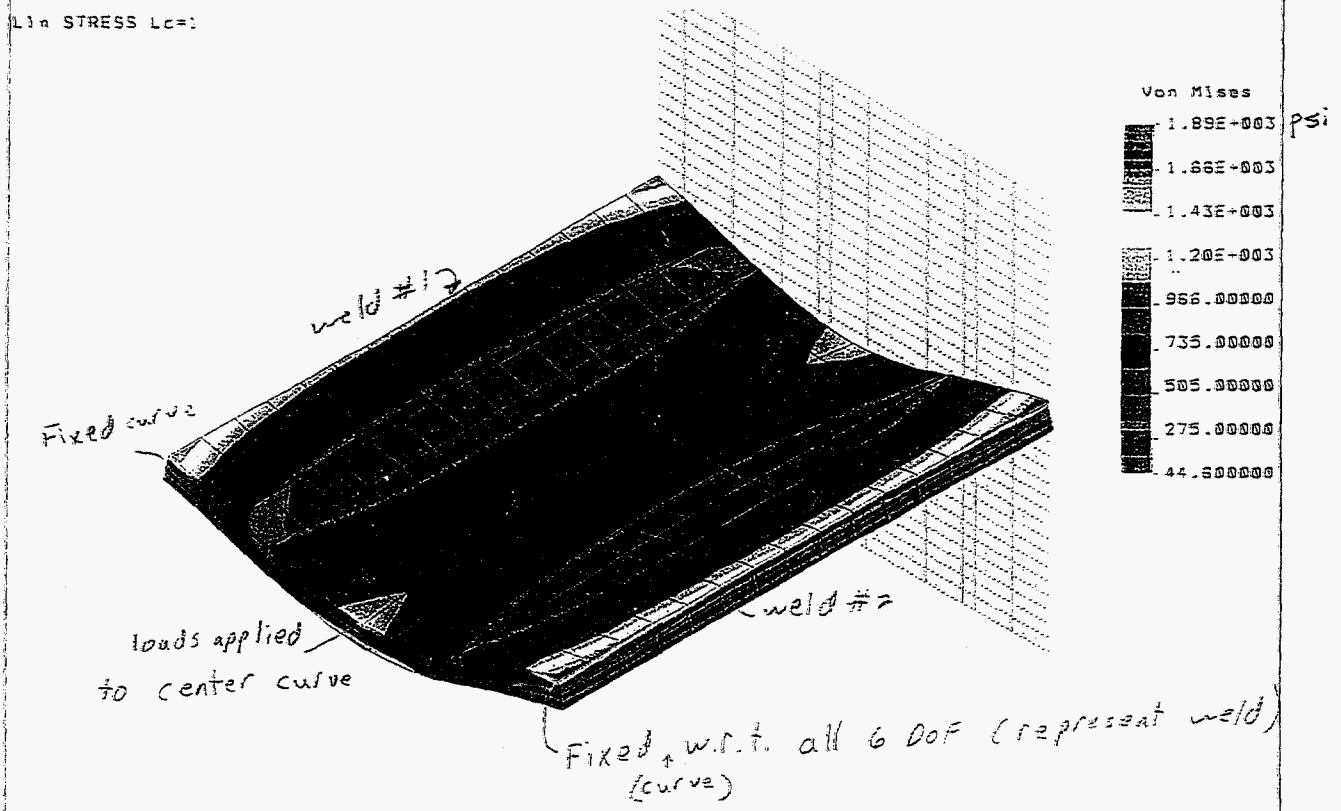

Note: The actual weld will be spread out (less concentrated than above model where just the edge curve is fixed). Thus the stresses will be more spread out along edge, max stress will be < 1.9 ksi. Even so, S.F. > 3 $\quad S.F. = \frac{35}{1.9} = 18.4$

GeoStar 1.75: QF021

Deformed Stress Plot
Ceiling Plate

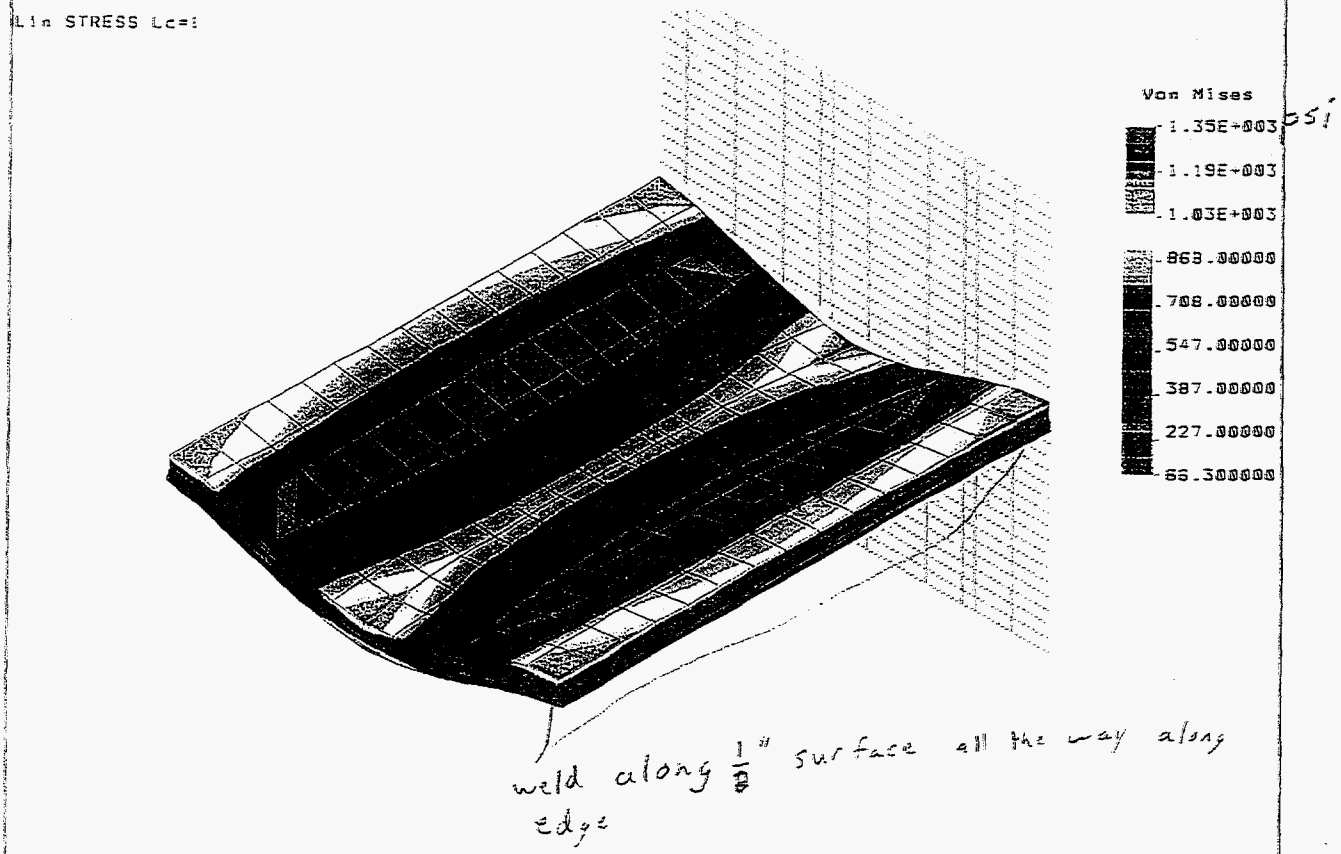

weld along $\frac{1}{8}$" surface all the way along edge

GeoStar 1.75: QF022b

stress plot
upper plate

edges of all 4 bolt holes fixed with respect to all 3 translations.

loading spread out to a contour with a radius of 1" representing the riser body through which the loads will be transmitted.

attachment

L1a STRESS Lc=1

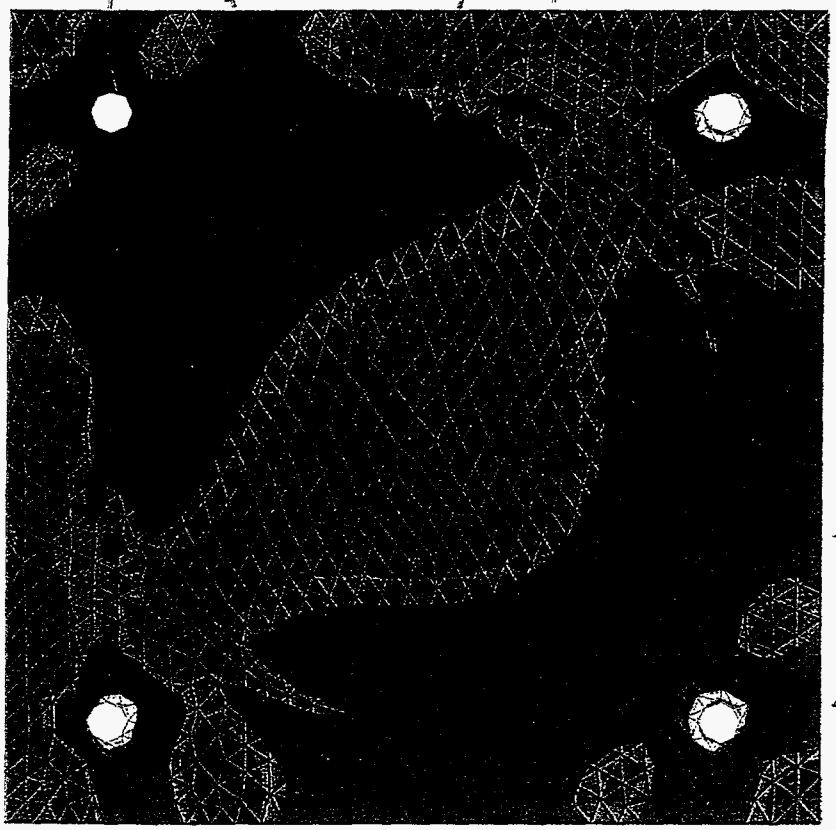

Shell 3 elements (0.75" thick)

worst loaded bolt (nodes 145-152)

Y
Z X

$\sigma_y = 35$ ksi

Comments

Except for small regions of high stresses (≈10-12 ksi) All stresses are low with S.F. > 3. In actuality, washers at the bolt holes will spread out the loading at the bolt location and reduce these stresses below 10 ksi, thus easily giving a S.F. > 3.

GeoStar 1.75: QF022b

Stress plot with Deformations

Upper Plate

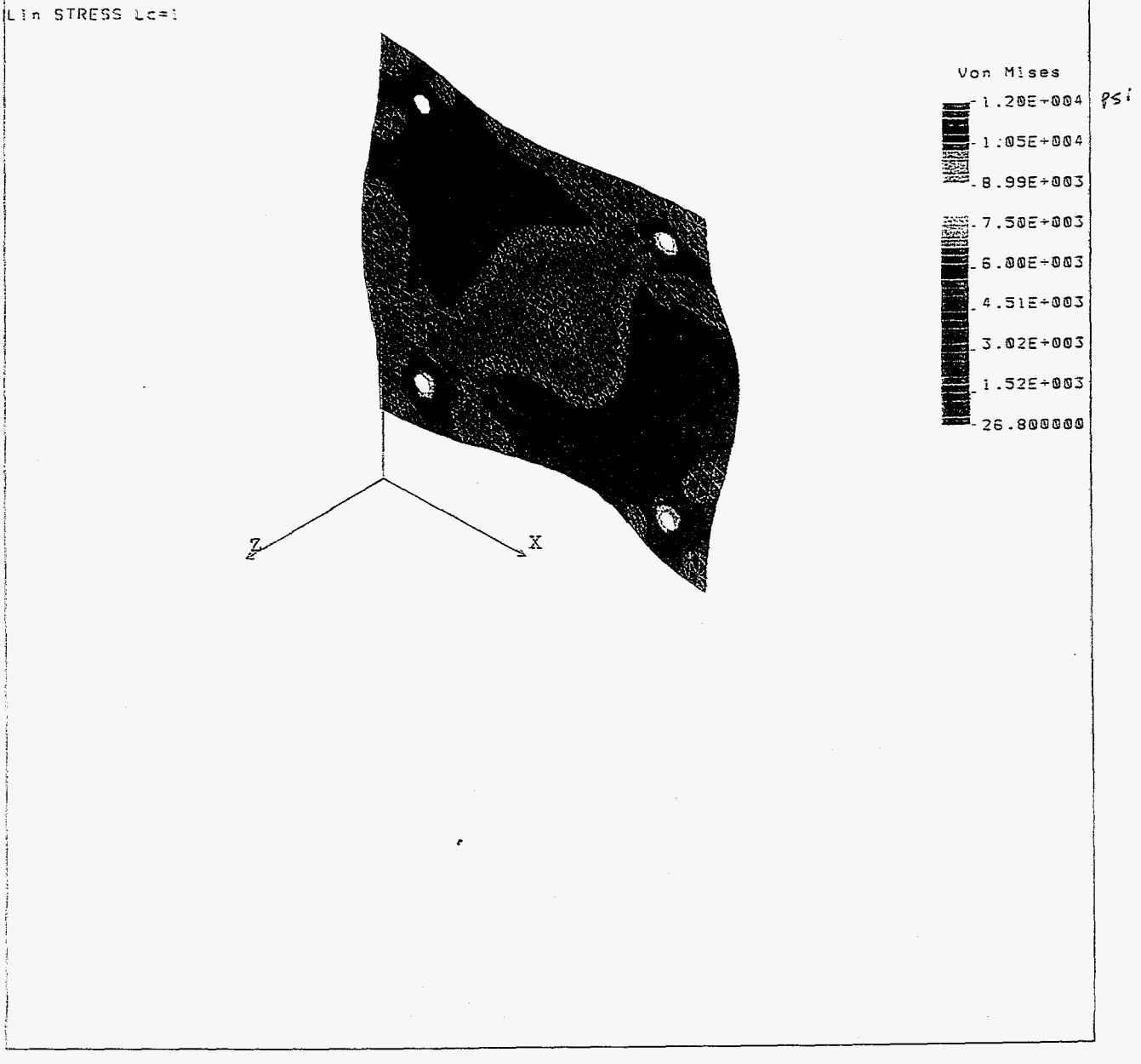

model

Riser Tube

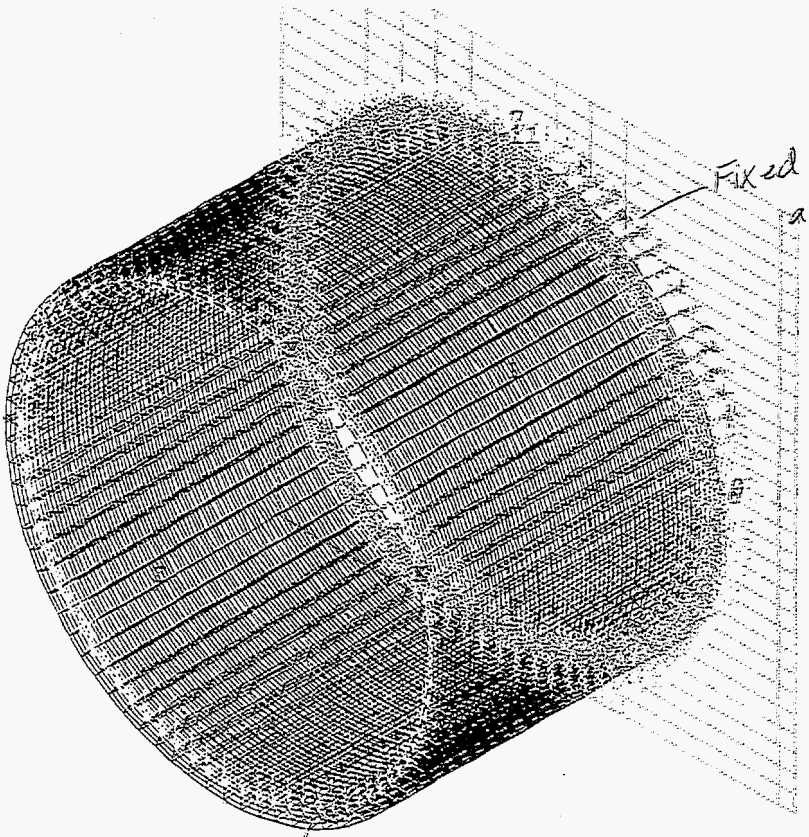

GeoStar 1.75: QF023

Riser Tube

Lin STRESS Lc=1

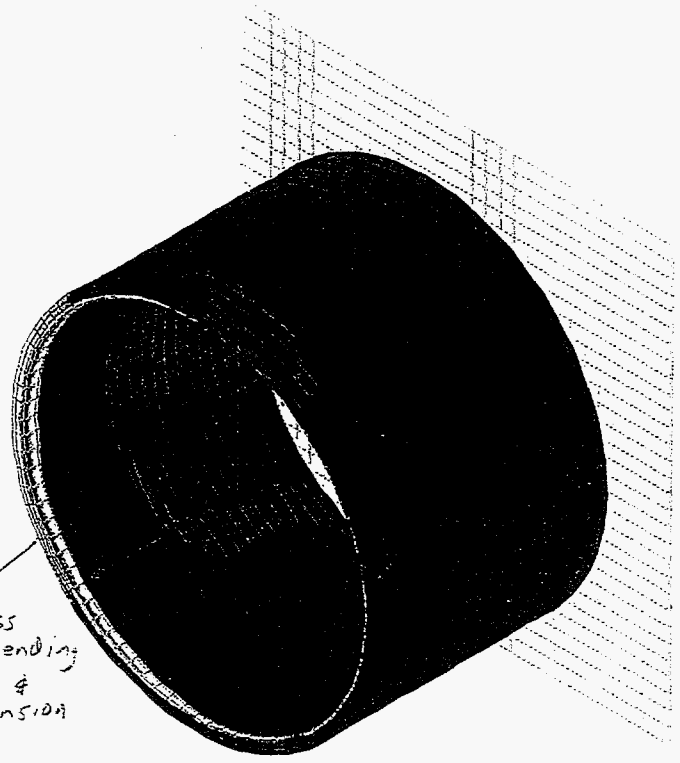

max stress due to bending (tension) & axial tension

Comment

Stresses are well below σ_y

$S.F. = \frac{35}{1.1} = 31.8$

GeoStar 1.75 : QF023

Stress plot
alternate view
Riser Tube

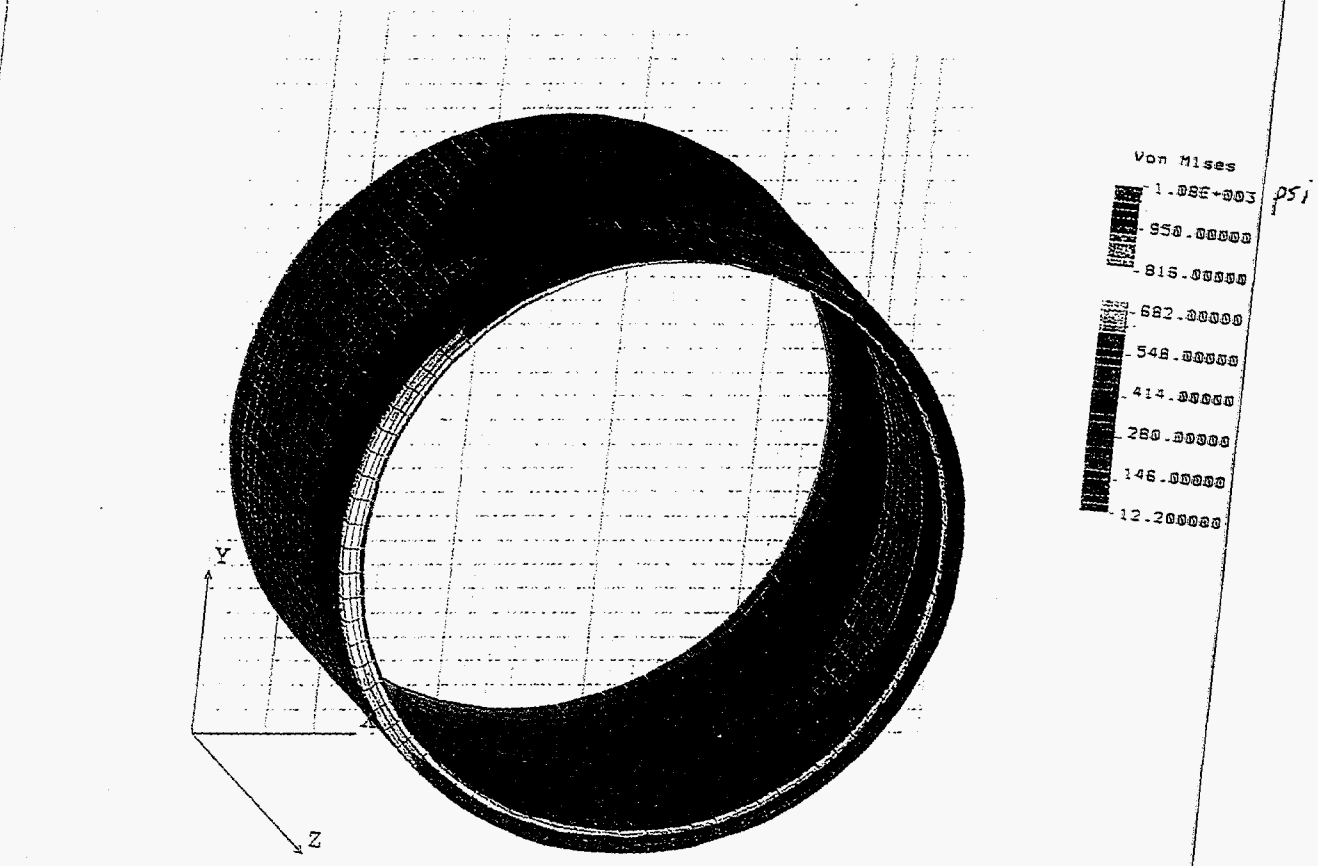

GeoStar 1.75 : QF023

stress Plot with exaggerated deformations

Riser Tube

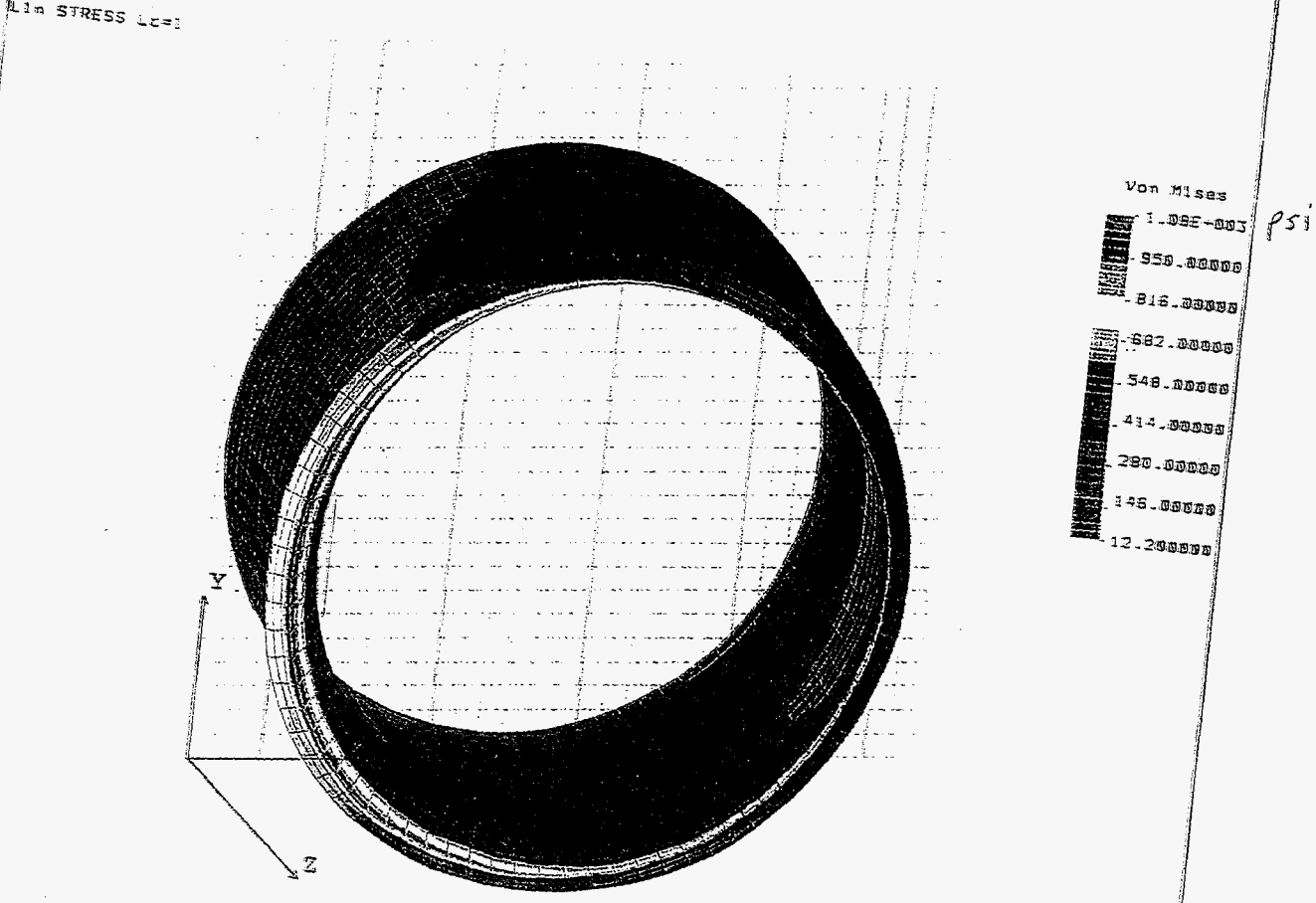

GeoStar 1.75: QF024

upper adjuster plate

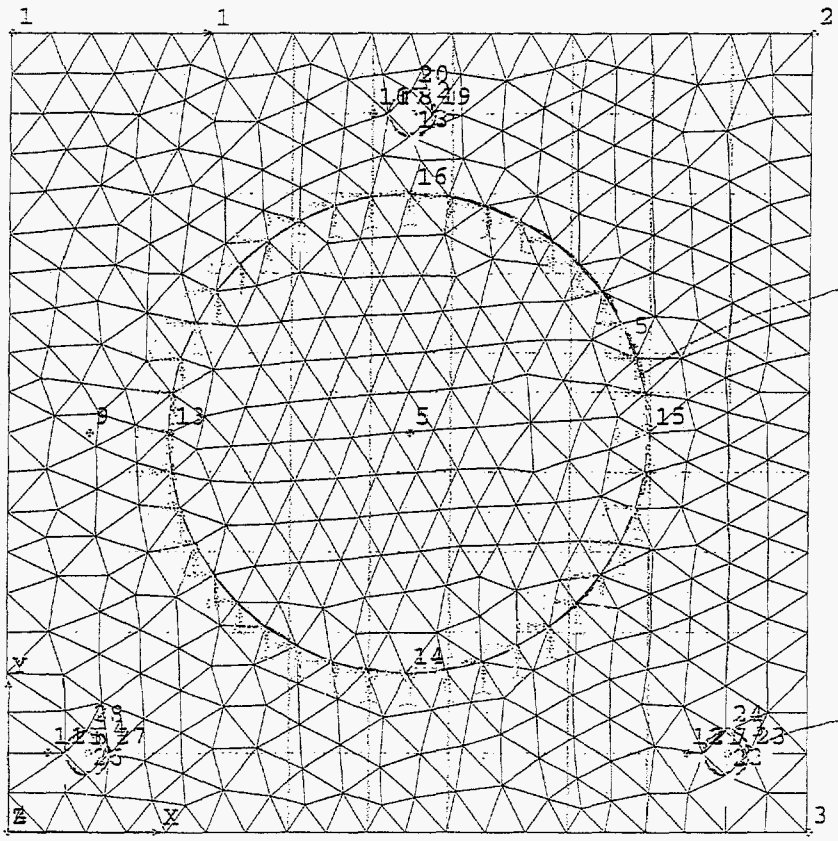

fixed w.r.t. all 6 DOF (along riser weld line, gusset neglected)

loading applied to edge of threaded rod

two loading orientations considered

orientation 1

P_s

orientation 2

P_s

GeoStar 1.75: QF024

orientation 1
von Mises stress plot

Upper Adjuster Plate

Lin STRESS Lc=1

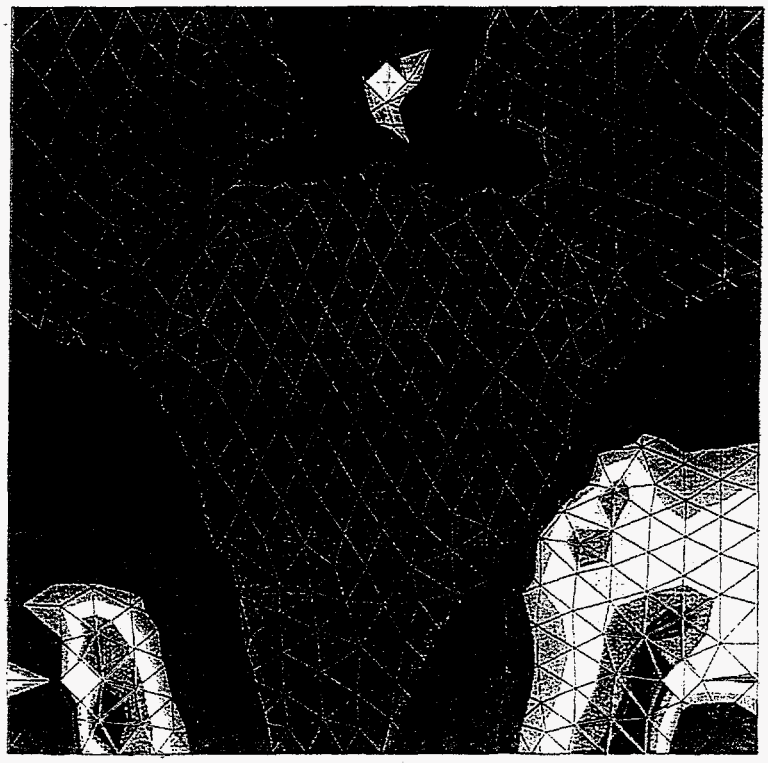

Comment: all stresses are relatively low, S.F. ≥ 3

Note: use of washers will distribute load & thus reduce stresses near holes

$S.F. = \frac{\sigma_y}{\sigma}$ $\sigma_y \simeq 35$ ksi S.F. = 3.2

GeoStar 1.75: QF024

orientation 1 : Stress plot with exaggerated deformations

Upper Adjuster Plate

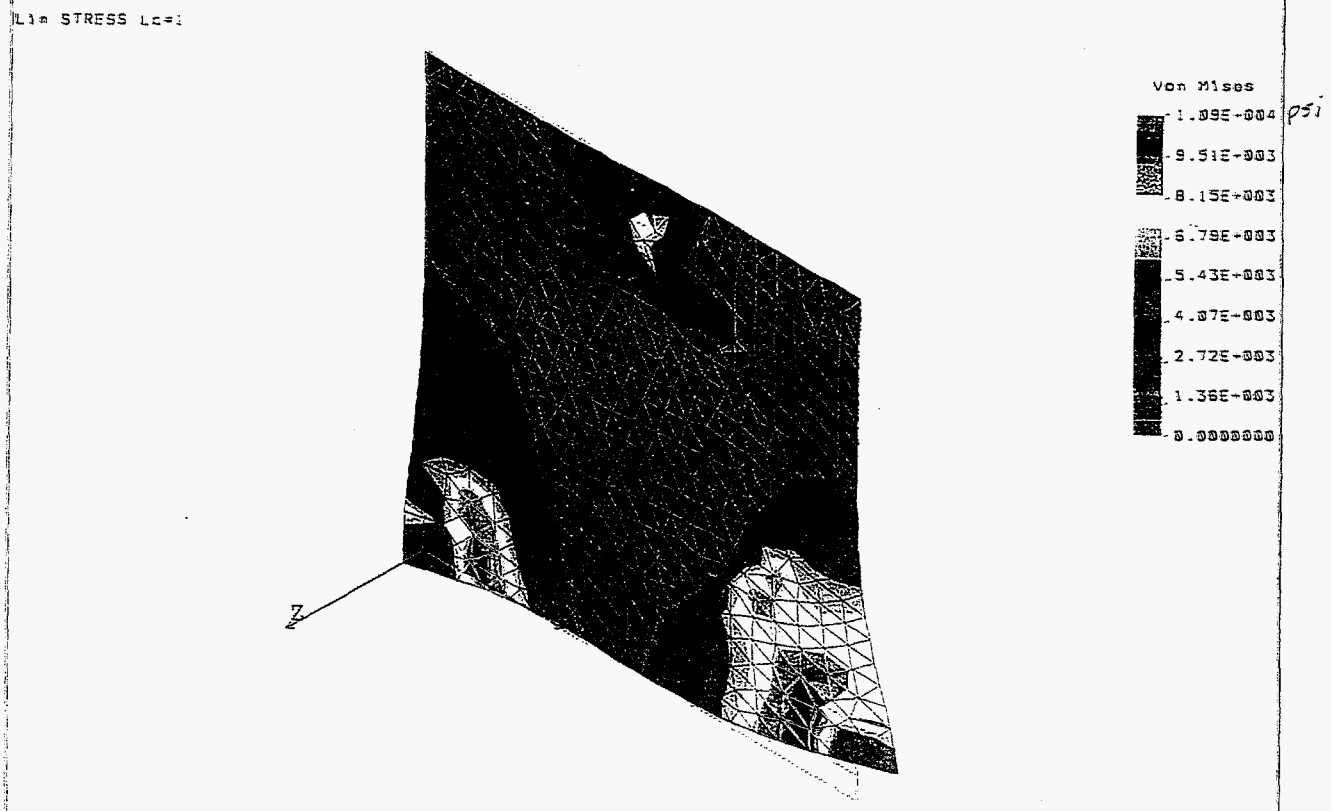

GeoStar 1.75: QF024

orientation 2

stress plot

Upper Adjuster plate

Lin STRESS Lc=1

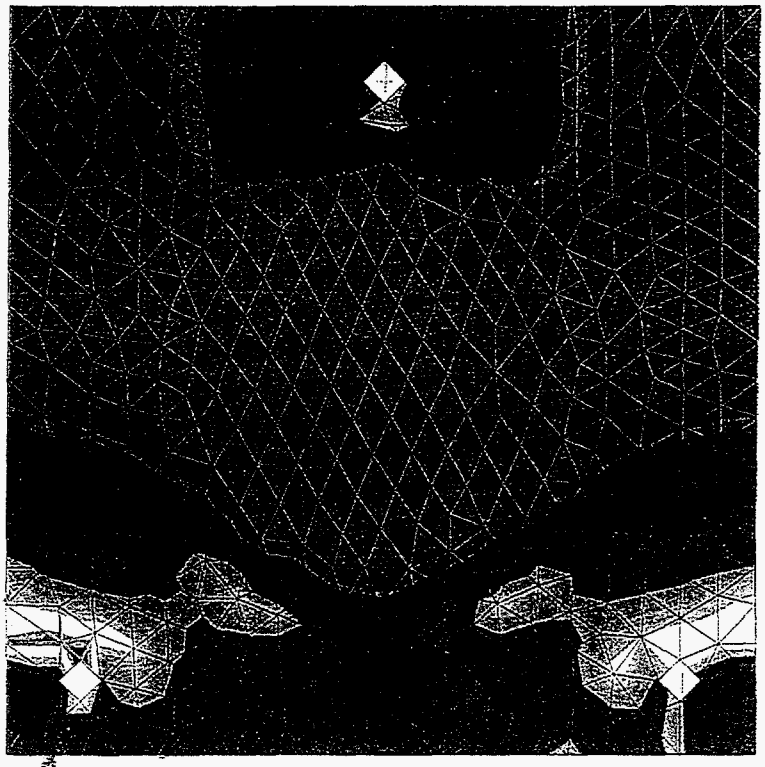

psi

comment — Majority of stresses are relatively low, S.F. ≥ 3

Note: Use of washers will distribute loads & thus reduce stresses near holes

GeoStar 1.75: QF024

Orientation 2 - stress plot with exaggerated deformations

Upper Adjuster Plate

Lin STRESS Lc=1

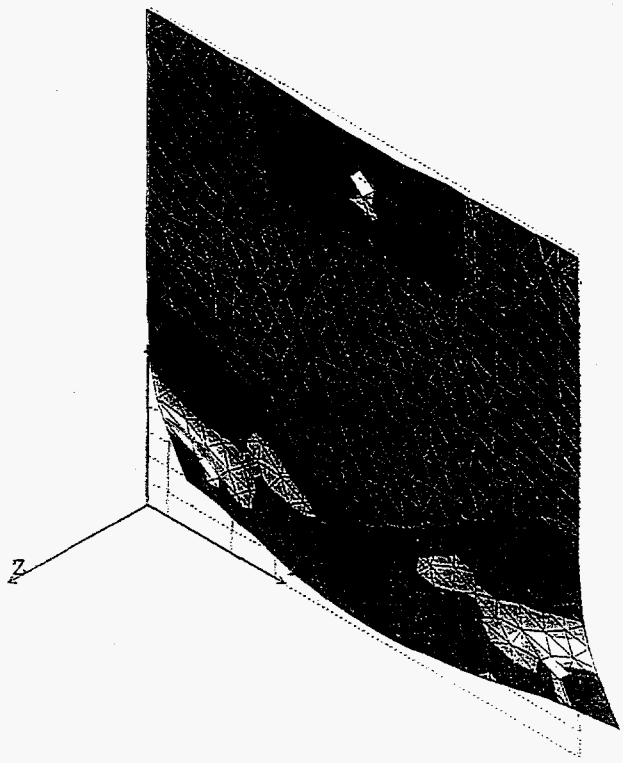

Von Mises

psi

1.43E+004
1.25E+004
1.07E+004
8.92E+003
7.14E+003
5.35E+003
3.57E+003
1.78E+003
0.0000000

GeoStar 1.75: QF024b

~~Lower~~ Adjuster Plate
Upper

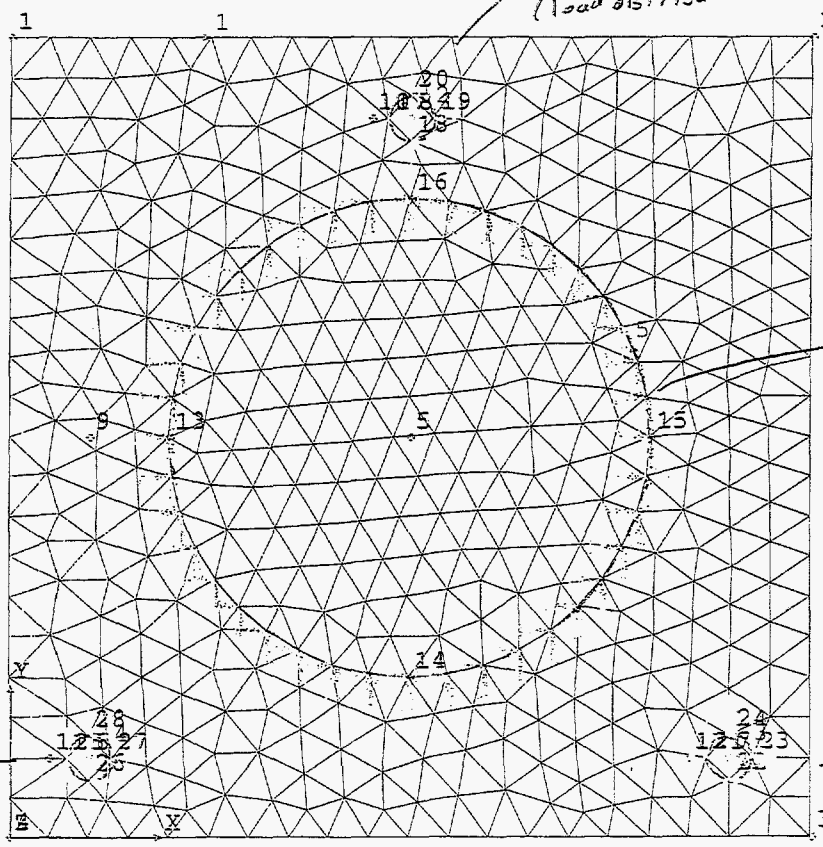

loading orientation 1 only

$P_s \longleftrightarrow P_m$

GeoStar 1.75: QF024b

orientation 1
Von Mise stress plot
~~Lower~~ Adjuster plate
Upper

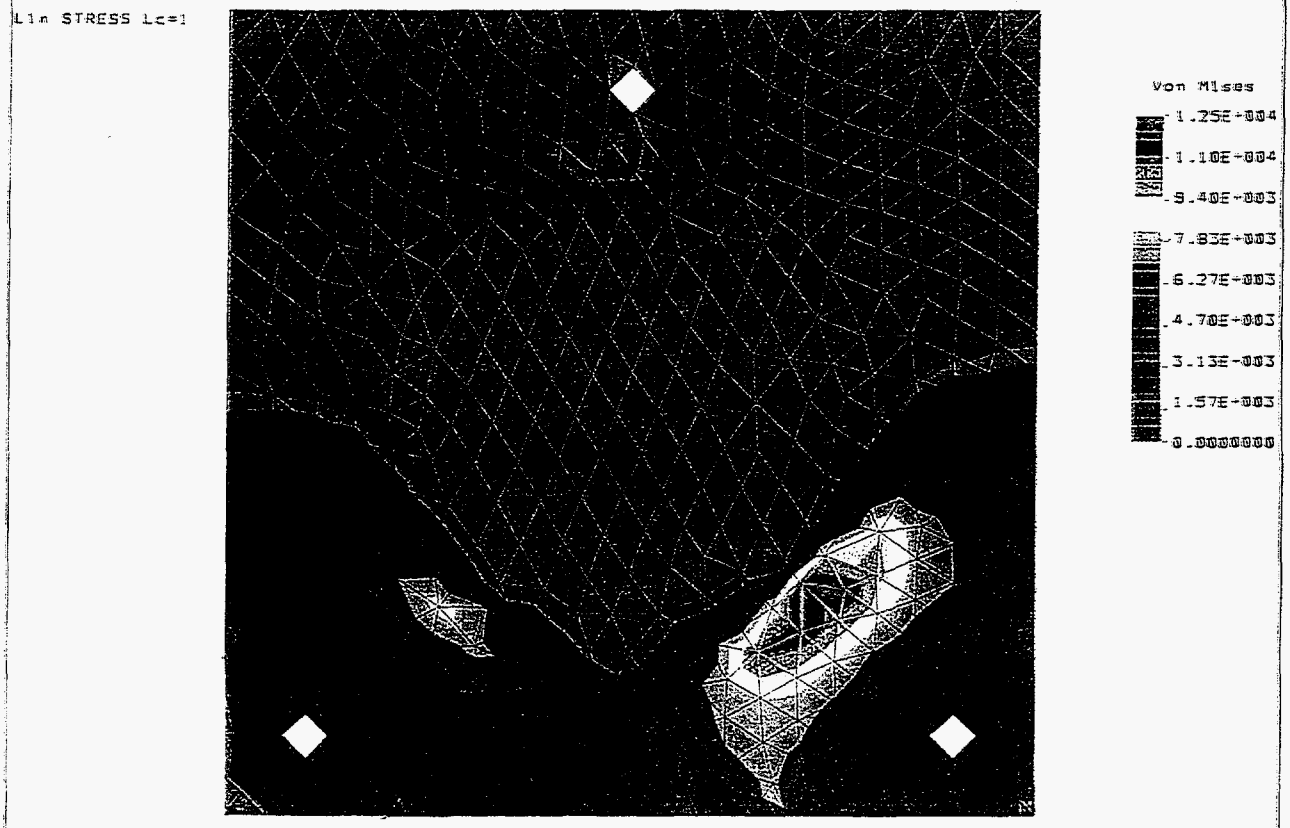

comment: Max stress in plate still gives high safety factor

$$S.F = \frac{\sigma_y}{\sigma_{max}} = \frac{35\ ksi}{12.5\ ksi} = 2.8$$

GeoStar 1.75: QF024b

Upper ~~Bracket~~ Adjuster Plate stress plot showing exaggerated deformation

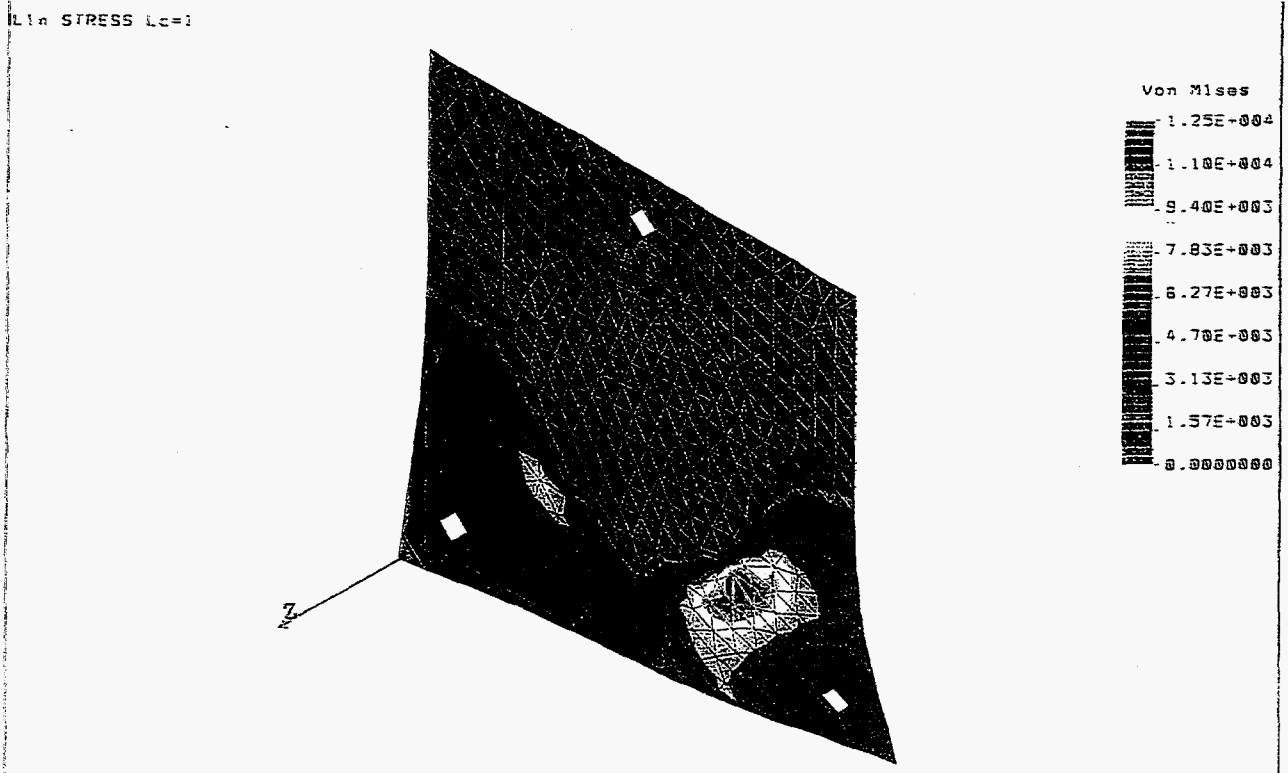

GeoStar 1.75: QF025b

Stress plot
Threaded rods

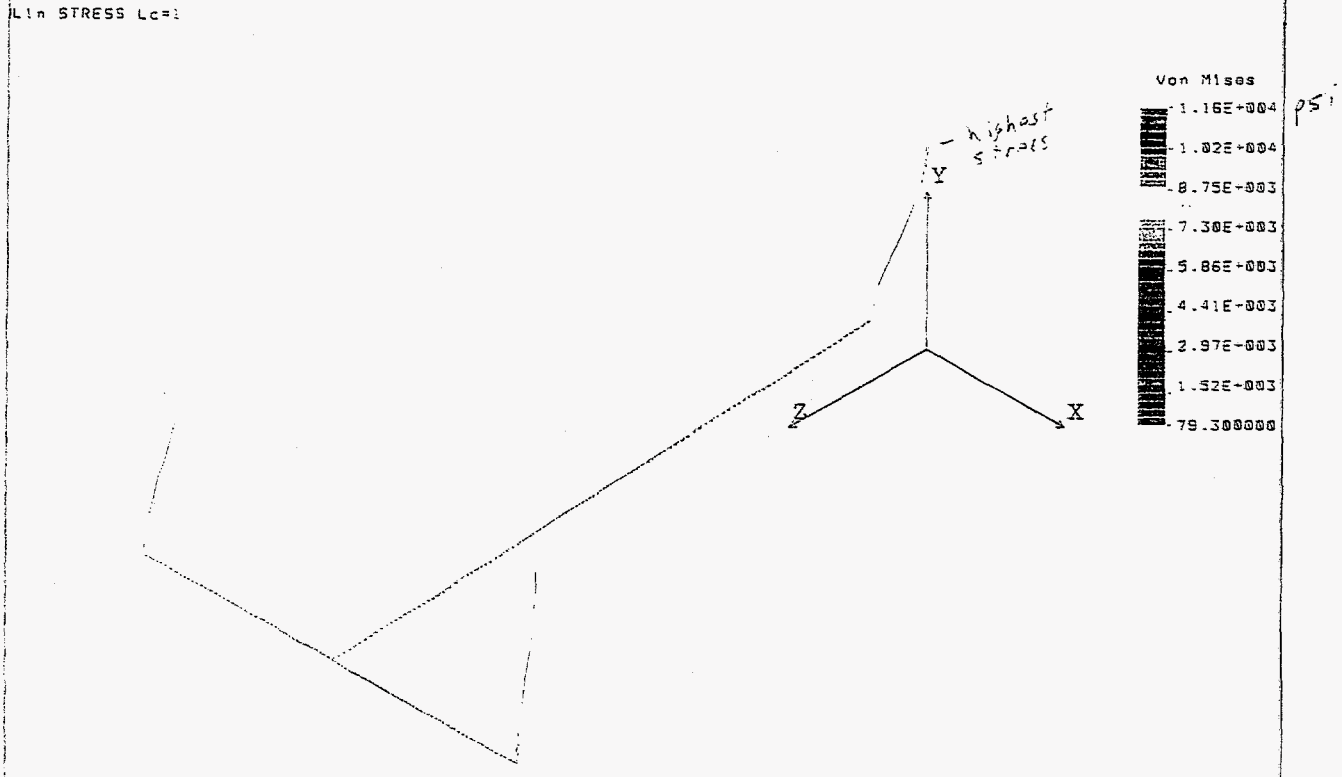

comment: Stresses are quite low.
For worst case, safety factor is:

$$S.F. = \frac{105\ KSi}{11.6\ KSi} = 9.1$$

GeoStar 1.75 : QF027

Threaded Rods

Win 1 (Active)

Lin STRESS Lc=1

Von Mises

1.39E+004 (psi)
1.16E+004
9.30E+003
8.35E+003
7.43E+003
6.51E+003
5.58E+003
4.65E+003
3.72E+003
2.79E+003
1.86E+003

Y
Z X

Main

fixed w.r.t, all 600F

1

20 beam elements
1" O.D. steel rod,
5" length

2 — loaded end ← 300lbs
↓ 600lbs

Y
Z X

GeoStar 1.75: QF027

Threaded rods

Win 1 (Active)

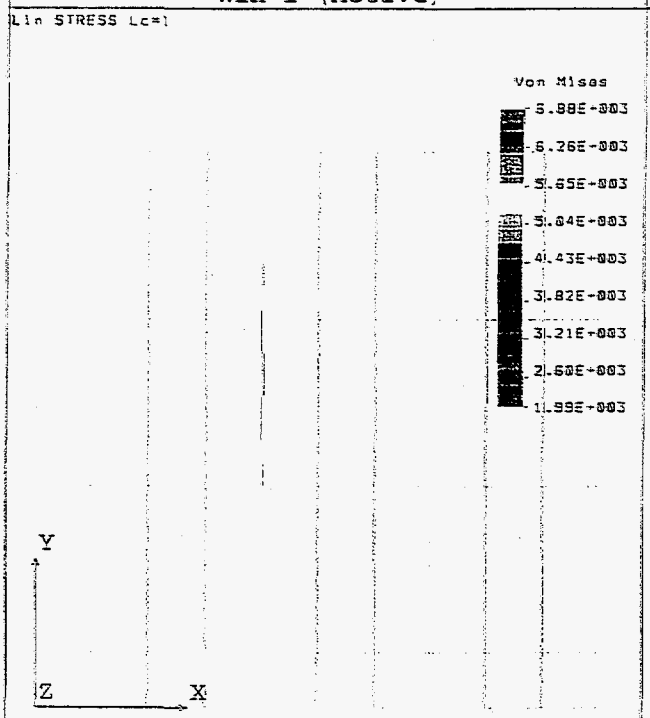

Main

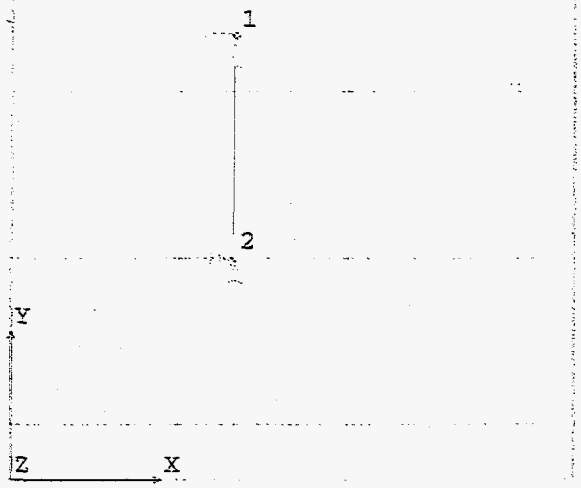

GeoStar 1.75: QF026b

model

Lower Adjuster Plate

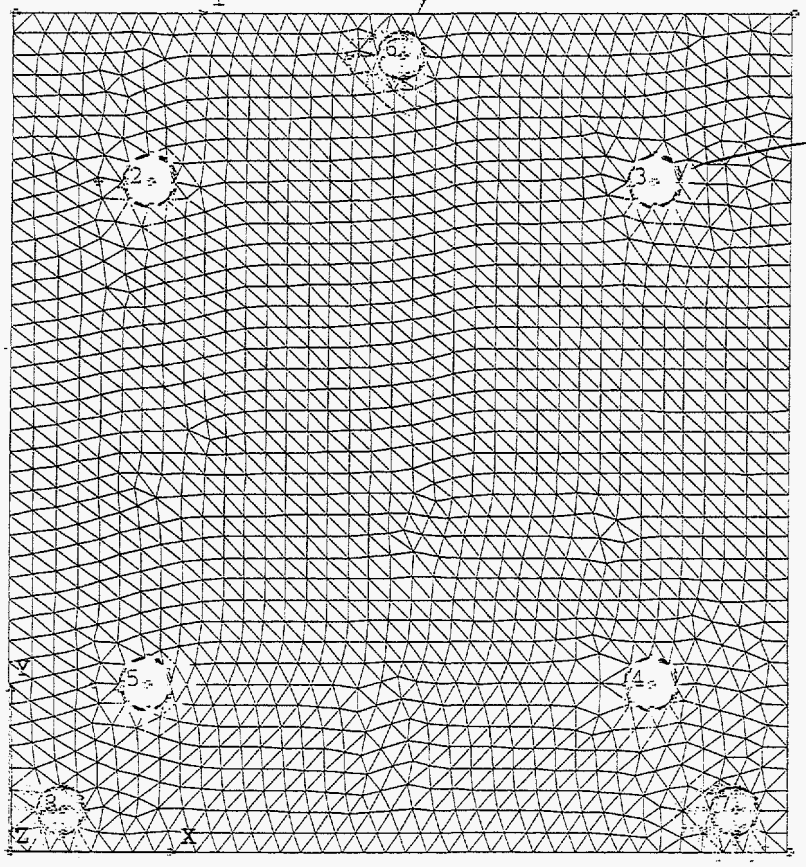

Shell 3 elements

loads distributed evenly across 4 holes.

Total loads

$F_x = -797$ lbs

$F_z = -1770$ lbs

$M_y = 18331$ in.lbs

Fixed w.r.t. all 6 DOF

GeoStar 1.75: QF026b

stress plot
Lower Adjuster Plate

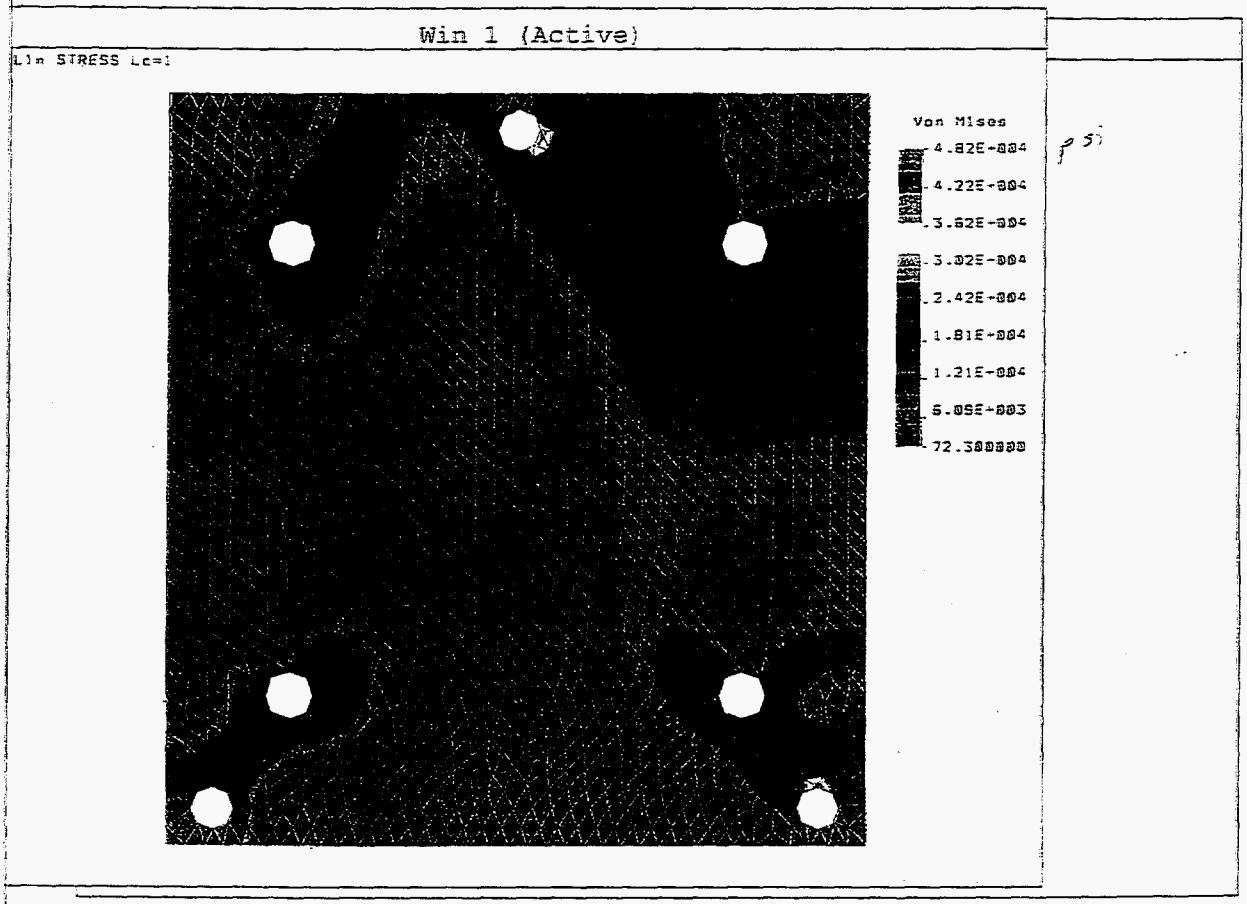

Comments

Only small regions near outer holes are stressed above 15 ksi. In actuality, the washers & nuts located at these holes will spread the load & effectively reduce the stresses. In addition, there is $\frac{1}{2}$" thick steel plate bolted to the underside of this plate, which covers most of the underside. This additional plate, along with the washers & nuts, effectively makes the plate 1" thick. For this model, see next page.

GeoStar 1.75: QF026b

Lower Adjuster Plate

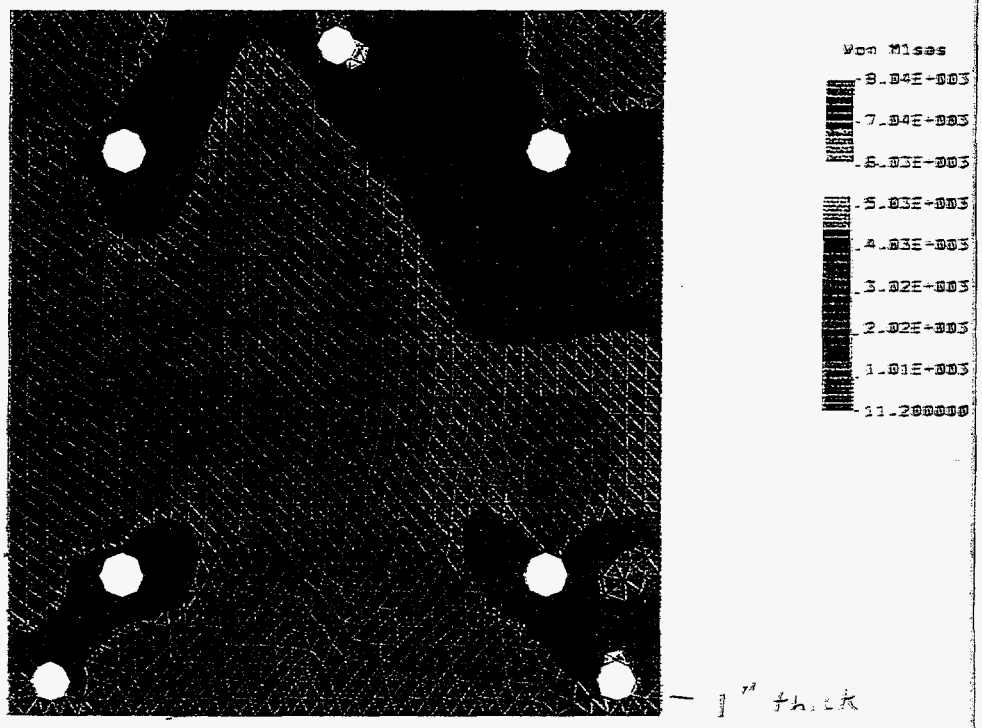

— 1" thick

Comment modelling the lower adjuster plate as 1" thick, reduces stresses & gives a safety factor $S.F = \frac{35}{8} = 4.4$

The actual plate is somewhere between this case and the $\frac{1}{2}$" plate, and it is reasonable to expect S.F. > 3

References

[1] LANSCE Phase II Upgrade Technical Design Report, Draft 7/26/96, Los Alamos National Laboratory.

[2] 1994, DOE Standard: Natural Phenomena Hazards Design and Evaluation Criteria for Department of Energy Facilities, DOE-STD-1020-94, U.S. Department of Energy, Washington, D.C.

[3] 1995, Seismic Vulnerability of Selected Structures, Systems and Components at the Los Alamos National Laboratory, Meson Physics Facility (LAMPF, TA-53), Report 52315-Rev. 0, prepared by EQE International, Inc., Irvine, CA, and Engineering Analysis Group, Los Alamos National Laboratory.

[4] Juvinall, R. C., 1983, Fundamentals of Machine Component Design, John Wiley and Sons, Inc., New York, NY.

[5] Pytel, A. and Singer, F. L., 1987, "Strength of Materials," 4th edition, Harper and Row, Publishers, New York, NY.

[6] Young, W. C., 1989, "Roark's Formulas for Stress and Strain," 6th edition, McGraw-Hill, Inc., New York, NY.